CTI JOURNAL

WINTER VOL. 42, NO. 1
2021

www.cti.org

In the Office.
Online.
Anywhere.

The CTI Journal

(ISSN: 0273-3250)

PUBLISHED SEMI-ANNUALLY
Copyright 2021 by The Cooling Technology Institute, PO Box #681807
Houston, Texas 77268. Periodicals postage paid at Houston, Texas.

MISSION STATEMENT

As a broad based industry association, our mission is to advocate and promote, for the benefit of the public, the use of all environmentally responsible, commercial cooling technologies, such as wet cooling towers, air-cooled condensers, dry coolers, indirect cooling, and hybrid systems, by encouraging:

- Education on these technologies
- Development of codes, standards, and guidelines
- Development, use, and oversight of independent performance verification and certification programs
- Research to improve these technologies
- Advocacy and dialog on the benefits of cooling technologies with Government Agencies and other organizations with shared interests
- Technical information exchange

LETTERS/MANUSCRIPTS

Letters to the editor and manuscripts for publication should be sent to: The Cooling Technology Institute, PO Box # 681807 Houston, TX 77268.

SUBSCRIPTIONS

The CTI Journal is published in January and June. Complimentary subscriptions mailed to individuals in the USA. Library subscriptions $45/yr. Subscriptions mailed to individuals outside the USA are $45/yr.

CHANGE OF ADDRESS

Request must be received at subscription office eight weeks before effective date. Send both old and new addresses for the change. You may fax your change to 281.537.1721 or email: vmanser@cti.org.

Contents

Feature Articles

8 **Extending The Life of Reinforced Concrete Cooling Towers**
David Whitmore, P.Eng. and Garth Fallis, P.Eng.

24 **Vibration Monitoring And Instrument Control In Cooling Towers**
Frank Fang and Everett Jesse

28 **Survey of Laboratory and Field Test Methods for *Legionella***
Loraine Huchler, P.E., CMC®, FIMC

32 **38 Ft Test Rig: A Step Forward In Fans Knowledge**
Nicola Romano

44 **Constructing Non-P Passivation Films for Cooling Applications: Surface Science Perspective**
Paul R. Frail

54 **Using An Ultrasound Measurement Technology To Monitor Real-Time Biofilm Activity Cooling Systems**
Shihhsiang Sean Chien, Michael Bluemle

Special Sections

62 CTI Licensed Testing Agencies
63 CTI Sound Testing and Thermal Performance
64-65 CTI ToolKit
66-71 CTI Certified Towers
72 Index to Advertisers

Departments

2 Multi Agency Press Release
2 Meeting Calendar
4 View From the Tower
6 Editor's Corner

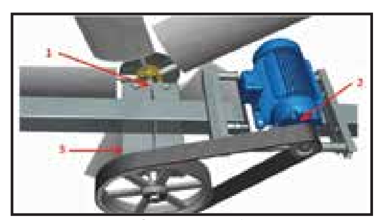

See Page...25

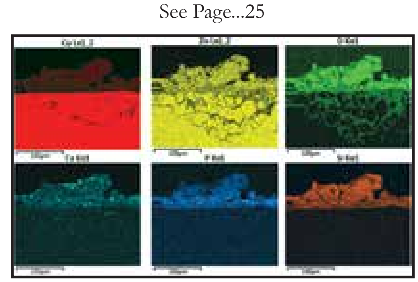

See Page....51

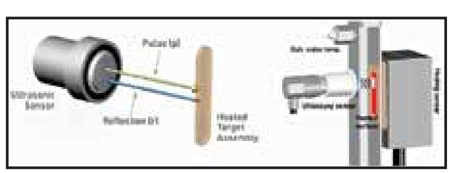

See Page....55

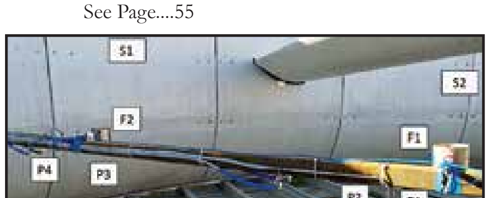

See Page...40

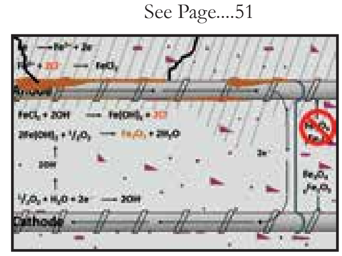

See Page....9

CTI Journal

The Official Publication of The Cooling Technology Institute

Vol 42 No.1 Winter 2021

Address all communications to:

Virginia A. Manser, CTI Administrator
Cooling Technology Institute
PO Box #681807
Houston, Texas 77268
281.583.4087
281.537.1721 (Fax)

Internet Address: http://www.cti.org
E-mail: vmanser@cti.org

For Immediate Release

Contact: Chairman, CTI
Multi-Agency Testing Committee
Houston, Texas

2-October-2021

Cooling Technology Institute, PO Box 681807, Houston, Texas 77268 – The Cooling Technology Institute announces its annual invitation for interested thermal testing agencies to apply for potential Licensing as CTI Thermal Testing Agencies. CTI provides an independent third party thermal testing program to service the industry. Interested agencies are required to declare their interest by March 1, 2021, at the CTI address listed.

Future Meeting Dates

Committee Workshop	Annual Conference
July 11-14, 2021 The Inn at Loretto Santa Fe, NM	April 12-14, 2021 Virtual
July 10-13, 2022 The Steamboat Grand Steamboat Springs, CO	February 7-11, 2022 The Westin Galleria Houston, TX

Quality & Workmanship Backed By
Amarillo Gear 1 Year Warranty.

RENEWING YOUR AMARILLO® GEAR AS EASY AS 1-2-3.

Great Value!

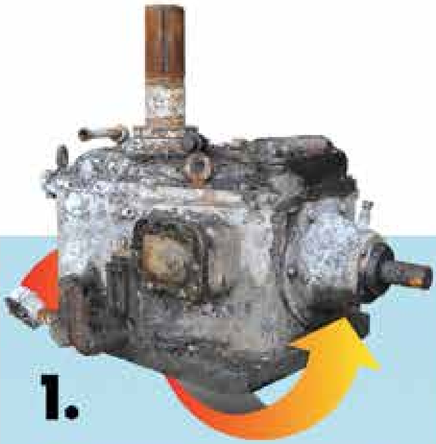

1. When you contact **Amarillo Gear Service™** about RENEWING your drive, we will send you a Not To Exceed quote to give you an idea of the potential total cost of RENEWAL.

2. After receiving your drive, an Amarillo® Gear Technician will inspect for wear and damage. Many times there are parts that can be cleaned and reused providing you, the customer, with considerable cost savings. You will then receive an As Found Condition Report, photographs and an updated quote.

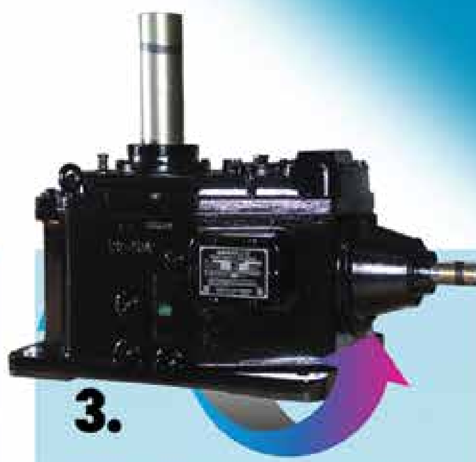

3. Finally, after your approval, your drive will be **RENEWED**, inside and out, tested, painted and returned to you with an As New one year warranty.

(806) 622-1273 • info@amarillogear.com • **AmarilloGearService**.com

Amarillo Gear Service™

Amarillo Gear Service™ is focused on keeping existing gear boxes,...*existing.* A gear drive that you may have thought was ready to be replaced, may now have the opportunity for a new life with quality, Amarillo parts and service. Ask us about our ACC and Industrial gear box renewal programs.

Contact us and let's see if we can take the ***stress*** out of your old gear drive.

*Ask about our added support in the **Gulf Coast** with our **New Orleans location.***

Amarillo Gear Company LLC — A division of Amarillo Gear Company, LLC

A Marmon Water / Berkshire Hathaway Company

CTI MEMBER

View From The Tower

HAPPY NEW YEAR!!!

Chris Lazenby

We are only a few days into 2021 as I write this, and everyone still seems to be relishing the fact that 2020 is in the rearview mirror. It was certainly a year like none other that most of us can recall, and there certainly is a lot that happened to support the idea that 2020 was the "worst year ever".

But…

As my wife reminded our own family recently, the year was not a complete loss. In fact, as we talked about it at our house, we recalled a lot of good things that happened to the four of us over the course of 2020. For instance:

Our kids' schooling was reduced to a few hours a day at our dining room table or on the couch, but they spent more time exploring the woods and creeks behind our house and playing outside this spring than they had in the previous decade combined.

The big vacation that we had planned to celebrate my wife's 40th birthday was canceled, but her birthday present became a new four-legged member of the family that raises the happiness quotient daily at our house.

I was sent home in mid-March and haven't been able to work a day inside my Southern Company office since then, BUT…okay, really there's no downside to that.

So, while 2020 was different, that didn't necessarily mean it was all terrible. And I think that view can also apply to the CTI. While COVID-19 impacted some people's ability to attend our Winter Meeting in February and caused us to cancel our annual summer meeting entirely, we were able to successfully hold the first ever Virtual CTI Committee Workshop in July. Not only did this allow us to keep moving forward with the important work of maintaining our Codes and Standards documents, it also gave us extremely valuable experience with technology platforms necessary to stream and connect with a virtual audience. This type of experience is invaluable to us as an organization as we continue to operate in a world that becomes more and more digitally based. And quite frankly, while I love all the people in the CTI, let's just agree that we are not always the most innovative, cutting-edge organization, so it may have taken something like this to force us to get this point!

Also, while not directly related to the pandemic, we had the rare occurrence of all three of our standing Technical Committees: Water Treatment, Engineering Standards & Maintenance, and Performance & Technology, changing their Chairs in 2020 (Water Treatment actually had two new chairs over the course of the year). Yet despite the turnover in leadership and without being able to meet in person, each committee continued to move forward issuing needed revisions to our existing Codes and Standards documents and working on new ones. A big thank you to James Blake, Jared Medlen, Dwight Emerich, and Brian Corbin for their leadership and to everyone who participated in these efforts.

Finally, as many are aware, we have been working for some time now on starting a Materials Certification program. However, after spending years spearheading that effort, Denny Shea, decided that he needed to step down from his role as coordinator. But, longtime CTI member and former President, Frank Michell, graciously agreed to take over from Denny and continue working to get that program started. Thank you, Denny, for all your efforts over the years, and thank you Frank for being willing to help us move forward!

Speaking of moving forward, while the world does seem to be moving more and more in a digital direction, I believe there are things that happen during face-to-face gatherings that cannot be duplicated entirely across a screen. So, while I think we need to keep working to broaden our digital presence, meeting in person will continue be of vital importance to the CTI. That is why we have taken the unprecedented step of moving our 2021 Annual Conference from its traditional February date back to April 11-15. It is our sincere hope that by this point in time, the pandemic may have subsided enough that an in-person meeting might still be possible. If that ends up not being the case, it will certainly be disappointing, but if this year has taught me anything it is that you as the CTI will continue to be flexible, adapt, and move forward.

So, here's to hoping we can see each other in New Orleans! And whatever happens, thank you for being the CTI, and please continue to stay safe!

Editor's Corner

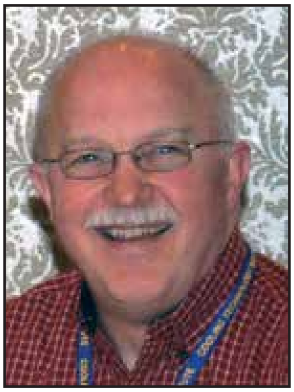
Paul Lindahl

Writing this in the 9th month of pandemic impacts and counting down to a new year. Vaccines have started, and are likely late spring for my wife and me. We are looking forward to some return to normalcy in 2021, let it be so… On behalf of many friends who are providing health care and who are at risk for infections, thank you to all who are wearing masks to protect others.

CTI continues to be active in working to influence governmental and other organization standards actions that impact our members, note that activity has slowed somewhat. A brief overview:

California Title 24 – We believe that they will push for increased energy efficiency for evaporative heat rejection equipment in future revisions, but not in the current one.

California Title 20 – It appears that they will hold to the exemption for heat rejection equipment fan efficiency requirements. We have still not yet seen language to confirm that.

ASME Boiler & Pressure Vessel Code – The scope task force is still pushing to remove the exemptions for less than 6" vessels and for those with non-boiling water. CTI has joined other organizations in written opposition to this since other standards have evolved to cover such equipment. It was not in the current revision, but it still on the agendas for the BPVC scope task force.

Legionnaires' – CTI has published GDL-159 for evaporative heat rejection equipment (cooling towers (open and closed loop) and evaporative condensers). ASHRAE Guideline 12-2020 has been released. Both are important enhancements to writing Water Management Programs per ASHRAE Standard 188-2018. ASHRAE Standard 514P is in development to cover other building water system hazards, and CTI has official organization representatives, Helen Cerra and Frank Morrison. An advisory public review is planned for Spring 2021.

CTI R&D is continuing to be active in exploring and developing R&D projects. They should be proposed through the standing committees and program committees.

Our goal is to introduce a new CTI regulatory update newsletter this Spring for CTI members only. Be looking for it by email.

The Virtual meetings in July went well, I think. The winter meeting for 2021 has been delayed to April in New Orleans, time will tell whether it can happen by April. Check the CTI website for updates. Hope to talk with many of you then, whether in person or virtual!

Extending The Life of Reinforced Concrete Cooling Towers

David Whitmore, P.Eng. and Garth Fallis, P.Eng.,
Vector Corrosion Technologies

David Whitmore

Abstract

Reinforced Concrete Cooling Towers are a mainstay of industries that require the cooling of systems and process water. The environment these cooling towers see varies widely from forced-air cooling towers for mineral water to natural draft cooling towers for brackish water. All these environments can have a detrimental effect on the condition and longevity of the reinforced concrete. This presentation will look at options for repairing and extending the life of these reinforced concrete cooling towers. The topic will be explored using two case studies; Coal Creek Station in North Dakota using structural concrete repair, waterproofing, beam replacement, and protective coatings; and a Mid-Atlantic Generating Station with a variety of impressed current and galvanic cathodic protection systems. Each repair and restoration is expected to extend the life of the cooling tower in excess of 25 years.

Cooling Towers

Cooling tower are used to cool process water for industrial facilities. The two cooling towers we are discussing in this paper are very different in design and process.

The Mid-Atlantic Cooling Tower is a reinforced concrete hyperbolic shell natural draft cooling tower. The tower is the main component of a closed-cycle water cooling system, in which the process water is sourced from the nearby brackish river. The hot water is sprayed into a basin at the base of tower to cool it. The steam (hot moist air) raises via convection, through a filter bed and out the top of the tower.

The Coal Creek Station Cooling Tower is a mechanical draft cooling tower. Three mechanical draft cooling towers operate at the power station, each 42' high and 225' in diameter, equipped with eight 28' diameter fans. Hot water from the plant is introduced to the top of the tower and is cooled by a counter-flow of air drawn from below. The water is finally collected in the cool water basin at the base of the cooling tower. The cooling water basin and the interior beams and columns are built with cast-in-place reinforced concrete and the elevated hot water basin is constructed with precast concrete elements.

Mid-Atlantic

The Mid-Atlantic Generating Station (Fig. 1) is a combination coal and natural gas generating station the brackish water from a local river as it's cooling water. Over the years as this brackish water rose up with the positive draft of the Cooling Tower the chloride penetrated into the concrete causing the reinforcing steel to corrode.

Structure Description

The diameter of the cooling tower varies with height, creating its distinct hyperbolic shape with the throat (smallest diameter) at approximately two-thirds height. Horizontal construction joints spaced at approximately 5-foot intervals form 70 identifiable concrete placement "lifts." The shell is 8-inches thick over its height and tapers over five lifts to a 36-inch thick bottom ring beam and over three lifts to a 26-inch thick top cornice ring. The shell is reinforced with a mat of vertical (meridional) and horizontal (circumferential) steel reinforcing bars at both the interior and exterior faces and is supported by 32 precast reinforced concrete X-columns that are approximately 60-feet tall with a 20 by 33 inches cross section.

Fig. 1 Mid-Atlantic Generating Station Cooling Tower

Operational History and Deterioration

The cooling tower was placed into service in 1975. The unit is a peaking unit that runs intermittently to meet peak energy grid demands and uses brackish process water sourced from the nearby river.

In the mid-1980s, the exterior face of the tower shell began to experience concrete deterioration. By the early 2000s, similar issues were apparent at the supporting X-columns. Since then, concrete deterioration caused by corrosion of the embedded reinforcing steel progressed significantly, including large areas of concrete delamination and spalling at the shell exteriors, large areas of concrete delamination at the shell interiors, and cracking and delamination in the supporting X-columns.

- Several condition assessments of the tower were conducted during the period 2006 to 2013 to characterize deterioration mechanisms and extent, assess structural integrity, and develop repairs to meet the owner-defined 25-year service life extension. The resulting comprehensive repair program, conducted from 2014 to 2018, included an engineered demolition and rebuild of the upper third of the tower as well as substantial repairs and installation of cathodic protection systems across the nearly 200,000 square foot concrete shell. Critical to plant operations, the tower remained fully operational throughout construction.

Cooling Tower Rehabilitation

The rehabilitation of the Mid-Atlantic Cooling Tower included:

- Removal and replacement of the top 100 ft of the tower
- Concrete spall repairs on the exterior and interior of the shell
- Cathodic Protection of the entire structure
  - Galvanic Cathodic Protection (GCP) on the X Column legs
  - Impressed Cathodic Protection (ICCP) in the new top of the tower
  - ICCP on the shell

Tower Cathodic Protection

To extend the useful life of the cooling tower it was decided that a cathodic protection system would be installed on the tower.

Corrosion Basics

To better understand the repairs, we need to understand the corrosion mechanism (Fig. 2).

Steel is manufactured in a process in which raw iron ore is extracted from the ground and goes through a process of adding energy to the iron to transform it into the steel that we know and use for reinforcing steel in concrete. This steel is constantly trying to return to its natural state by giving off the energy and transforming back to iron oxide.

In concrete, external agents accelerate this corrosion process with the most significant of these being chlorides, or salt. Once the chloride penetrates to the level of the reinforcing steel through the pores in the concrete, it initiates and accelerates the corrosion activity.

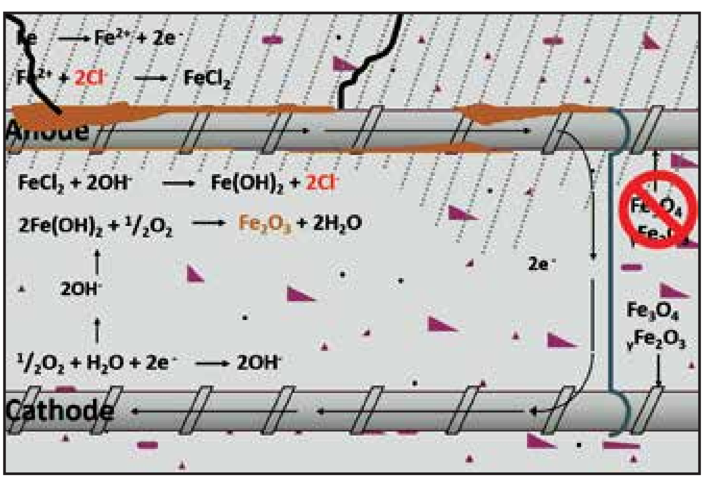

Fig. 2 Reinforcing Steel Corrosion Process

This corrosion starts with breaking down the protective passive layer on the reinforcing steel that has been generated by the high pH of the surrounding concrete. Once the passive layer is destroyed, a corrosion cell between the contaminated reinforcing and other reinforcing, that is still passive, is developed creating an anode and a cathode. At the anode the corrosion of the reinforcing continues developing ferrous oxide (Fe2O3). This ferrous oxide has volume of 8 to 10 times that of the original steel from which it has transformed. This volumetric expansion puts pressures on the concrete and over time causes it to crack and eventually spall.

Corrosion Mitigation

On the Mid-Atlantic Cooling Tower, to provide optimal corrosion mitigation, four different sections of the tower (Fig. 3) used four different corrosion mitigation methods:

- The X Column support legs used a galvanic system
- The top section of the tower, which was removed and replaced, used an Impressed Current Cathodic Protection (ICCP) system with titanium ribbon embedded in the new concrete
- The middle section of the tower, with an ICCP system with titanium ribbon embedded in slots in the existing concrete
- The lower section of the tower, with an ICCP system with ceramic titanium discrete anodes embedded in holes drilled in the existing concrete

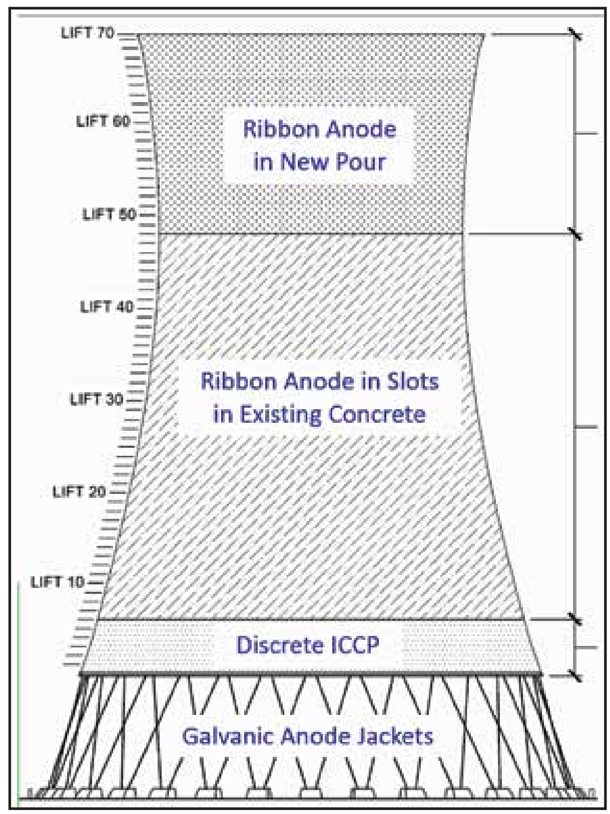

Fig. 3 Cathodic Protection Systems Layout

X Column Rehabilitation

Thirty of the 32 X-columns exhibited visible deterioration. The lower half of the X-columns, below the water distribution media, exhibited the greatest deterioration, which primarily consisted of longitudinal cracking and delaminations at the corners associated with corrosion of embedded reinforcement.

X-Column Cathodic Protection

The X-column environment is wet and subject to a wide range of service temperatures (0 °F to 125 °F). The GCP jackets are comprised of alkali-activated zinc anodes installed on the column faces that are encapsulated with cement grout inside stay-in-place fiber reinforced polymer forms. To protect the X Columns, distributed galvanic anodes were installed on the surface of each X Column legs and connected to the reinforcing steel. To protect the anodes, and enhance their performance, the legs were surround by a fiberglass jacket with the space between the jacket and the columns, where the anodes were located, being filled with a cementitious mortar (Fig.7 to 8).

Fig. 4 Remove Delaminated Concrete

Fig. 5 Install Linear Anodes

Fig. 6 Install and Grout Jacket
Sequence of X-column galvanic jacket installation.

The galvanic system essentially operates as a low-voltage battery supplying protective current to the column reinforcing steel. Four X-columns were instrumented with reference electrodes to monitor and assess the GCP performance over time.

Fig. 7 Connecting Anode to Reinforcing Steel

Fig. 8 Completed Jacket

Galvanic Cathodic Protection

Galvanic cathodic protection provides the electrons to the corroding steel by means of connecting dissimilar metals, ie. connecting a metal that is more electro-negative than steel, such as zinc or magnesium, to the steel. The more electro-negative metal releases electrons that flow to the steel and replaces the electrons being lost in the corrosion process, thus stopping the corrosion activity.

There are embedded galvanic anodes that are specifically designed for use to protect reinforcing steel in concrete. The embedded galvanic anodes for concrete are designed with a zinc core surrounded by a special highly alkali mortar, which keeps the zinc actively corroding over time. These galvanic anodes come in variety of shapes and sizes so they can be best designed to suit specific applications. (Fig. 9 to 11)

fanTR
TECHNOLOGY RESOURCES

Soluciones innovadoras para ventilación subterránea

FanTR fabrica equipos y sistemas de ventilación para la renovación del aire en ambientes subterráneos o confinados, desarrollados por un experimentado equipo profesional de ingenieros especializados en ventilación.

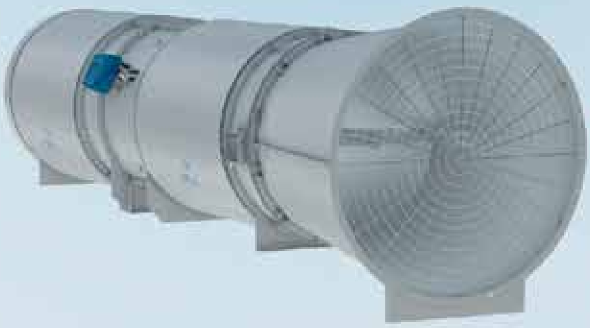

Número 1 en el mercado de ventilación subterránea en Brasil

Presencia local en Perú y Colombia

EQUIPOS DE VENTILACIÓN DE MINAS SUBTERRÁNEAS

Desarrollados para la realidad de las minas, nuestros ventiladores ofrecen una mayor resistencia y garantizan una durabilidad superior, incluso an las condiciones más adversas.

VENTILADORES Y SISTEMAS DE EXCAVACIÓN Y APERTURA DE TÚNELES

Siguiendo la misma línea de diseño de los ventiladores de minería, estos equipos son más robustos y están diseñados para condiciones extremas de operación, muy comunes en los sitios de construcción.

VENTILADORES AXIALES DE CHORRO DEFINITIVOS DE ALTA TEMPERATURA

Los ventiladores con certificado F400, según la norma EN12101-3, soportan temperaturas de hasta 400°C de funcionamiento sin comprometer su estructura o rendimiento durante dos horas.

fantr.com

fanTR
TECHNOLOGY RESOURCES

GRUPO PROSUMISAC
PROVEEDORES DE SUMINISTROS MINEROS E INDUSTRIALES S.A.C.

FAN TECHNOLOGY RESOURCES

Rodovia Waldomiro Corrêa de Camargo, km 53,7
Bairro Cruz das Almas - Itu/SP - Brazil

fantr@fantr.com **+55 (11) 4025-1670**

VENTAS PERÚ - PROSUMISAC

Urb. Los Rosales Mz. B Lote 12 - San Martín de Porres
Lima - Perú

+51 (01) 484-4298
+51 991909007

ventas@prosumisac.com

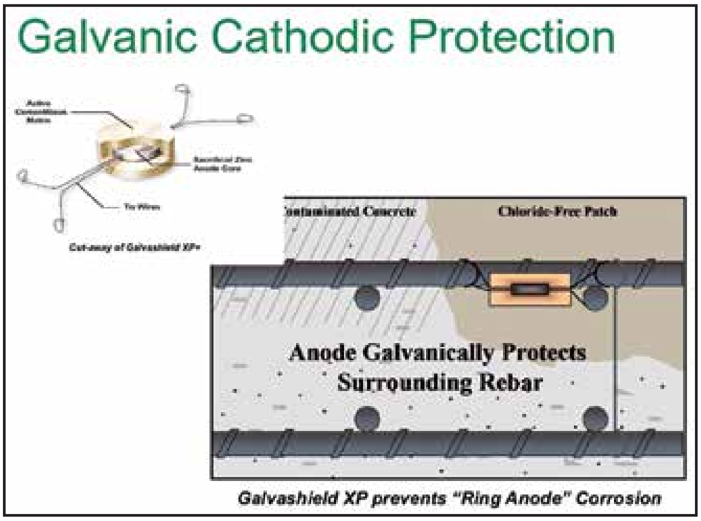

Fig. 9 Galvanic Anode for Patch Repair

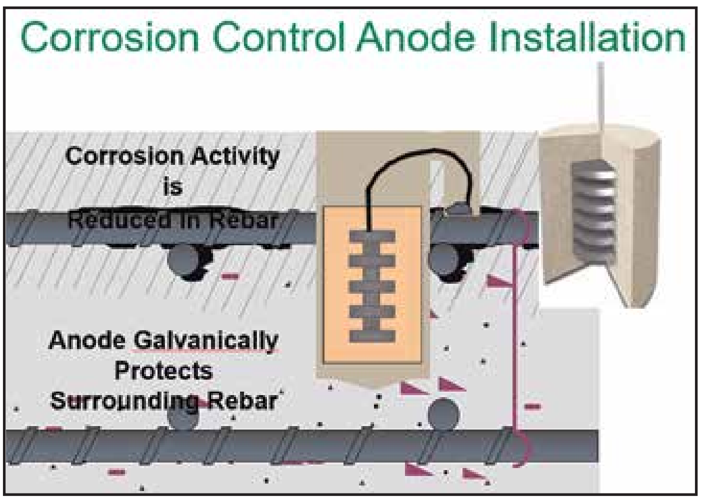

Fig. 10 Galvanic Anode for Drilled in Application

Note: "Ring Anode" Corrosion is the corrosion of the reinforcing steel immediately outside a repair due to clean reinforcing the new repair becoming a cathode and increasing the corrosion of the reinforcing steel just outside the repair.

Fig. 11 Galvanic Anode for Marine Application

Other forms of galvanic anodes for protecting reinforcing steel are surface applied. Again these are zinc, but in this case it is arc-spray applied to the concrete surface, then attached to the reinforcing steel to provide the protection. (Fig. 11A & 12) These anodes are design to provide protection to a large area, such as the outside of a bridge pier, marine facility, chimney or cooling tower.

Fig. 11A Activated Arc Sprayed Zinc Anode Installation

Fig. 12 Activated Arc Sprayed Zinc Project Installation

Shell Rehabilitation

Shell Engineered Demolition and Rebuild

Demolition of the upper third of the shell was performed by saw cutting roughly 5-foot by 8-foot sections of the tower shell from project-specific fabricated moveable saddle platform rigs that traversed around the tower circumference. (Fig. 13 & 14) Cut concrete panels were secured and lowered to ground via cranes positioned around the tower. In total, approximately 60,000 square feet of concrete shell were safely removed.

Fig. 13 Demolition of upper third of the tower in progress.

Fig. 14 Saw-cut demolition panel showing delamination cracking at both interior (top) and exterior (bottom) faces.

The shell rebuild matched the geometry of the original design and was constructed from a propriety full-circumference, self-climbing (up and down) three-level work platform with a built-in jump-form system. (Fig.15 & 16)

Fig. 15 Rebuild of the upper third of the tower, in progress.

Fig. 16 Three-level self-climbing work platform

Shell Repair

Partial-depth and full-depth concrete repairs using dry-mix shotcrete were performed on the lower two-thirds of the interior and exterior faces of the shell. (Fig. 17 &18) Exterior face access was provided by the proprietary climbing work platform used during the rebuild, and the interior face was accessed from heavy duty suspended platforms. (Fig. 19) Repairs followed ICRI and ACI guidelines and shotcrete nozzlemen were prequalified on-site specifically for the project.

Fig. 17 Partial-depth concrete repair area. Note horizontal saw-cut slots for ICCP ribbon anodes.

Fig. 18 Shotcrete installation.

Fig. 19 Heavy duty interior work platforms.

Shell Cathodic Protection

Three types of ICCP systems were used at different sections of the shell. In the heavily reinforced, thickened concrete base of the shell, over 4,300 discrete titanium suboxide ceramic tube anodes were installed in drilled holes and grouted into the center of the thick wall section to provide protection to both the interior and exterior reinforcing mats. Mixed metal oxide-coated titanium ribbon mesh anodes, grouted into slots cut in the exterior surface of the shell (Fig. 20) using ionically conductive cement grout provide protection to both mats of reinforcing in the 8-inch thick shell section. In the reconstructed upper shell portion, ribbon mesh anode was installed between the reinforcing layers prior to placing the concrete. In the rebuilt shell, the ICCP is only "trickled" to prevent corrosion from initiating. In total, over 6 miles of ribbon mesh anode were installed.

Fig. 20 Grouting ribbon anode in continuous saw-cut slot at shell exterior.

Impressed Current Cathodic Protection (ICCP)

Impressed current cathodic protection also stops the corrosion actively by providing electrons to the corroding steel, but in this case the electrons come from an external power supply. An ICCP system consists of an anode and a DC power rectifier. The DC power supply receives power from an outside source and then with it connected on the positive side to the anode and the negative side to the reinforcing steel it creates a corrosion mitigating circuit. Once energized the DC rectifier sends electrons to the reinforcing steel providing the corrosion protection. (Fig.21)

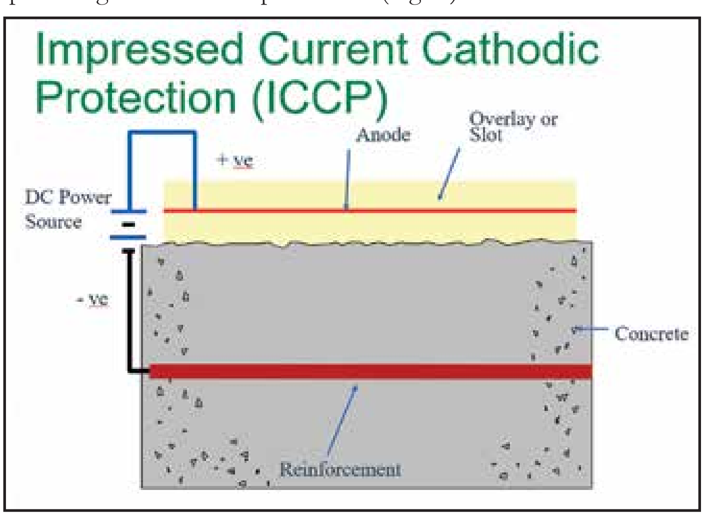

Fig. 21 Impressed Cathodic Protection Schematic

The key variation in an ICCP system is the anode. The anodes come in a variety of forms, mixed metal oxide titanium ribbon, titanium mesh, ceramic titanium discrete anodes, and others. (Fig. 22 & 23) The mixed metal oxide titanium is chosen because even though it "corrodes" it does not lose its effectiveness or change in volume.

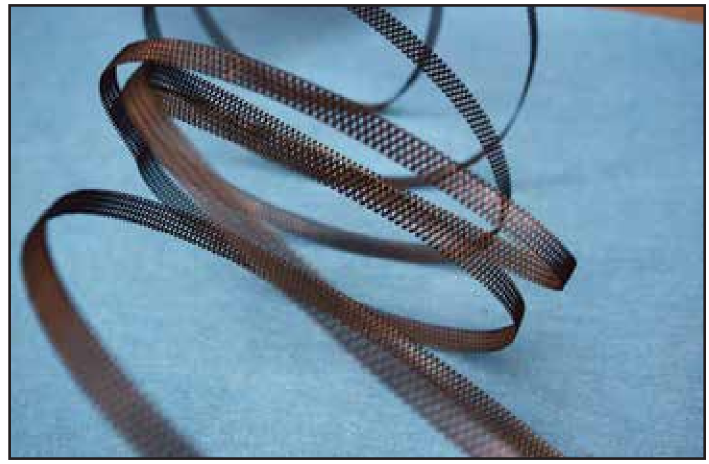

Fig. 22 Titanium Ribbon Anode

Fig. 23 Ebonex Discrete Anode

ICCP system with titanium ribbon embedded in the new concrete

The top portion of the tower concrete damage due to the corrosion of the reinforcing steel was so extensive the entire top 100 feet was removed and replaced. Knowing that if left unattended that the corrosion activity on the top of the tower would continue to be severe, it was decided to install an ICCP system in the new concrete. In this case, a titanium ribbon anode was embedded into the new concrete. (Fig. 24 & 25) These anodes were connected to the DC rectifier located at the base of the tower.

Fig. 24 Ribbon anode installed in new concrete

Fig. 25 Ribbon anode ready for new concrete

ICCP system with titanium ribbon embedded in slots in the existing concrete

In the middle portion of the tower, the reinforcing steel had corroded to the point of causing some concrete damage, but not enough to cause it to have to be replaced. To stop future corrosion and concrete damage an ICCP system with titanium ribbon anodes embedded in slots on the concrete were installed.(Fig. 26 & 27) Again these anode were connected to the DC rectifier located at the base of the tower.

Fig. 26 Sawcutting slots for ribbon anode

Fig. 27 Grouting slots after ribbon anode installed

ICCP system with ceramic titanium discrete anodes embedded in holes in the existing concrete

On the lower section of the tower the reinforcing steel was also corroding. In this case, the concrete was up to 40 inches thick with reinforcing steel that needed to be protected on both the inside and outside face of the tower. To provide protection to both layers of reinforcing ceramic titanium discrete anodes embedded in holes was chosen as they could be installed in the middle of the wall close to both layers of reinforcing. (Fig. 28 & 29) Again these anode were connected to the DC rectifier located at the base of the tower.

Fig. 28 Drilling for Ebonex Discrete Anodes

Fig. 29 Installing Ebonex Discrete Anodes

Power Supply and DC Rectifier

An extensive system of wiring and conduits were required to connect the three different anode systems to the DC Rectifier. (Fig. 30 to 34) To best operate the ICCP system the tower was divided into 48 zones, with no splices, each with its own connection to the rectifier. Each zone had to be connected with a full length wire with no splices.

Fig. 30 Installing Conduit and Wiring

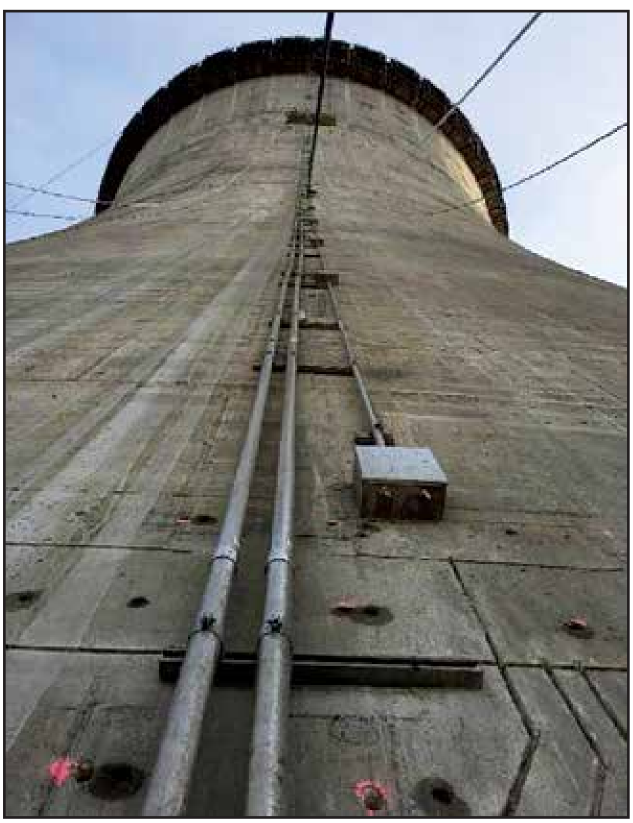

Fig. 31 Conduit

Fig. 32 Rectifier Control Panel

Fig. 33 Rectifier Control Panel Box

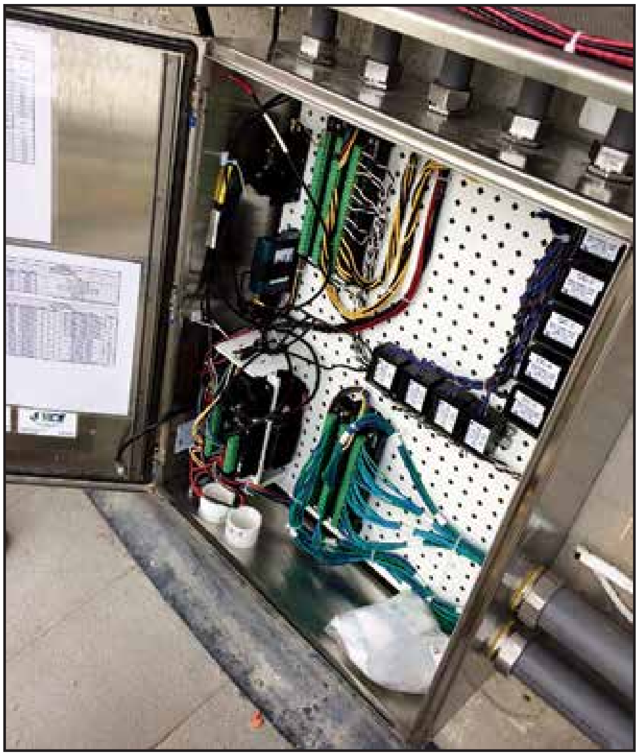

Fig. 34 Rectifier Control Panel Wiring

Controlling and Monitoring the ICCP System

The entire ICCP system is able to be monitored and controlled remotely using the StructureView remote monitoring system. (Fig. 35) Each zone has its own controls, and constant readings are taken to access its performance. Should adjustments need to be made to optimize the systems performance they can also be made remotely.

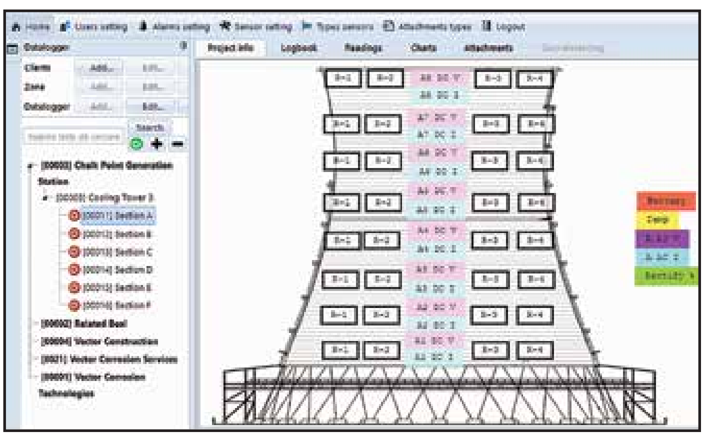

Fig. 35 ICCP Monitoring System Readout

With the installation of the Galvanic Cathodic protection system installed on the X Column support legs and the ICCP system installed on the tower, the life of the Mid-Atlantic Cooling Tower # 3 has been extended 25 years and beyond.

Coal Creek Station

Coal Creek Station is located about 50 miles north of Bismarck. Coal Creek Station is North Dakota's largest power plant and distributes electricity into the Twin Cities of Minnesota, Minneapolis and St. Paul. Coal Creek Station operates two late 70's vintage lignite-fired generators and combined have a capacity of more than 1,100 MW.

Tower Restoration

After 40 years of use, cooling tower #91 was showing its age and required extensive attention. If the entire cooling tower was demolished and rebuilt, including the interior concrete structure, it would be very costly and require a long downtime. Even though the cooling tower was showing signs of advanced deterioration, it was determined that the concrete could be preserved, and so an extensive restoration and rebuild of the cooling tower was planned during an extended 6-1/2 week shutdown in May, 2017.

A large amount of work was to be completed in a short amount of time; planning and coordination between the owner and contractors was critical to completing the time sensitive project efficiently and safely. It was determined that the cooling tower rebuild required the following steps:

- Demolition of the exterior structure which was originally built with pressure treated lumber framing and sheet metal, thus exposing the interior concrete structure. (Fig. 36)
- Concrete rehabilitation work including structural concrete repair, crack repair, waterproofing, beam replacement, and protective coatings.
- Installing the new field-erected FRP exterior structure connected to the rehabilitated concrete frame.

Fig. 36 Demolition of the outer structure of the cooling tower to expose the interior concrete structure.

The structure's age, years of constant heavy use, leaking water through joints in the precast concrete hot water basin (Fig. 37) and freeze thaw cycling were the primary sources of the concrete deterioration as evidenced by rust staining, cracking, spalling, concrete delaminations and general wear. The North Dakota environment is rather extreme with a 180 oF variation between its highest and lowest recorded temperatures, the 3rd largest variation of any U.S. State.

Fig. 37 Leaking joints in precast concrete hot water basin led to deterioration throughout the concrete structure.

Project Planning

During autumn 2016, the project team was able to inspect to gather information for pre-planning an efficient shutdown the following May. A visual inspection and sounding survey was conducted to identify defects, estimate quantities, develop a repair strategy, and to create a detailed project schedule. This planning phase was a key to successfully completing the critical path concrete repair work within an allotted 5 weeks' timeframe.

To preserve the structure, the concrete repair scope of work included:

- Epoxy injection to bond and seal cracks
- Remove delaminated and spalled concrete and replace with high performance concrete
- Installation of an alkali-activated embedded galvanic anodes to mitigate patch accelerated corrosion
- Precast concrete joint repair and waterproofing
- Removal and replacement of severely deteriorated precast concrete beams
- Installation of new reinforced concrete pedestals into the cold water basin and trench to support the new FRP structure
- Installation of epoxy coating on the hot water basin's vertical directional fins

Hot Water Basin Repair

The floor of the hot water basin was essentially constructed using upside-down precast double tee beams such that the beam stems (or upright "fins") created a channel for steady water flow and reduced turbulence.

The primary deterioration in the floor was the vertical fins. Deteriorated and freeze-thaw damaged concrete was removed and additional steel, anchors and galvanic anodes were installed to protect the corroding fins. (Fig. 38 to 41) After temporary formwork was installed, the concrete was replaced with a high early strength / high performance concrete consisting of microsilica, fly ash, water reducer, air entrainment and a 0.45 water:cement ratio that was custom designed for the application. High range water reducers were added to achieve the desired slump for workability.

The ready mix repair material placed into a concrete bucket and lifted by crane to the hot water basin where it was wheel barrowed to the fins to complete the form and pour concrete repairs. To protect the fins, a 100% solids hybrid novolac protective coating was applied at an approximate 15 mils dry film thickness. The selected protective coating exhibits excellent water immersion resistance after only 3 days of curing.

Fig. 38 Completed hot water basin floor repairs including concrete repairs and waterproofing Prepared precast fins with galvanic anodes awaiting new high performance concrete.

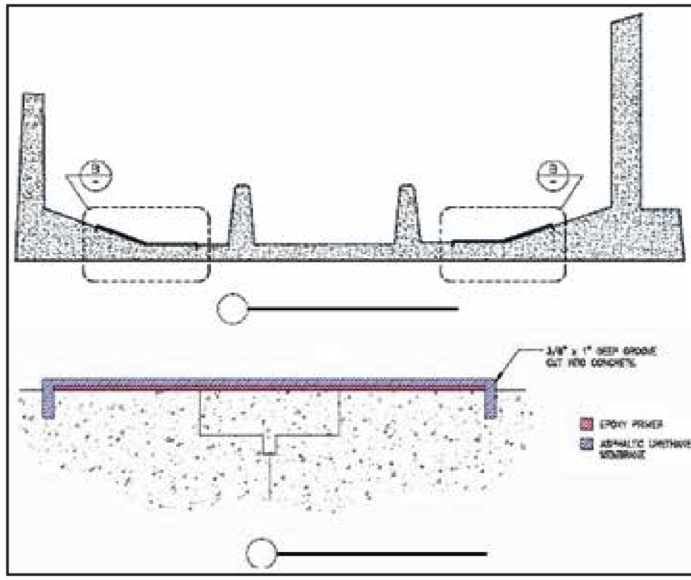

Fig. 39 Concrete fins repaired, prior to protective coating application.

Construction joints between the precast floor and wall sections, a source of unwanted water leakage onto the lower columns and beams, were waterproofed with an elastomeric urethane asphalt membrane system for concrete. First, 3/8" wide by 1" deep grooves parallel to the joints were sawcut about 4" on both sides. After the concrete surface was sandblasted, an epoxy primer was placed. Finally the chemically cured urethane asphalt membrane was placed across the epoxy primer and anchored into the sawcut grooves. The system is designed to remain elastic to temperatures as low as -40°F with very good physical abrasion resistance.

Basin wall cracks were repaired using the epoxy injection process. (Fig. 42) Plastic injection ports and epoxy paste seals were placed over cracks as thin as 4 mils in width and filled under pressure using purpose-built plural component pumps capable of maintaining the proper mix ratio under pressure. The injection port spacing was relatively narrow to promote adequate filling of the fine cracks.

Fig. 40 Prepared precast fins with galvanic anodes awaiting new high performance concrete.

Fig. 41 Concrete fins repaired, prior to protective coating application.

Fig. 42 Epoxy adhesive injected to seal fine cracks in the basin walls

Concrete Column and Beam Repairs

Leaking water from the hot water basin had contributed to the deterioration of the substructure. Deteriorated beam ends and columns were repaired with the same high performance ready mix concrete as used for the precast fin repairs. (Fig. 43 & 44) Preparation of the cast-in-place beam ends followed procedures as outlined in ICRI Technical Guidelines such as 310.1R-2008 – Guideline for the Surface Preparation for the Repair of Deteriorated Concrete from Reinforcing Steel Corrosion. The concrete repairs also include embedded galvanic anodes for enhanced long term durability. For the column repairs, only spalled and delaminated concrete cover was removed to save time and to mitigate the need for structure shoring which would impact the budget and schedule. To improve durability of the column repairs, additional anchors were installed into the repair areas such that the repairs would have both chemical and mechanical bond.

Cold Water Basin

As previously mentioned, Cooling Tower #91 is one of three cooling towers. When repairing the adjacent cooling towers, the precast beams that support the outer wood/sheet metal structure were repaired then strengthened using surface bonded carbon fiber.

Fig. 43 Deteriorated beam end with concrete removed and embedded galvanic anodes installed

Fig. 44 Example of damaged column under the hot water basin, prior to concrete repair.

Fig. 45 Previously repaired beams strengthened with CFRP.

The same strengthening technology was expected to be used on Tower #91. (Fig. 45) However, advanced deterioration was discovered during the fall inspection. Based on this new information, it was decided to completely replace the severely deteriorated precast beam that spanned the outlet flume. Based on the relatively short shutdown schedule, utilizing precast concrete was deemed to be the most effective approach to replace the roughly 24'x4'x1.5' beam. (Fig.46)

Fig. 46 Precast concrete beams were cast in temporary beds inside the contractor's shop.


World's Largest Ethanol Event
Where Producers Meet
& Business Happens
Grow Your
Network
Enhance Your
Knowledge
Producers Receive
FREE Registrations
Register Today
FuelEthanolWorkshop.com
37th ANNUAL
INTERNATIONAL
FEW
FUEL ETHANOL
WORKSHOP® & EXPO
2021
MINNEAPOLIS
July 13-15
Produced By Ethanol Producer Magazine BBI International 866-746-8385 | service@bbiinternational.com | #FEW21 @ethanolmagazine

In preparation of the shutdown, new precast concrete replacement beams were constructed in the contractor's shop months before they were taken to site. The beams were constructed with a high performance ready mix concrete and shop-fabri¬cated stainless steel connection plates were used for added long term durability. The new replacement beam was precast in two sections to facilitate ease of handling. (Fig. 47) The controlled environment of the shop provided excellent curing conditions for the new beams. The existing beam was wire cut, removed and replaced with the new beam.

Fig. 47 Severely deteriorated beam was wire cut, removed and replaced with new freeze-thaw resistant precast beams.

In addition to the beam replacement, major concrete repairs were required at the wall-to-floor joint in the cold water basin. (Fig. 48) The concrete repairs were also completed according to ICRI guidelines with the same high performance ready mix concrete mix.

Another aspect of the repairs in the cold water basin was to fix the deterioration and leakage at the vertical joints between the cold water basin wall to the flume wall, which is the outlet for water passing under the new beam. This joint was completely rebuilt with epoxy anchored dowels and waterproofing was provided with the use of hydrophilic butyl rubber waterstops and elastomeric sealant at the new construction joints.

Fig. 48 Concrete repairs at the wall-to-floor cold joint in the cold water basin.

Finally, in the cold water basin, new reinforced concrete pedestals were installed into the floor to support the new FRP framing. (Fig. 49) \According the design, the round pedestals were to be of various diameters and heights. As part of the project planning process, innovative adjustable formwork was devised using multiple rings of engineered concrete fiber forms to allow the proper pedestal elevation to be efficiently achieved in the field.

Fig. 49 Concrete pedestals installed to support new FRP cooling tower framing.

Summary

Even though very different designs and operations, the Mid-Atlantic and the Coal Creek cooling towers experienced extensive concrete deterioration due to their constant contact with hot steamy water. The repairs in the two projects show that there are many restoration and protection systems that may be employed. The key, as demonstrated with these towers, is to investigate the damage and then select the best rehabilitation method for the situation.

References

ICRI

510.1-2013 - Guide for Electrochemical Techniques to Mitigate the Corrosion of Steel for Reinforced Concrete Structures

310.1R-2008 - Guideline for Surface Preparation for the Repair of Deteriorated Concrete Resulting from Reinforcing Steel Corrosion

320.1R-1996 - Guideline for Selecting Application Methods for the Repair of Concrete Surfaces

320.2R-2018 - Guide for Selecting and Specifying Materials for Repair of Concrete Surfaces

ACI

ACI 562-19 - Code Requirements for Assessment, Repair and Rehabilitation of Existing Concrete Structures

ACI 563-18 - Specifications for Repair of Concrete in Buildings

364.1R-19: Guide for Assessment of Concrete Structures Before Rehabilitation

546R-14 Guide to Concrete Repair

Vibration Monitoring And Instrument Control In Cooling Towers

Frank Fang and Everett Jesse
Metrix Instrument Company

Frank Fang

Abstract:

Cooling towers are an important component for refineries, power generation plants, and many other industrial process facilities. Monitoring the cooling tower condition and conducting proper machinery control provide enormous advantages to production. Great benefits in avoiding downtime losses can be achieved through predictive and preventive maintenance. Vibration is one of the key parameters that is used to provide early warning of machine failure. In this paper, vibration fundamentals are briefly elaborated, and then followed by a discussion of vibration monitoring requirements for cooling tower applications. In the end, an optimal vibration detection solution for cooling towers is explored.

Vibration Fundamentals

Vibration is defined as "Periodic Motion" due to disturbed equilibrium. Vibration can be characterized by:

1. Frequency: Number of oscillations in a period of time
1. Amplitude: Severity, how big is the vibration
1. Phase Angle: When and where the vibration is happening

The following graph illustrates an unbalanced motor shaft at running speed, 1,200 revolutions per minute (rpm), with vibration at 1,200 cycles per minute (cpm) or 20 cycles per second (Hertz, Hz).

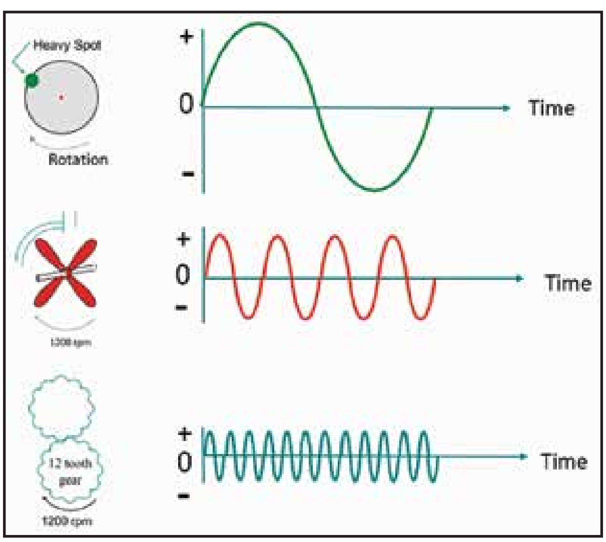

We call the vibration coincident with running speed 1X. The 4-blade fan driven by the motor vibrates at 4,800 (4x1,200) cpm or 80Hz or 4X, and the 12-tooth gear mesh driven by the same motor vibrates at 14,400 (12x1,200) cpm or 240Hz or 12X. These three frequencies are the characteristic vibration frequencies in the system.

When we discuss vibration, we talk in terms of orders of running speed (e.g. 1X, 2X, 1/2X, nX, etc.), cycles per second (cps) or Hertz (Hz). Revolutions per minute (rpm) only pertains to the running speed of the machine.

If an accelerometer is used to measure vibration, especially when mounted on gear box, the overall output from the accelerometer is a mixed signal with the vibration frequencies superimposed.

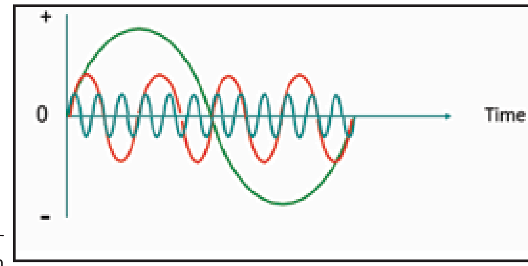

The typical time-based waveform looks like the following. From the mixed signal it is very difficult to extract the essence of vibration in the system.

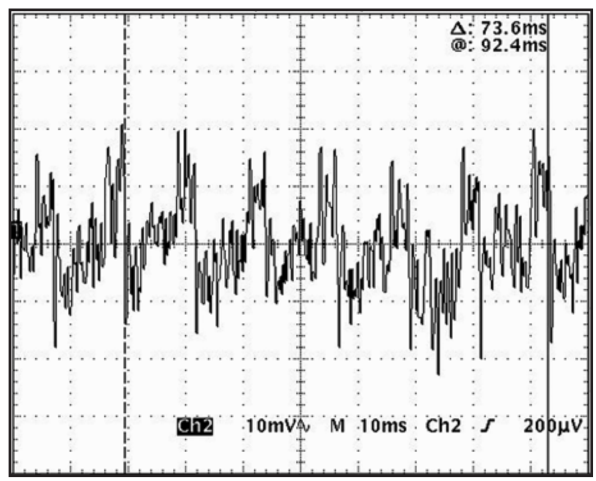

In order to truly understand what is going on when a rotating machine is vibrating, it is necessary to retrieve the raw vibration signal from the vibration sensor and then use an advanced algorithm such as an FFT (Fast Fourier Transform) to transfer the time-based waveform into the frequency domain. As a result, the elements of the vibration turn into discrete values and then the nature of the vibration could can be investigated in a comprehensible manner.

Vibration Sources in Cooling Towers

A motor is used to drive a fan to force air to pass through the cooling tower. Based on the driving mechanism, two types of fans are commonly used: gearbox driven fans and belt driven fans. With a gearbox driven fan, the motor is mounted to the side of the fan's cell and the fan is driven by the motor by the shaft. In the belt driven case, the motor drives the fan by a belt. Gearbox driven fans are normally used in larger towers, and belt driven fans are often used in smaller towers. These two types of fans are illustrated below.

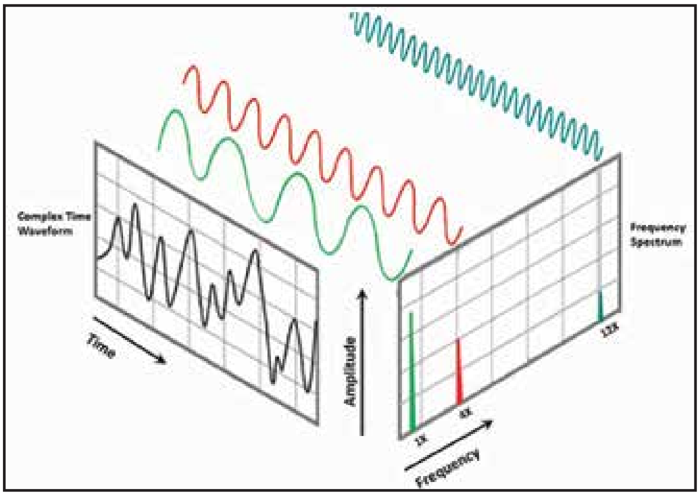

Gearbox Driven Fan

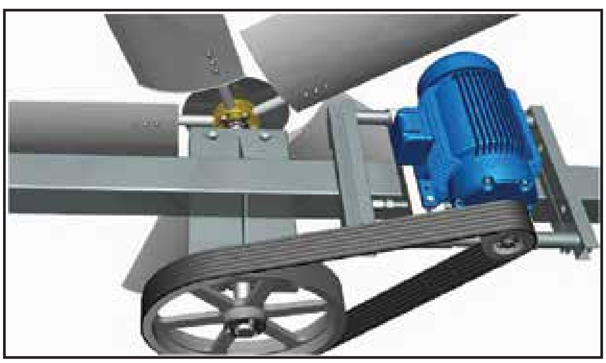

Belt Driven Fan

Causes of Failure in Cooling Towers

Excessive vibration, mostly due to misalignment or unbalance, can cause rapid deterioration and result in catastrophic failure. The fan, motor, and gears are the three major rotating components in a cooling tower. They are also the source of vibrations in the system. 1 The failures of a motor can be caused by motor imbalance, shaft misalignment, rotor bar defects, bearing defects and foundation issues. The gearbox may fail due to the stress it experiences from the airflow, misalignment of the gear with the motor, cracked gears, lack of lubrication, and worn bearings. Unbalanced fan blades or errors in blade pitch are some of the reasons causing fan blade failure.

Vibration Control and Monitoring in Cooling towers

To prevent disastrous failure due to vibration in a cooling tower, a vibration sensor is typically employed to measure machine vibration severity. The output of vibration device is used to trigger system alarms and shutdown signals when a preset vibration threshold is exceeded. Either the 4-20 mA output from a vibration transmitter to a Control System, Programmable Logic Controller (PLC) or SCADA (Supervisory Control and Data Acquisition) System, and or an open/close relay from a vibration switch are commonly used in a cooling tower to achieve the safety goals of the organization.

To maintain the cooling tower in a good operating condition, vibration monitoring is often used to provide vital early warning of problems and enable scheduled service prior to any substantial damage. Raw dynamic vibration data is retrieved locally or remotely into a signal acquisition system. Further data analytics will be performed to comprehend the meaning of vibration data. When necessary, advanced diagnostic techniques could be used to probe the root cause of problems.

Vibration condition-based machinery monitoring is critical to cooling tower operation. Vibration monitoring brings another level of benefit by not only helping to keep the mechanical system healthy, but by maintaining or increasing production profit through an effective maintenance and service strategy.

Vibration Device Requirements in Cooling Towers

From application experiences, the authors recommend installing at least one vibration sensor on the gearbox and/or fan bearing. The sensor installation positions are illustrated in below graphs:

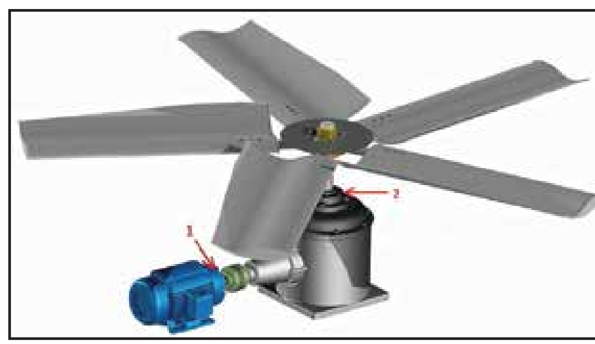

Gearbox Driven Fan

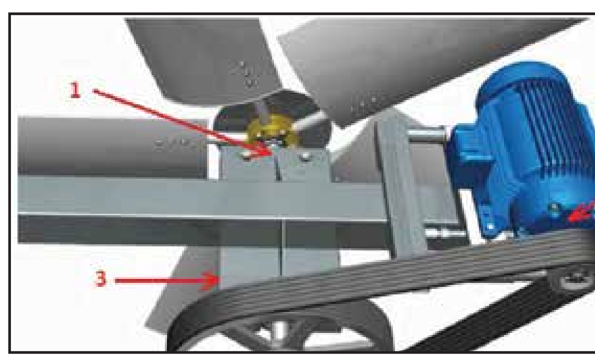

Belt Driven Fan

On gearbox driven fans, it is preferred to collect vibration data from both the motor and the gearbox. On a belt driven fan, the locations to collect vibration data are on the fan inboard pillow block bearing, on the motor inboard bearing and intermediary bearings on the fan shaft.

Cooling towers are usually operating in harsh environments. The rigorous condition demands highly reliable vibration devices to ensure their vital functional performance. A robust design and assembly are also needed to guarantee superior accuracy and high quality of the vibration signal output. In addition to 4-20mA output, switch for automatic alarm and shutdown, and raw signal for monitoring, the vibration device is required to incorporate many other features suitable in a cooling tower environment:

- Water resistance
- Corrosion resistance
- Wide frequency range
- Extended temperature range
- Hazardous area approvals
- Field adjustable or configurable vibration thresholds

Machine Protection Solutions in Cooling Towers

There are two basic machine protection implementations: centralized and distributed applications.2 A centralized system is used in plants with a more traditional setup where data from all sensors is sent to a central, rack-based system where instrument monitoring and control are integrated. A distributed setup is suitable for smaller or less critical equipment, remote locations or for plants with a distributed structure. The great advantages of distributed systems are the simplicity of the systems, the lower costs, and the reduction of infrastructural requirements. Cooling Tower Systems are one of the best applications where distributed monitoring fits the best. The switching function of a vibration device is an ideal solution for stand-alone machinery protection. When the raw data is retrieved and processed either locally or remotely by a vibration monitoring system, the hybrid system has advantages to replace rack based centralized systems, with significant cost reduction, without compromising features.

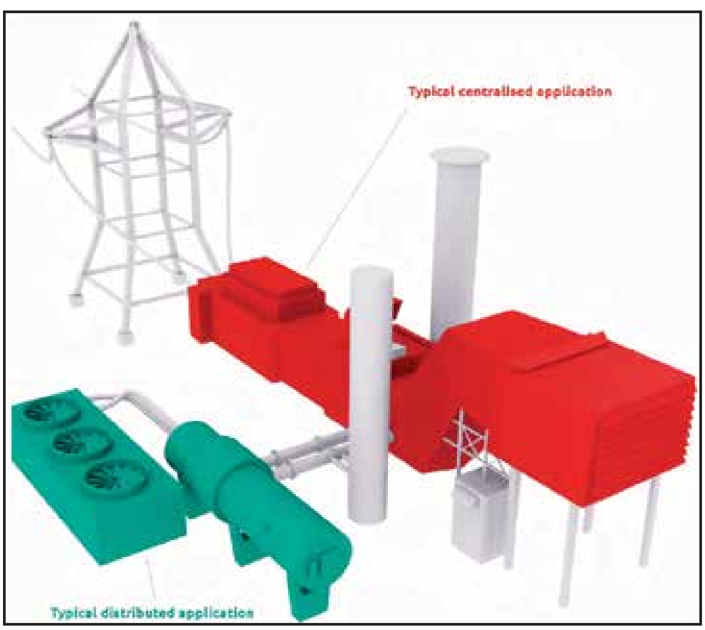

Instances of Centralized and Distributed Applications

Compact Configurable Vibration Switch

In cooling tower applications, it is desirable to have one compact vibration device incorporating all demanding functions and features into one package. The availability of many other options makes the product even more versatile, effective, and attractive to cooling tower users.

1. 4-20 mA output, for trending and early warning
2. Dual channel switches, for alarm and shutdown
3. Raw vibration signal output, for signal analysis
4. Software configurability for switch
   - Startup delay
   - Independent channel trigger level and delay
   - Latching and non-latching switch operation
   - English and metric unit selection
5. 316 stainless steel housing material, for durability.
6. Factory order versatility:
   - Full scale range
   - Housing stud size
   - Low and high pass filter
   - Hazardous area certification
   - Connection type
     - MIL style connector with mate cable
     - Flying leads with integrated cable
     - Combo of switch with elbow for explosion proof

Conclusion:

Vibration is a phenomenon common to any rotating machinery. Measuring the vibration is a best practice for a machine protection in many industries. A compact vibration switch integrated with a 4-20 mA transmitter and dynamic data capability provides a flexible and economic solution to suit a wide variety of applications in the cooling tower industry. The vast feature versatility and intuitive field configurability help different cooling tower users to meet their unique requirements over an extensive range.

References:

1. John McConville, Bristol-Myers Squibb and Tom LaRocque. "Simple, Low-cost Vibration Monitoring of Cooling Towers at Bristol-Myers Squibb." Connection Technology Center, Inc., Aug. 1999. Retrieved from https://www.ctconline.com/university/4_casestudies/4-01.pdf on August 8, 2019.
2. ISTEC, The protection of rotating machinery using vibration measurements. Retrieved from https://www.istec.com/en/machine-protection-solutions-and-systems/ on June 17, 2019.

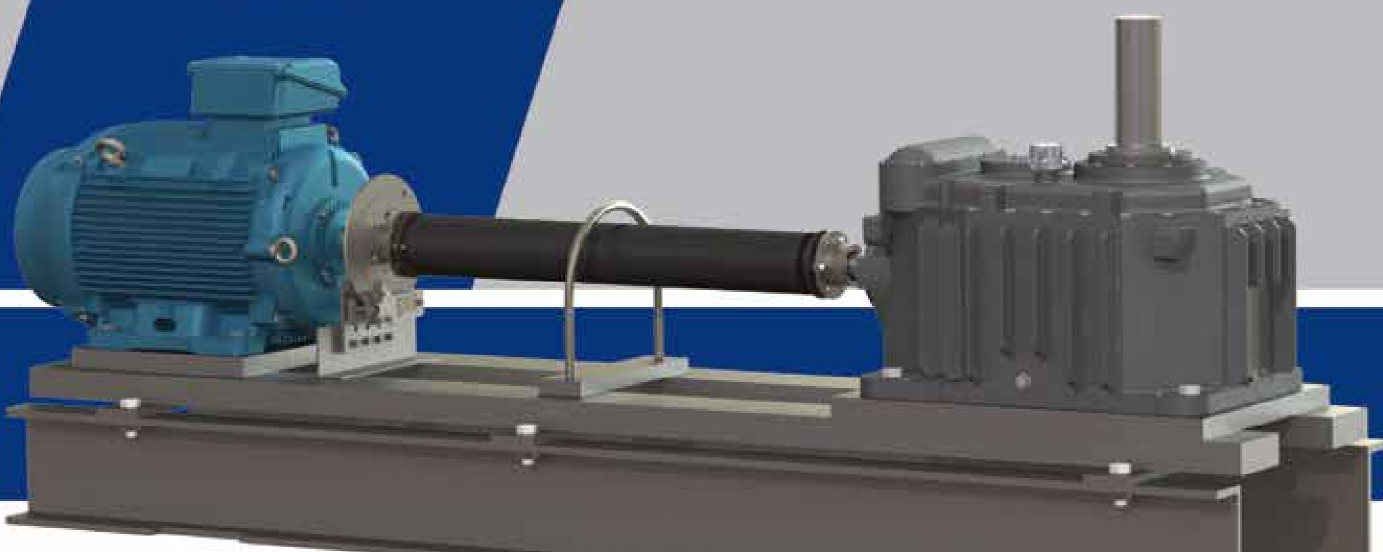

Survey of Laboratory and Field Test Methods for *Legionella*

Loraine Huchler, P.E., CMC®, FIMC
MarTech Systems, Inc.

Loraine Huchler

Abstract

The Centers for Disease Control (CDC) requires a spread-plate culture legionella test during investigations of a known or suspected outbreak of Legionellosis. While owners of cooling towers are concerned about managing their legal liability, they also must manage their operating risks. The culture method is a poor fit for routine assessment of operating risk of *Legionella* in cooling water systems because operators cannot make timely decisions about corrective actions.

Field test methods can provide valuable information about the *Legionella* population and allow the cooling system owner to promptly assess the operating risk and implement corrective actions – reducing the risks to public health.

This paper discusses the selection criteria for field test methods *Legionella pneumophila* (sensitivity, specificity, time, and legal defensibility (accreditation)) and reviews the commercially-available field test methods and test kits, including the technology, the accuracy of the test results, and the proper interpretation of test results.

Introduction

With the publication of ASHRAE SPC-188 and the passage of legislation in New York City and New York State for registration of all cooling towers with routine monitoring and reporting of *Legionella* bacteria populations in the cooling water, the issue of *Legionella* test methods has become more relevant for water treatment professionals and owners of cooling towers.

The Centers for Disease Control (CDC) and most legislation requires the use of the standard culture test that assesses the viability of the *Legionella pneumophila* bacteria – the ability of the bacteria to not just survive, but to reproduce. From a medical diagnostic perspective, a culture makes sense to confirm an infection in a patient. The lengthy incubation period (7 – 14 days) makes this test method wholly inappropriate to identify risks in cooling water systems or validation (proof that the corrective actions have controlled the hazard (presence of > 10 CFU/ml population of *Legionella pneumophila* bacteria in cooling water)).

In addition, the presence of competing HPC[1] bacteria often requires special heat or acid treatment to improve the readability of the cultures; the trade-off is an unknown mortality of *Legionella pneumophila* bacteria that increases the uncertainty of the culture results.

For the owner of a cooling tower, this lengthy delay and potential bias of the results creates a "Catch-22:" should the owner proactively disinfect the cooling water system or delay any corrective actions until the receipt of the test results, risking additional infections should the cooling tower be a source of legionella-infected drift?

There are numerous other laboratory and field test methods that provide faster results, allowing more effective management of the risk of Legionellosis infections from a cooling tower and, in turn, reduce the legal and reputation risks that occur following a confirmed or suspected infection from your cooling tower.

Discussion

Monitoring for *Legionella* bacteria starts with defining the objectives for monitoring.

As defined in the ASHRAE SPC-188-2018, "Legionellosis Risk Management for Building Water Systems," managing the risks of Legionellosis infections from your cooling tower does not automatically require testing for *Legionella pneumophila* bacteria in the cooling water. The standard describes a methodical analysis of the risks for each water system, including the cooling tower.

Legionellosis infections require three conditions:

1. Aerosols (water droplets) infected with *Legionella pneumophila* bacteria…
2. …that are present in an airspace…
3. …and breathed into the lungs of a vulnerable person.

If any one of these three conditions are not met, then the risk of a Legionellosis infection dramatically decreases. For example:

Control the hazard.

Many experts subscribe to the concept of "control the hazard" by minimizing the presence of *legionella* bacteria in the cooling water and/or minimizing the generation of water droplets – drift – that leave the cooling tower with the plume of water vapor. This approach will reduce, but not eliminate the risk of infected water droplets.

Define the drift zone.

Minimizing or preventing the drift from being present in an airspace where people are present is difficult, but not impossible. Cooling towers in "good condition" located far from parking lots or areas where people congregate or in a place where the prevailing winds direct the drift away from these populated areas have a low risk. In contrast, cooling towers located in close proximity to pedestrians and/or that have damaged drift eliminators or other structural or operating problems that create high concentrations of drift have a higher risk.

Identify at-risk individuals in the drift zone.

Identifying the presence of vulnerable persons in the drift zone is a nearly-impossible task due to the confidentiality of personal medical information and the complexity of accuracy assessing exposure to *Legionella pneumophila*-contaminated aerosols in the drift zone.

The less knowledge or control you have over preventing infected water droplets from leaving the cooling tower, defining the drift zone and identifying the presence of at-risk individuals in the drift zone, the greater the risk of an infection. As the risk of infection increases, the more likely that the monitoring program will include routine testing for *Legionella pneumophila* bacteria.

Monitoring For *Legionella* Bacteria Includes Monitoring Sessile Bacteria.

There is no correlation between the population of sessile and/or planktonic HPC bacteria and *Legionella pneumophila* bacteria; however, the presence of sessile anaerobic bacteria ("slime") is as an indication that the environmental conditions may be conducive to the proliferation of *legionella* bacteria because the *legionella* bacteria require a symbiotic relationship with a host organism such as an amoeba or protozoa to reproduce.

Monitoring for *legionella* bacteria includes identifying the optimal samples and sample locations.

Selecting the optimal sample type and location depends on the objective of the *legionella* testing. For example, if the objective is to confirm the source of a Legionellosis outbreak, then the CDC recommends spread plate culture tests for a set of bulk water and biofilm swab samples[2] from the cooling tower (Figure 1).

COOLING TOWERS[1]

Site	Approximate number of samples	Type of samples	Sample processing[1]
Make-up water (water added to replace water loss because of evaporation, drift, or leakage)	1	1L bulk water	Direct
Collection basin (an area below the tower where cooled water is collected and directed to the sump)	2	1L bulk water and a biofilm swab at the water line	Direct
Sump (a depressed chamber contiguous to the basin, where water flows to facilitate pump suction; may also be used as collection point for silt and sludge)	2	1L bulk water and a biofilm swab at the water line	Direct
Storage tank or reservoir in the system	1	1L bulk water	Direct
Drift eliminators or other surfaces that remain moist	1	1 biofilm swab	Direct
Heat sources (e.g., chillers)	1	1L bulk water	Direct

Figure 1 – CDC Sampling Procedure and Potential Sampling Sites – Cooling Towers2

If the objective of testing is to confirm the efficacy of the biocide treatment program in a cooling water system, then faster field test methods that measure both viable-and-culturable and viable-but-not-culturable *legionella* bacteria would be appropriate.

A robust assessment of the risks includes samples of both bulk water and sessile bacteria ("slime"). Ideally, the bulk water sample should be representative of the water droplets that may leave the cooling tower with the plume – the "hot" water returning to the cooling tower, flowing into a distribution header or onto the top deck of the cooling tower. Locations for collecting samples of sessile bacteria are more challenging. In a crossflow cooling tower, it might be possible, albeit difficult, to obtain a sample of sessile bacteria in the sediment that accumulates on the hot deck; in a counterflow cooling tower, it's impossible to obtain a sample of sessile bacteria from the interior surface of the distribution header.

On-line monitoring of sessile bacteria. A mesh coupon (Figure 2) is an excellent way to monitor sessile bacteria.

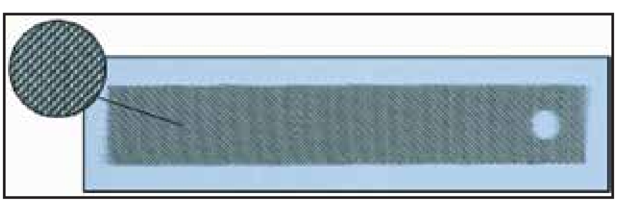

Figure 2 – Bio-Mesh Coupon for Anaerobic Bacteria Measurements[3]

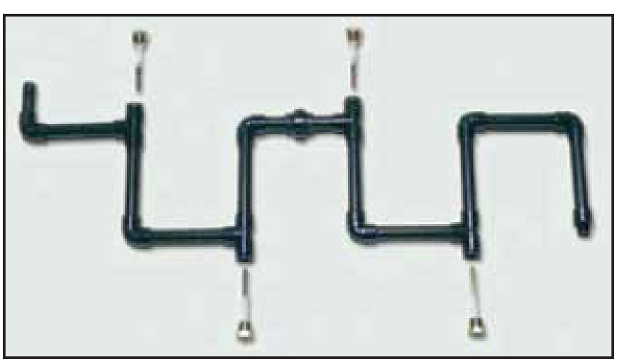

.Figure 3 – Bypass Rack and Corrosion Coupons

A more sophisticated method to measure biofilm is Bio-GeorgeTM, a monitoring system that allows real-time monitoring of the presence of sessile bacteria and the effectiveness of the biocide chemistry and treatment protocol. The system consists of a probe, integrated electronics and display software. (Figure 4) The probe is installed into a piping system, heat exchanger water box, cooling tower, or side stream via a 2-inch threaded connection. Special probes can also be built for "hot tap" type fittings or flow-through probes.

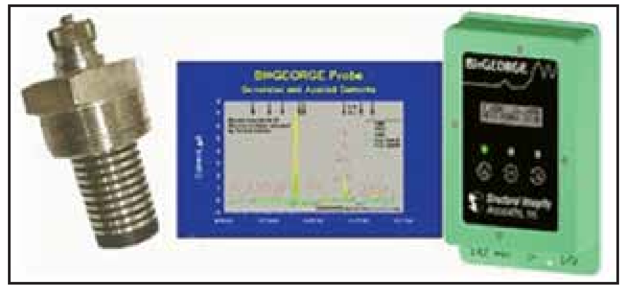

Figure 4 – BioGeorge™ System

Monitoring for *Legionella pneumophila* requires determining the optimal laboratory and/or field test methods.

The specific objective for measuring *Legionella pneumophil*a in cooling water will determine the optimal laboratory and/or field test methods.

Selection Criteria for Laboratory and Field Tests

Table 1 lists the selection criteria for various technologies for laboratory and field testing of *legionella* bacteria.

Test	Technology	Sensitivity	Specificity	Time	Legal Defensibility
Culture Test - Traditional Spread Plate	Laboratory - Culture	10 CFU/ml	Addition analysis for serogroups	7 days – preliminary 14 days - final	Very high, definitive test per CDC
Culture Test - IDEXX Legiolert	Laboratory - Bacterial Enzyme	10 CFU/ml	No differentiation of serogroups	7 days	CDC validation in progress
Quantitative polymerase chain reaction (qPCR)	Laboratory or Field - Analysis of DNA	8 CFU/ml (MPN[5])	LpSG1[6]	<1 hour	CDC validation in progress
Immuno-magnetic Method (IMM)	Field - Tagged Antibodies	100 CFU/ml	LpSG1	25 minutes	Low due to poor sensitivity
Biophotonic Light Sensor	Field - Surface Plasmon Resonance (SPR)	*No information available; technology under development.*			

Table 1 – Selection Criteria for Laboratory and Field Tests for *Legionella pneumophila* Bacteria

Culture Test - Traditional Spread Plate (ISO11731:1998, CDC)

The traditional spread plate measures the population of live *Legionella pneumophila* bacteria and is the definitive method to measure the ability of the bacteria to not just survive, but to reproduce. With additional analyses, technicians can determine the populations of different le*gionella* species and serogroups. The primary challenge of this method is that *Legionella pneumophila* bacteria are very slow growing, requiring 14 days for final results. In addition, the test does not measure "viable but non-culture-able" *Legionella pneumophila* bacteria – i. e. *legionella* bacteria that simply do not "like" the agar media. The lower sensitivity of the spread plate test is about 10 CFU/mL of *legionella*; lower numerical values are not reliable.

Filtering the sample to concentrate the bacteria can improve the sensitivity of the test. The sample is then spread onto a nutrient-rich plate (Buffered Charcoal Yeast Extract [BCYE] agar) and incubated in optimal conditions for several days to promote growth.

During this incubation period, *Legionella* and other bacteria may flourish, resulting in a very high concentration of *Legionella pneu-*

mophila on a spread plate that may have little or no resemblance to the concentration of *Legionella* pneumophila in the original water sample. These results support medical diagnostics but is not predictive for assessing these risks in a cooling water environment.

The test method allows laboratory technicians to use an acid or heat treatment to be able to "read" the results – a process that can destroy some of the *legionella* bacteria in addition to the HPC bacteria. Consequently, the information provided by spread plate cultures are not sufficient to support efforts to control the hazard in cooling towers.

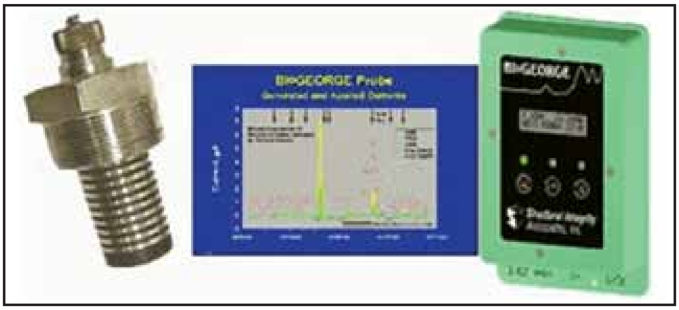

Figure 4 – Legiolert Test Results[7]

Culture Test-IDEXX Legiolert (ISO 13843:2017)

Legiolert is a modified culture test that uses a bacterial enzyme detection technology to provides the concentration of viable cells as Most Probable Number (MPN) instead of colony-forming units (CFU). The test uses a proprietary reagent that contains nutrients as well as a substrate metabolized by *Legionella pneumophila* that produces turbidity and/or a brown color.

Results of a recent study published in AWT's trade journal show that this technology detects *Legionella pneumophila* with equal or greater accuracy than traditional spread plate culture methods in water samples from cooling towers.[8] The CDC does recognize the Legiolert as an alternative to the traditional spread plate method for situations other than investigations of a known or suspected outbreak of Legionellosis. For non-potable waters, the sensitivity limit in the Legiolert test is 10 CFU/mL of *legionella*; this technology does not provide any information about serogroups.

Quantitative polymerase chain reaction (qPCR) (ISO/TS 12869:2012)

This is a rapid molecular test method that can detect and quantitate *Legionella* pneumophila and serogroup 1 in water samples by identifying an amplified gene sequence using a fluorescent signal. Results are semi-quantitative based on comparison to a standard curve of fluorescence of a known quantity of DNA of the target gene. Instead of colony-forming units, the results may be reported in Modified Fishman Units to account for bacteria that are viable but non-culturable.

Bacteria populations from the standard qPCR results are typically higher than culture because the standard assay cannot discriminate between of live and dead or impaired Legionella pneumophila and the test may detect *Legionella pneumophila* bacteria that are not culturable (NVBC). By using proprietary sample preparation procedures, the Viability-qPCR assay can differentiate between live and dead cells, providing a test result for live *Legionella pneumophila* but cannot measure non-culturable bacteria.

qPCR methods traditionally required a full-service microbiology laboratory. Two examples of portable qPCR devices suitable for use in a "field-laboratory" are iQ-Check® Legionella Real-Time PCR Kits from Bio-Rad[9] and Spartan Cube from Spartan Bioscience[10]. The iQ-Check provides results in four (4) hours; the Spartan Cube provides results in under an hour.

Results of a recent study[11] published the Journal of Water & Health showed a concordance between the results from the on-site qPCR using the Spartan Cube and laboratory culture methods but showed poor correlation between the laboratory and on-site qPCR tests. The risks of compromising the water sample during shipping is real; on-site testing at a cooling tower with the Spartan unit showed high concentrations of *Legionella* pneumophila in a cooling tower that had "passed" the laboratory culture test.[12]

Lateral Flow Immunochromatographic Assay (LFICA).

Immunochromatographic assay uses the same technology as home pregnancy tests. Water samples must be filtered prior to testing. Antibodies of *Legionella* pneumophila serogroup 1 tagged with red nanoparticles, bind to any bacteria in the sample and make them visible as a thin line on the device. Hydrosense[13] provides a test result after a 25-minute reaction period. The sensitivity of this test is 100 CFU/ml of *legionella* bacteria for water samples (standard kit) and 200 CFU/ml for sessile bacteria samples (swab kit). The test has limited value to assess the risks of efficacy of the corrective actions because the test is not sufficiently sensitive.

Biophotonic Light Sensor.

A consortium of European researchers funded by investors is developing POSEIDON,[14] a plasmonic-based automated lab-on-chip sensor for the rapid in-situ detection of *Legionella* that uses biophotonic technology to detect *Legionella* bacteria in less than an hour. Tiny sensors allow the device to use the photonics technique of Surface Plasmon Resonance (SPR) to read information from a refracted laser beam, providing a fast, highly sensitive and inexpensive detection from a small sample without the need for 'labelling' - binding the bacterium to a protein to permit detection. This device matches the refracted energy to the electronic signature of a pre-programmed pathogen such as *Legionella pneumophila* bacterium, providing an unambiguous detection of the bacteria in situ.

References

1. HPC = Heterotrophic Plate Count
2. https://www.cdc.gov/legionella/downloads/cdc-sampling-procedure.pdf
3. http://www.alspi.com/
4. Dresty, John E., Puckorius, Paul, "Testing Cooling Tower Water for Total Bacteria and Legionella," https://www.process-cooling.com/articles/89404-testing-cooling-tower-water-for-total-bacteria-and-legionella
5. Most Probable Number
6. Legionella pneumophila serogroup 1
7. https://www.idexx.com/water/legiolert-info.html
8. The Analyst: The Voice of the Water Treatment Industry: Association of Water Technologies, Spring 2019, https://123.index.idexx.com/resource-library/water/water-reg-article17N.pdf
9. https://www.bio-rad.com/en-us/product/iq-check-legionella-real-time-pcr-kits?ID=LS5I7MLPT
10. https://environmental.spartanbio.com/
11. journal of Water & Health, Volume 17, Issue 2, 1 April 2019, https://iwaponline.com/jwh/article-lookup/doi/10.2166/wh.2019.252
12. https://environmental.spartanbio.com/docs/norkem-case-study.pdf
13. Hydrosense
14. https://www.filtsep.com/water-and-wastewater/news/new-light-sensor-quickly-spots-deadly-bacteria/

38 Ft Test Rig: A Step Forward In Fans Knowledge

Nicola Romano, Cofimco

INTRODUCTION

Scope of this paper is to share the main features of the 38 ft test rig erected in summer 2018 at Cofimco's facility in Italy, figures 1.1 and 1.2, and the results of some of the measurements taken during the first year of activity.

This paper will mainly focus on:

- Stress measurements on blades.
- Performance measurements of fans.

Nicola Romano

Fig. 1.1: Rig aerial views

Abbreviations And Symbols

Abbreviations:

AoA – Angle of Attack
DG – Diesel Generator
DP – Dynamic Pressure
FR - Flow Rate
FRP - Fiber Reinforced Plastics
MS - Monitoring System
SP - Static Pressure
VFD - Variable Frequency Drive

SYMBOLS

Vy - Axial component of the flow
,ρ - Air density
,σ - Blade stress

Fig. 1.2: Rig south view

TEST RIG MAIN FEATURES

The rig is an induced cell equipped with louvers for the variation of the Static Pressure (SP) vs Flow Rate (FR) curve and a VFD for the fan speed setting. The structure is made of FRP beams and side panels.

The main dimensions of the 38 ft test rig are listed in table 2.1, see figures 2.1 & 2.2:

	SI	Imperial
Base	16 x 16 m	≈ 52' 6"
Fan stack	11.662 m	≈ 38' 3"
Stack height	2.44 m	8'
Louvers windows size	15.5 x 3 m	≈ 51' x 10'
Louvers windows count	2	
Total louvers area	93 m^2	≈ 1020 sqr ft

Tab. 2.1: Rig dimensions

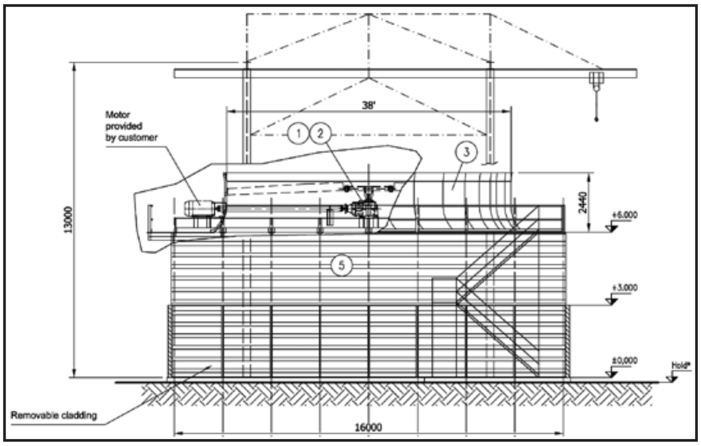

Fig. 2.1A: Rig dimensions – Side view (dimensions in mm)

Motor model	M2BA 355 SMA 4	
Voltage	400	V
Frequency	50	Hz
Power	250	KW
	335	Hp
Poles	4	
Nominal speed	1488	RPM
Max mechanical speed	1800	RPM
Current	445	A
Torque	1604	Nm
	1183	lb-ft
Tmax / Tn	2.6	
Power factor	0.85	
Efficiency	95.1	%

Tab. 2.2: ABB Electric Motor features

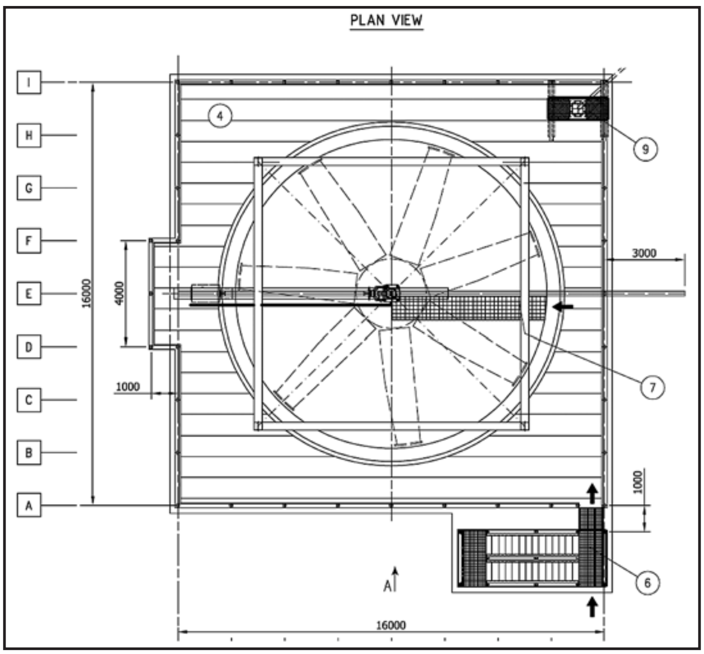

Fig. 2.1B: Rig dimensions – Top view (dimensions in mm)

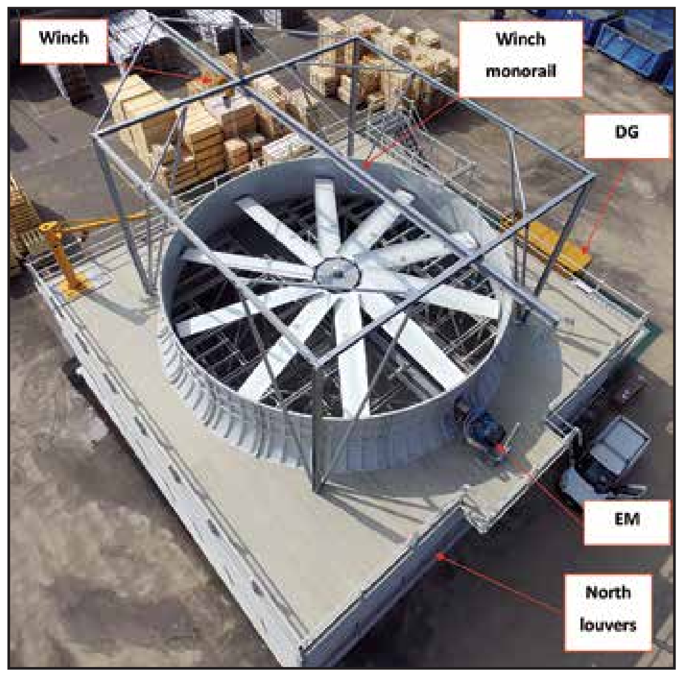

Fig. 2.2: Rig layout

The rig is equipped with an ABB Electric Motor (EM) model M2BA/BAX 355SMA 4, see fig. 2.3 and tab. 2.2. The motor is driven by an ABB VFD model ACS880, able to run the motor above 1800 RPM.

The EM torque is transferred to the fan through a Carbon Shaft (CS) and a Hansen Gearbox (GB), see fig. 2.4, with speed ratio 1:17.425. Therefore, the VFD system is able to run the fan from 30 RPM up to 103 RPM (62.4 m/s, 12296 ft/min) according to the torque curve shown in the fig. 2.5 with a peak power of 225 KW (≈ 320 Hp).

Fig. 2.3: ABB Electric Motor (EM) and Carbon Shaft (CS)

Fig. 2.4: Hansen Gearbox (GB)

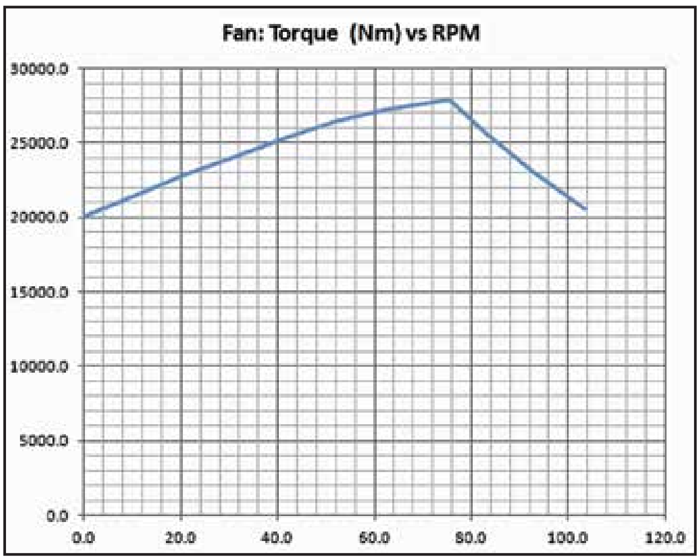

Fig. 2.5: Driving system torque curve

The power supply is autonomous by means of a Caterpillar Diesel Generator (DG) DE500E0, 450 KVA driven by a P-C15-DE500 diesel engine, see fig. 2.6.

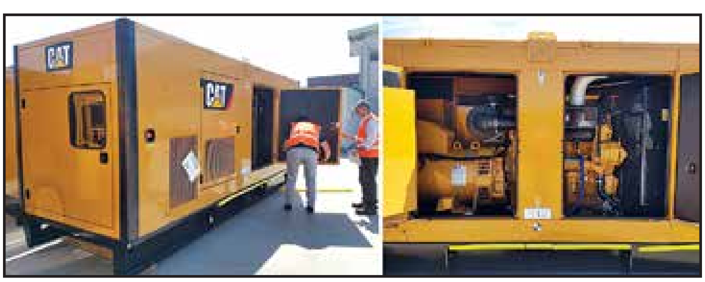

Fig. 2.6:Diesel Generator

Finally, on two opposite sides, the rig is equipped with two windows 15.5x3 m (≈51' x 10')[1] , each one fitted with 4 independent sets of electrically driven louvers, see fig. 2.7. Custom made hardware and software (Control Panel – CP) allow the operator to set the louvers opening percentage as well as the fan speed from the control room, fig. 2.8.

1. Total area 93 m^2, ≈ 1020 sqr ft

Fig. 2.7: Closed louvers (left) and open louvers (right)

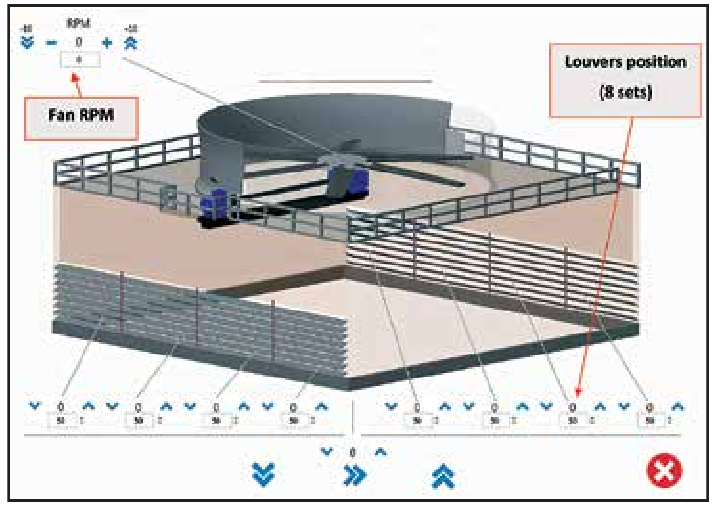

Fig. 2.8: Screen shot of the Louvers and fan speed Control Panel (CP)

Further features are, see fig. 2.9:

- Walkway settable as single-leg or two-leg to investigate the influence of an ACC-like bridge (two-leg) or CT-like bridge (single-leg)
- Walkway grid density settable as std FRP grid or fully-closed metal sheet.

Fig. 2.9: Walkway configurations – from grid single-leg to metal sheet double-leg.

A steel-structure monorail is also erected to support a winch in order to ease the installation and removal of hubs and blades. The said winch is shown in the previous figures 1.2, 2.1 and 2.2.

aggreko

Available now

The latest in cooling tower innovation

Modular design and interconnection for infinite expandability

Equipped with remote monitoring capabilities for:

- Increased efficiency
- Decreased downtime
- Real time temperature, water flow, and electrical status display

GT-40

900-4000 GPM

GT-20

400-1600 GPM

Aggreko's new GT Series Cooling Towers combine the modularity of our cooling towers with the portability of an Intermodule freight container

40%
freight cost reduction with ISO container

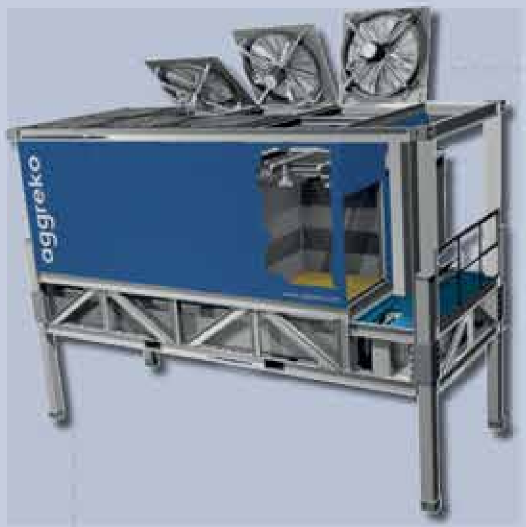

Direct drive, variable speed, high-efficiency fan motors provide precise temperature control and significant energy savings.

Telescoping substructure provides safe and easy extension during installation.

External sump provides easy access to two sets of dual sump screens and the make-up water float valve.

Service platform serves as a continuous walkway between towers and provides easy and safe access to controls and sump screens.

Measuring And Recording System

A dedicated tailor-made Monitoring System (MS) is installed for the monitoring and recording of the following parameters (see fig. 3.1):

a. Wind speed and direction
b. Blade stress (3 blades simultaneously)
c. 3-direction vibration amplitude
d. Plenum Static Pressure (SP)
e. Flow Rate (FR)
f. Shaft torque
g. Fan speed

Thanks to the MS software, the main parameters like SP and FR fluctuations, vibration and blade stress peaks can be related to each other and to wind intensity, direction and gusts, allowing the analysis of correlations among them.

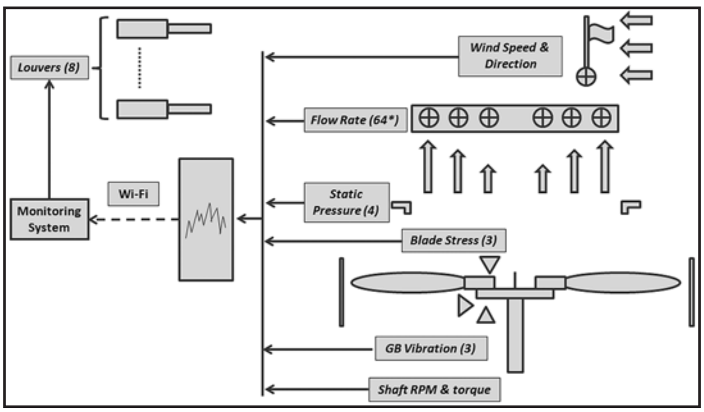

Fig. 3.1: Monitoring System block diagram

(*) Flow rate probes: presently 4x16= 64 measuring points

The MS allows the setting and the calibration of the parameters used for the measurement and visualizes the monitored parameters, see fig. 3.2.

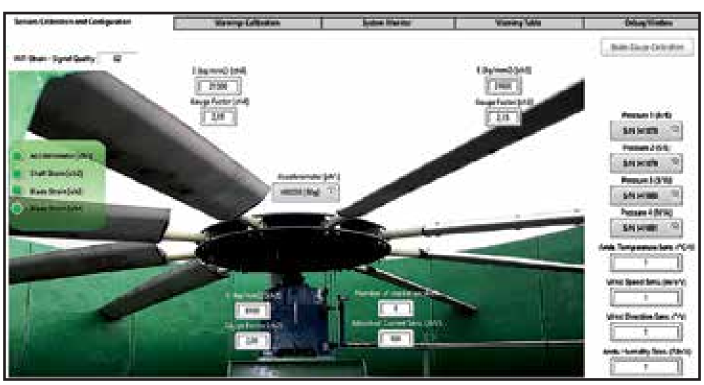

Fig. 3.2: Screen shot of the MS parameters setting and calibration page

The MS visualizes and records the measured parameters, see fig. 3.3.

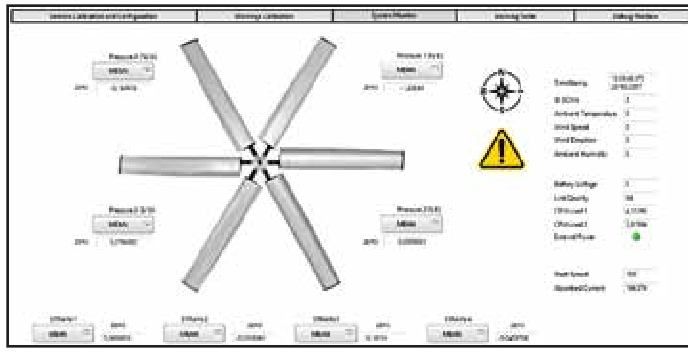

Fig. 3.3: Screen shot of the MS measurements page

Finally, the MS allows the setting of alarm thresholds on the main parameters in order to highlight peaks of stress, vibrations, pressures, etc., see fig. 3.4.

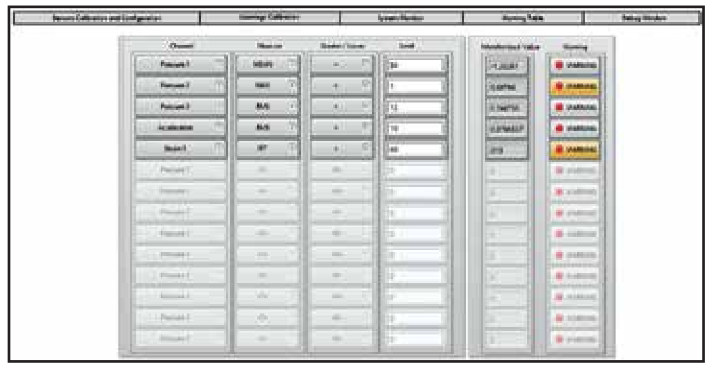

Fig. 3.4: Screen shot of the MS thresholds setting page

The shaft power is calculated and recorded as well by means of the shaft torque and fan speed and double checked from the VFD cabinet. In the same manner, the electric consumption and the fan speed are monitored as well for a double check.

Stress Measurements

Thanks to the described MS, some investigations were carried out in order to check the influence of several parameters like:

- Bridge configuration (single leg/double leg; grid density)
- Flow asymmetry (wind, occlusions, fans operating around, etc.)

In order to measure the impact of the above elements, several stress measurements were taken on a few fans with three different bridge configurations (single-leg with grid, double-leg with grid, double-leg with metal sheet) and with three different louvers configurations (both sides 100% open, one side 100% open and the opposite side completely shut, both sides completely shut).

The measured stress are summarized in the fig. 4.1. The top part of the graph shows the static component of the stress (average - blue); the bottom part of the graph shows the dynamic value of the stress (alternate - red).

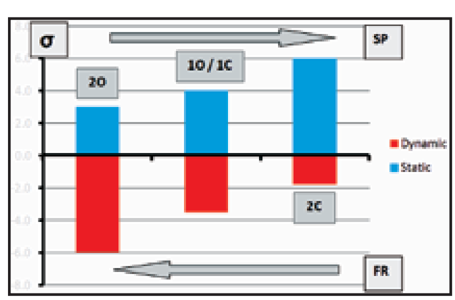

Legenda:

- **2O** – louvers 100% open on both sides.
- **1C/1C** – louvers on one side 100% open and 100% closed on the opposite side.
- **2C** – louvers 100% closed on both sides.

SP: Static Pressure

FR: Flow Rate

Fig. 4.1: Stress at different louvers settings.

The graphs in fig. 4.1 lead to some interesting considerations:

- the static (average) stress increases toward higher SP and lower FR;
- the dynamic (alternate) stress increases toward higher FR and lower SP;
- the asymmetry of the flow pattern increases the dynamic stress.

This phenomenon confirms what measured on site when a cross wind or the fan position in the plant generates asymmetric flow patterns at the fan inlet, see fig. 4.2.

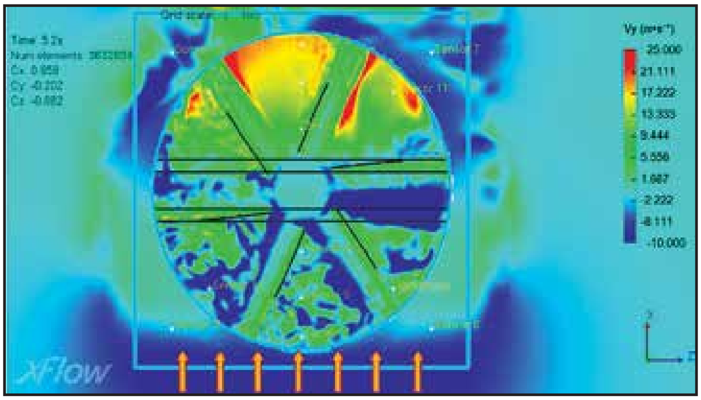

Fig. 4.2A: Asymmetry in the vertical flow component (Vy) in case of wind

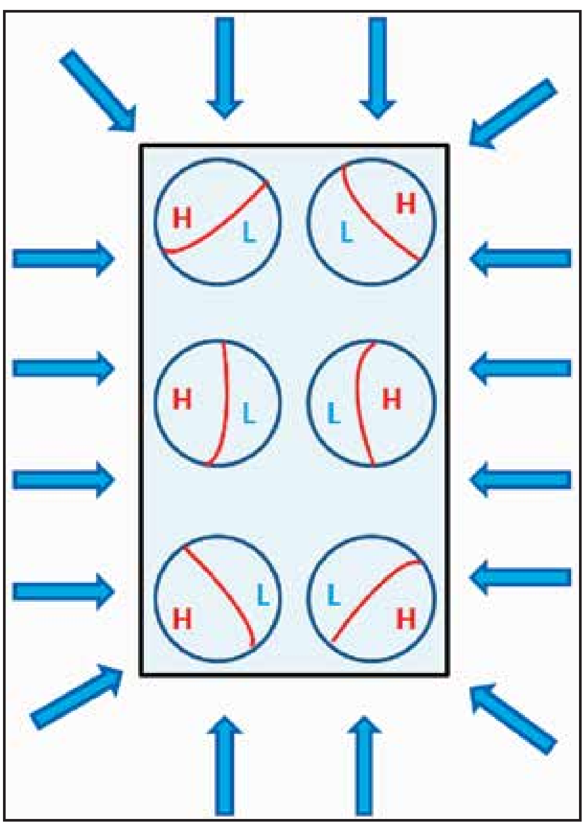

Fig. 4.2B: Asymmetry in the vertical flow component (Vy) in case of multiple-cell units.

H/red – high flow region (high Vy)
L/blue – low flow region (low Vy)

From the theoretical point of view, the above mentioned behavior can be explained with the help of the figures 4.3, 4.4 and 4.5.

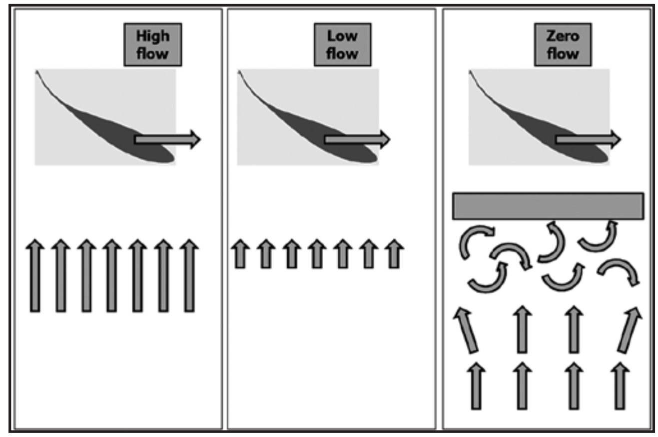

Fig. 4.3: Flow conditions
A – High flow B – Low flow C – Zero flow

When the flow is high, fig. 4.3A, the Average Aerodynamic Angle of Attack (AoA) is relatively low, putting the blade in condition D of fig. 4.4. On the contrary, when the flow is low, fig. 4.3B, the AoA is relatively high, so the blade is in condition B of fig. 4.4. Finally, when crossing an obstructed area (like above or underneath a broad obstacle, fig. 4.3C), the AoA is definitely high and the blade is in condition C of fig. 4.4.

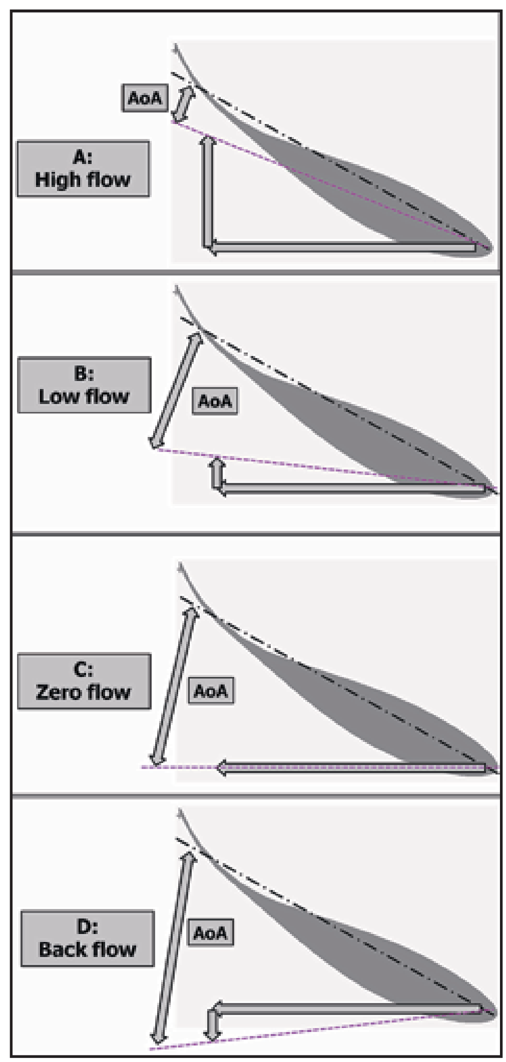

Fig. 4.4: AoA at different flow conditions

Looking at fig. 4.5, it can be seen that, in case of high flow, when crossing an obstructed area the blades moves from A to C with a high load variation (ΔL_{AC}). In case of low flow, the blade moves from B to C with a load variation (ΔL_{BC}) smaller than in the previous case, leading to a lower dynamic stress. The described situation gets even worse in the case of a blade moving from a zone of high flow to one of back-flow like in case of cross wind, fig. 4.2: in such a condition, the blade jumps from A to D with an extremely high load variation and, not rarely, overtaking the stall point of the lift curve in fig. 4.5.

The above analysis is carried out considering the same blade at constant speed and pitch in the four conditions A, B, C and D.

NOTE: *the blade speed, the flow vertical speed component (Vy) and the blade pitch vary along the blade span, so the vector components and the resulting AoA should be analyzed at each fan radius.*

It must be taken in to consideration that real-scale measurements of the above mentioned events are extremely difficult to carry out on-site but can be simulated with reasonably precision in a properly equipped test rig.

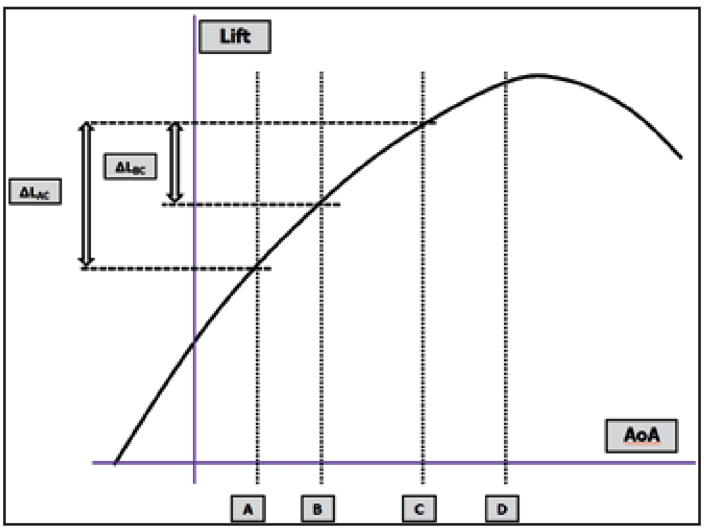

Fig. 4.5: Blade lift curve

Flow Rate Measurements

In order to set the most reliable measurements of fans performance, several different approaches have been followed. According to the ref. a), see fig. 5.1, the flow velocity measurements have been taken below the fan both using Pitot tubes and anemometers.

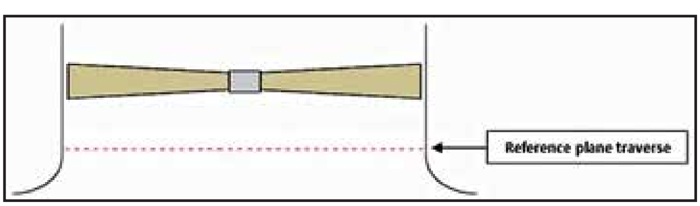

Fig. 5.1: Flow measurement according to ref. a)

A couple of sample measurements have been taken on 2 stations (S1 and S2) along a fan radius, see figures 5.2 and 5.3.

At each station, 2 Pitot tubes and one anemometer have been installed with the aim to compare the measurements. The flow measurements have been taken at different fan speeds.

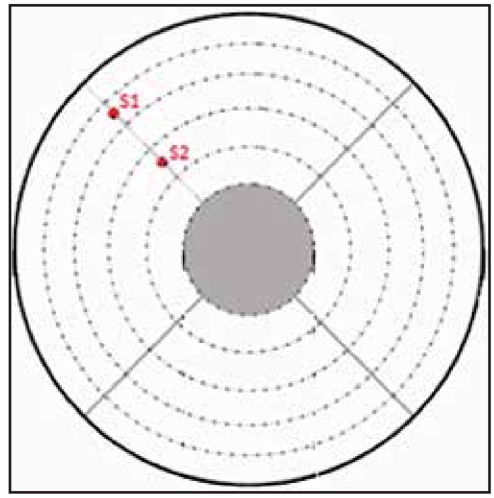

Fig. 5.2: flow measurement stations

Fig. 5.3: Flow measurement probes

Preliminary measurements, taken on a previously installed 6-blade fan used for the measurements optimization, is shown in the following fig. 5.4, where the Pitot measurements are highlighted. The signal was acquired at 1 KHz and then averaged.

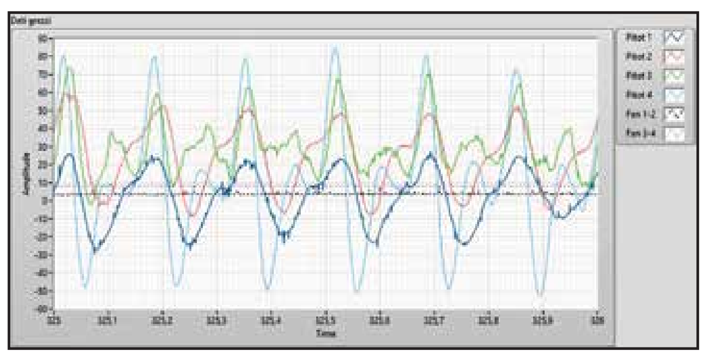

Fig. 5.4: Flow velocity measurements at 60 RPM, Louvers 50% open on both sides.

Two aspects immediately strike:

- the dynamic pressure has very high fluctuations and
- the dynamic pressure goes down to negative values.

One might think that the negative values mean reverse flow. This is likely true but, considering the physics behind the Pitot tube, fig. 5.5, the measured values during reverse flow are obviously not reliable.

Then, when elaborating the 1KHz signals, all the negative (unreliable) values affect dramatically the average value calculation.

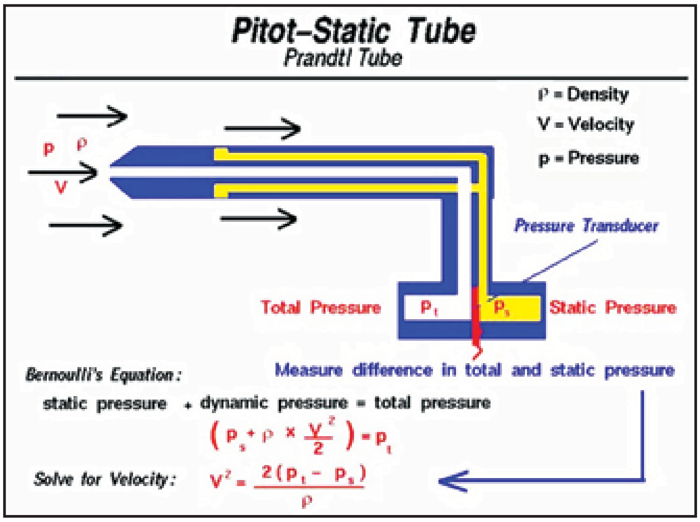

Fig. 5.5: Pitot's tube physics

So, from the above considerations, it was decided to equip the test rig with a set of anemometers.

The measurements reported in the followings were taken on a 38ft – 6 - 40F / G20 fan. Its main features are:

- 6 blades
- Root chord 890 mm (≈ 35")
- Tip chord 770 mm (≈ 30")
- Hub diameter 2 m (≈ 80")

Below, see figure 5.6, the flow measurements for the louvers position 80% closed. The fan axis is on the right. The measurements were well in accordance with the very same fan tested on site.

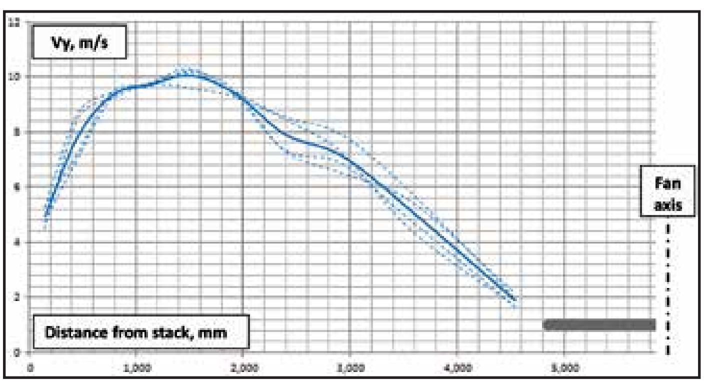

Fig. 5.6: Louvers 80% - four radii flow velocity measurement and average value

A couple of points were highlighted by the measurements:

1. The dynamic pressure at the fan outlet is always higher than the result of the simple axial velocity averaging;
2. The dynamic pressure in the plenum is higher than the result of the analogous calculation carried out in the plenum.

Since the DP component is of relevant importance in the evaluation of the fan performance, the above points need to be carefully taken in to consideration during performance measurements.

With the help of some CFD simulation, fig. 5.7, the mentioned test rig can help to verify or improve the present performance measuring procedures.

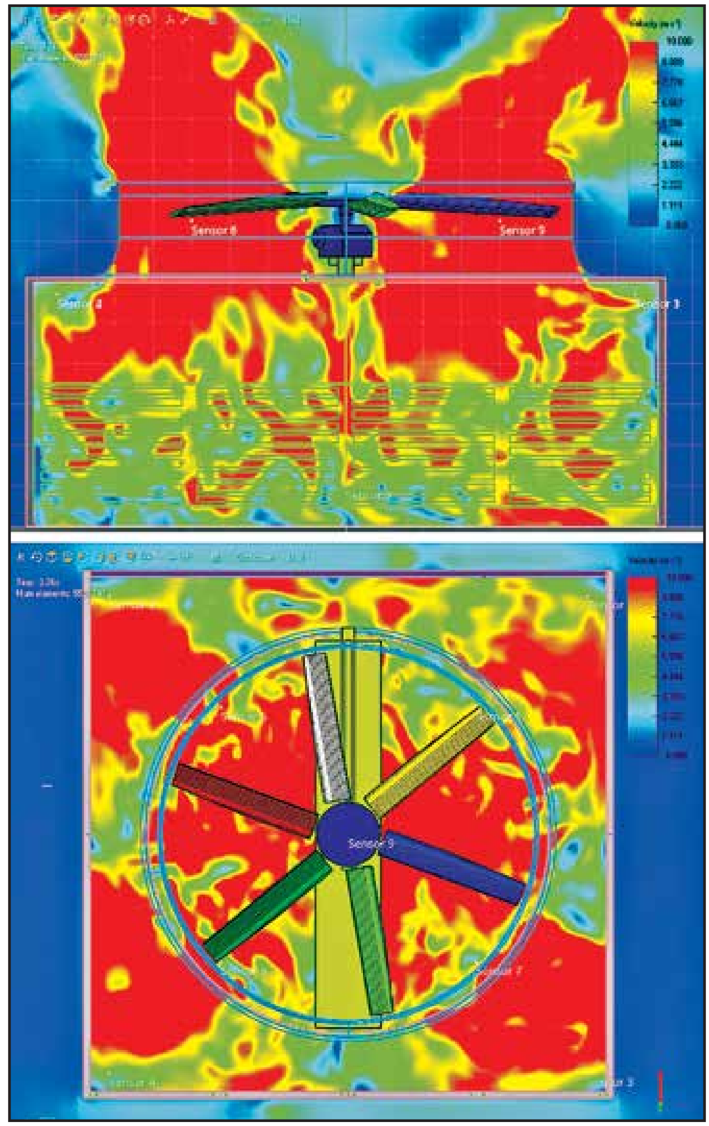

Fig. 5.7: Air velocity by CFD simulation.

Section at the symmetry plane (left) and horizontal section at static pressure probes level (right).

Conclusions

In the previous chapters the main features of the 38 ft test rig have been shown. Some results of the measurement of the first year of activity have been shared as well.

The following points deserve to be highlighted:

- The unit allows real-scale measurements of fans performance and noise both in design conditions as well as related to cells singularities that can be mocked-up on the rig.
- The size and the features of the rig were chosen following the recent trend of several plants with the aim to simulate and study the dynamic effects on both ACC and CT fans as well as their performance and noise characteristics. Thank to the rig, the interpolation algorithm of the fan curves can be adjusted removing excessive safety margins unavoidable when applying the fan rules to a very broad size range.

- Large fans are subjected to dynamic load of primary importance that are difficult to foresee but can be simulated with satisfactory approximation and at real scale with a proper setting of the rig and the related instrumentation. The unique features of the rig allow to set the cell configuration in order to replicate some standard situations as well as anomalous working conditions like flow asymmetry due to cross wind or fan position, bridge shape or size, bridge distance from the fan, blades operating in resonance range and so on. All the mentioned conditions are extremely difficult, if not possible at all, to capture on site or to simulated on scaled-down models.

References

1. CTI PFM 143 – Recommended Practice for Airflow Testing of CTs

Constructing Non-P Passivation Films for Cooling Applications: Surface Science Perspective

Paul R. Frail

SUEZ – Water Technologies & Solutions

Paul R. Frail

Abstract

To comply with environmental regulations or to ameliorate an existing calcium phosphate fouling issue, more customers are looking for non-P cooling corrosion control programs. Simply transitioning from a calcium phosphate to a non-P corrosion control program is relatively seamless due to the slow dissolution of the existing calcium phosphate passivation film to the new non-P passivation film. A more difficult transition is when the surface is neat due to a freshly cleaned surface or a re-tubing of a heat exchange bundle. Utilizing surface analysis techniques coupled with traditional corrosion monitoring for cooling applications the necessary means to construct effective passivation films will be discussed while exploring the various options available: (i) use of metal additives such as Al, Zn, Sn, etc.; (ii) non-P polycarboxylic acid derivatives; and (iii) potential new approaches.

Introduction

Industrial cooling systems must mitigate and tolerate the various forms of corrosion.[1] Thermodynamically, all metals are driven towards reaching their highest oxidation state, meaning that all base metals, under oxidative conditions, are looking to transfer electrons into the electrolytic medium to reduce oxygen or chemical oxidizers. Over time, an oxide layer can form that retards the electron transfer processes until the now cationic metal ion dissolves into the aqueous phase via chlorides or sulfates. The base metal, without an oxide layer, is the most reactive. Nobel metals, such as titanium, zirconium, etc., are not always an economical option to replace lower noble metals, such as low carbon steel. Mitigation using chemical treatments is often the best course of action. Unfortunately, inadequate passivation of exposed base metal after re-tubing a heat exchanger, system cleaning, start up of a new system, etc. often occurs resulting in corrosion damage that impacts the asset's use lifetime.

Industrial cooling systems rely on a variety of chemical inhibitors to form a protective passivation layer on the metal surface. Chemical inhibitors include the use of heavy metals (Cr, Mo, Zn, etc.), inorganic phosphate, organic phosphonates, and polycarboxylic acids. The inhibitor is described based on the which of the two corrosion reactions they inhibit: anodic or cathodic reaction (Equation 1). Determination of whether a corrosion inhibitor is anodic or cathodic is done via electrochemical experiment such as a Tafel plot. To passivate an exposed metal surface, chemical inhibitors are typically applied under low hardness conditions at 2-3 times the maintenance dose under cycled up operating conditions. The expectation is that by feeding 2-3 times the maintenance dose the system is saturated with a chemical inhibitor, which drives the passivation film formation on the exposed base metal with complete coverage of the metal piping.

Passivation with a heavy metal often results in positive outcomes. Unfortunately, heavy metals have negative impacts on the environment and the individuals that handle these chemical reagents. As the industry moved away from the use of chromium corrosion inhibitors and replaced them with phosphorus, comparable performance could be achieved[2-6] This is due to the thicker passivation film that phosphorus-based chemical treatments form.[2] Phosphorus chemical treatments may have provided adequate passivation films, they also run the risk of fouling or can have negative impacts on the environment. Phosphorus chemistries are not inherently toxic to individuals and the environment directly. Rather, as a micronutrient, they accelerate microbiological growth that can result in biofilms, toxic levels of pathogens such as *Legionella*, or algal blooms that deplete oxygen from bodies of water and/or release toxic levels of respiratory bioproducts. For these reasons, regulations are becoming stricter regarding the use of phosphorus-based chemistries in industrial cooling systems.[7-10]

M = base metal
n = number of electrons

$$M^0 \longrightarrow ne^- + M^{n+} \quad \text{Anodic Reaction – Generates electrons}$$

$$O_2 + 2H_2O + 4e^- \longrightarrow 4OH^- \quad \text{Cathodic Reaction – Accepts electrons}$$

Equation 1 – Anodic and cathodic half reactions

Polycarboxylic acid chemistries, without the presence of P in the molecular composition, have been investigated as corrosion inhibitors. Organic, carbon-based chemistries remain largely unexplored as a sole passivating agent in industrial systems.[11-13] These polycarboxylic acid chemistries are common in industrial water systems as scale-inhibiting treatments and have been used in junction with heavy metals or phosphorus chemistries to achieve desirable corrosion rates. With increased scrutiny over the use of phosphorus and/or heavy metals there is a resurgence of interest in new, phosphorus-free, polycarboxylic acid corrosion inhibitors for industrial water treatment.[19-27]

Previous work has shown the use of specific Carbon-Hydrogen-Oxygen (CHO) based inhibitors to be effective in corrosion control for industrial cooling applications without the addition of phosphorus chemistries such as phosphate, pyro-phosphate, or organic phosphonates. CHO inhibitors work with the ionic species in the water solution to form effective corrosion protection films that can achieve less than 2.0 mpy and sometimes less than 1.0 mpy without localized corrosion. Additionally, these inhibitors could be enhanced to further lower the corrosion rates with the use of exceptionally low doses of soluble cationic aluminum species.[14] The low levels, less than 0.5 ppm, act as a catalyst for forming a CHO-salt capping matrix without the addition of phosphorus to the chemical treatment program.[27]

This work examines the use of CHO inhibitors, with and without the use of a soluble cationic aluminum film catalyst, to passivate low carbon steel surfaces under low hardness conditions.[27] Surface analysis techniques aide in elucidating the films chemistry, construction, and relationship to the chemical treatments and water chemistry. Passivating a fresh and exposed metal surface is critical to ensuring asset longevity. Key learnings from the surface science compliments the development of non-phosphorus corrosion programs that enrich the metal oxide interface and catalyze a capping matrix that revels calcium phosphate programs and heavy metals.

Methods and Materials: Full experimental details concerning the design and capabilities of testing equipment have been described previously. Corrosion rates were measured by weight loss or calculated using the linear polarization method and reported as mils of penetration per year, mpy.[27]

Beaker Corrosion Testing: Beaker testing methods and materials have been described in detail previously. The method utilizes the standard 3 electrode corrosion cell in synthetic cooling water with treatment doses. Instantaneous corrosion rates are acquired as Rp vs. Time plots for a predetermined time: generally, 18 to 40 hours. The total average of the instantaneous corrosion rates is used to evaluate performance; as well as, evaluating inserted coupons for deposit and density of corrosion cells.

Cooling Recirculating Tests: All coupons, heat exchange surfaces, and corrosion data were acquired using Bench Top Units (BTU) with various water conditions. Specifics regarding the test methodology have been reported previously.

Coupon Preparation: Laboratory coupons were polished with corn cobb media, sonicated, rinsed with distilled water (DI) and isopropanol, and polished with acid/pumice prior to use. Field coupons were used as received in protective sleeves. All coupons are inserted at the start of an experiment or field coupon cycle. At the end of the testing duration the coupons are removed, rinsed with DI water to remove the application water, and air dried prior to shipping. Coupons were stored under dry conditions prior and during shipping to the GE Global Research Center in Niskayuna, NY for surface characterization.

Surface Analysis: X-Ray Photoelectron Spectroscopy – XPS measurements were performed on a Kratos Axis Ultra DLD instrument (Kratos, Manchester, England) using a monochromatic AlKa X-ray source (1486.6 eV). The analysis area is 700 x 300 mm2. Compositional survey scans were acquired using a pass energy of 160 eV. Three spots on each coupon were analyzed. The compositional data are an average of the values determined at each spot. Compositions were calculated with CassXPS software.

Time of Flight Secondary Mass Spectroscopy – ToF-SIMS measurements were performed using an ION-TOF.SIMS 5-100 (ION-TOF) GmbH, Munster, Germany). The instrument was equipped with 25 kV and bismuth liquid metal ion gun (LMIG). The analysis Bi3+ beam was rastered over a 100 x 100 mm2 area on the coupon's surface. A low energy electron flood gun was used to stabilize surface charge and the high current bunched mode was used for analysis. Data analysis was performed using a SurfaceLab 6 software from ION-TOF GmbH.

Transmission Electron Microscopy – TEM analysis were conducted using FEI Osiris TEM operating at 200 kV equipped with 4 SDD detectors for faster acquisition of EDS signal. The image was collected in the STEM mode. Due to the presence of organic layers on top of the sample STEM mode was selected to give lower dose to the sample and minimize possible beam damage. TEM samples were prepared with Focused Ion Beam (FIB) lift-out technique to extract cross section specimens. The dual beam FEI NOVA FIB was used to prepare the TEM cross section.

Discussion

Recently, an admiralty brass heat exchanger tube from a west coast refinery was examined using surface analysis techniques. The tube itself was replaced for no specific reason or cause. Rather, the tube had been in service beyond the expected lifecycle of 42 years. During this time the tube itself had experienced a wide range of chemical treatments and conditions. Visibly, there were no remarkable corrosion features, Figure 1. SEM and TEM images reveal the tube suffered significant intergranular cracking and build up of >10-micron thick scale, Figure 2. Both phenomena are expected from a heat exchanger tube with extended years of service under refinery conditions. Surface analysis techniques were used to better understand what was happening at the metal interface to allow for extended service time. Once the chemistry is elucidated via surface analytical techniques, could a similar surface passivation film be engineered under no added phosphorus conditions to provide equal performance.

The top surface layer was examined by XPS and an average elemental composition was obtained for the top 10 nm of the passivation film, Table 1. There were minimal amounts of nitrogen suggesting a very low concentration of azoles on the upper most surface layer.[16-18, 28] The XPS composition suggest the top passivation layer consists primarily of corrosion products that formed amorphous colloids with typical scaling salts found under industrial cooling applications: Zn and Cu from the ADM surface combined with Si, Ca, and P from the concentrated cooling water. Unfortunately, this alone does not reveal why the tube was able to have a 42-year life cycle without significant localized and general corrosion.

Cross sectional SEM with EDS mapping was performed on the heat exchanger tube, Figure 3. The SEM image reveals significant formation of grain boundary attack. An anticipated result given the longevity of the heat exchanger tube. The passivating surface film ranged in thickness between 10-100 microns with porous segments. Elemental mapping initially revealed a surface film rich in O, P, Ca, and Si. The elemental mapping of oxygen suggested that the grain boundary attack may be driven by internal oxidation and dezincification. Versus a standard phosphate program there appears nothing remarkable concerning a cause for the long term of service other than a thick surface film.[2,28] However, when one considers the life time of the heat exchanger tube it becomes relevant to investigate the Cr contribution since the tube life overlaps with chromate-based corrosion programs.

The EDS mapping of the cross-sectional SEM reveals the metal interface layer is enriched with a chromium film that is then capped by various salts that originate from the industrial water stream, chemical treatments, or corrosion products. A more defined picture of the Cr film was examined using FIB lifted sample under TEM with EDS mapping, Figure 4. The enrichment of the metal interface with chromium appears to be a critical step in forming passivation films that deliver extended protection within a corrosive environment. Despite decades of various chemical treatments and water conditions the chromium film remained intact at the interface while a capping matrix was building and transforming over time. This is a desirable design or engineering motif that would need to be present in any new corrosion control chemistries or program.

Thus, for non-phosphorus application it is necessary that a similar film is engineered on the surface. A film that enriches the metal interface and then allows a thicker capping matrix to form on top of the initial passivation, Figure 5. If this initial enrichment is not achieved the passivation film is weak and not robust enough to withstand the simultaneous chloride attack and dissolution with the electron transfer reaction. Traditional corrosion perspective would require one to develop inhibitors that impacted either the anodic or cathodic reaction as determined via a Tafel experiment. Engineered filming technology focuses on the ability to form surface films that enrich the metal interface and then are capped by electrically insulating salt-organic matrix. This matrix prevents the necessary electron transfer reaction involved in the corrosion process.

Phosphate or phosphorus inhibitors allowed the industry to move away from the use of toxic metals such as chromium, molybdate, and zinc because these chemistries formed thick surface films: 200 nm to several microns thick.[2,27] The film consisted mostly of calcium phosphate combined with calcium carbonate and some of the organic chemical treatments. Recently, surface analysis of corrosion protection films highlighted the important role the stress tolerant sulfonated dispersant polymer plays in forming calcium phosphate films. Similarly, the choice of polycarboxylic acid, or CHO inhibitor, plays an important function in facilitating the formation of surface films. The incremental removal of phosphate from a corrosion control program results in elevated corrosion rates and erosion of the protective phosphate matrix to the point where localized corrosion is evident. Under non-phosphorus conditions the ability to passivate a pristine surface, due to replacement of metallurgies or cleaning, would seem problematic and a cause for concern.

Previously, it was noted that to engineer protective surface films under non-phosphorus corrosion control programs, the correct CHO inhibitor needs to be selected. The CHO inhibitor has two necessary roles:

1. act as a surface buffering agent and
2. aides in constructing the salt-CHO capping matrix that is electronically insulating and prevents the electron transfer reaction to occur.

Similarly, the correct CHO inhibitor needs to be selected to passivate a fresh metal surface. Low hardness conditions were selected to represent a difficult to treat start up conditions. A series of CHO inhibitors, Table 2, were selected to illustrate that CHO-1 inhibitor is unique versus traditional CHO polycarboxylic acids derivatives commonly used in industrial water treatment.[2]

CHO-1 was compared to several polycarboxylic acid derivatives under the low hardness conditions, Table 3, to simulate passivation of a cleaned or replaced low carbon steel heat exchanger tube: CHO-1 inhibitor with and without aluminum, polyacrylic acid, polymaleic acid, and a polyhydroxy starch, Table 2. All were dosed continuously at elevated levels versus maintenance dose, 25 ppm active, while pH was maintained at 8.0. The first 24 hours no heat load was applied to the system or oxidizer fed. If the inhibitors were effective at enriching the metal interface no corrosion, general or localized, would be seen in the first 24 hours of circulation. If the inhibitor provided adequate protection a heat load would be applied to achieve 135 ^{o}F skin temperature (120 ^{o}F temperature in the sump). Once equilibrated at temperature and pH, oxidizer would be fed into the system. In some scenarios, the sump would be dumped and transitioned to typical cycled water conditions in efforts to highlight the robustness of the passivation film to withstand typical cycled cooling water, Table 3, without the presence of added phosphate. Or, a more difficult test, the low hardness conditions were continued with 0.3 ppm residual hypochlorite for the duration of the test.

Polymaleic acid, PMA, was tried as a potential CHO inhibitor for passivation. Under no heat load rapid appearance of localized corrosion was seen under low hardness conditions that did not have the presence of any phosphate or phosphorus chemistries. Doubling the concentration of PMA did not eliminate the localized corrosion during the initial passivation step. Comparing the two low carbon steel heat exchanger tubes it does appear that increasing the concentration reduced the density of pits and perhaps their overall thickness. Unfortunately, neither conditions were suitable as a passivating treatment. Polyacrylic acid produced similar results, with some improvement. Unlike the PMA, there were signs of a precipitated Fe-PAA complex in addition to the numerous localized corrosion cells. The overall passivation film is visually improved versus PMA. The poor performance can be related to the inability to fully cover the entire metal surface giving rise to localized corrosion. Increasing the dose of PAA was not attempted due to previous learnings that PAA can form insoluble salt complexes. Visual comparison between the runs can be distinguished from Figure 6.

One example of a polyhydroxy starch complex, saccharic acid, was screened as a potential passivating species. There have been numerous reports of such class of molecules being effective corrosion inhibitors. After the initial passivation of no heat load there were a small density, 10-20 localized corrosion cells on the heat transfer tube, slightly improved versus the PAA experiment, and the test proceeded with a heat load. When the heat load was applied the localized corrosion cells rapidly began to grow and eventually formed tubercle mounds. As seen in Figure 6, the corrosion was too severe to continue testing. Doubling the concentration was not considered as saccharic acid being a starch derivative is easily convertible to nutrients for microbiological growth and would not be advisable.26

CHO-1 outperformed the common industrial cooling polycarboxylic acid species. The inhibitor alone produced small pit density on the tube, < 10, and the surface film was able to withstand a heat load, Figure 7. The addition of oxidizer, as hypochlorite, increased the degree of corrosion and was still able to produce coupon corrosion rates less than 2.0 mpy under low hardness conditions. However, corrosion on the heat exchanger tube was too severe when a heat load and oxidizer were applied and would be suitable only for transfer piping. CHO-1 inhibitor outperformed the other polycarboxylic acids species because it can initially enrich the metal oxide interface with a thin protective layer. Even though the CHO-1 inhibitor could passivate the low carbon steel under low hardness conditions the passivation process still needs to be improved to achieve no localized or general corrosion and have instantaneous corrosion rates less than 1.0 mpy and preferably less than 0.5 mpy.

The performance of CHO-1 can be improved by using very low amounts of soluble aluminum, < 0.5 ppm.[14,27] Previously, aluminum was reported as a viable zinc and tin alternative.[27] Zinc is a primary pollutant and is highly regulated for discharge purposes and forms common fouling salts with phosphate and carbonate. Tin is relatively new to the industrial cooling applications space and has several concerning features: it is a redox active salt and can have an oxidizer


Denso®
BOLT & NUT
CORROSION
PROTECTION
FITTING
CORROSION
PROTECTION
VALVE
CORROSION
PROTECTION
PIPING CORROSION PROTECTION
STRUCTURAL STEEL CORROSION PROTECTION

demand; it is galvanically active, more so in the higher oxidation state; it is sparingly soluble under cooling conditions. The soluble aluminum complex used for enhanced corrosion protection is not redox or galvanically active. Aluminum solubility is highly predictable using competitive ion equilibrium modeling and use concentrations are often well below saturation limits. The effective dose is often well below potential permit limits.

Figure 8 is the heat exchanger tube after passivation and is clear of any localized or general corrosion. The robustness of the passivation surface film under low hardness was tested by applying heat and ~0.3 ppm residual chlorine. The aggressive conditions did not break the passivation film and resulted in a clean tube with varying hues of colors. The color formation is indicative of an amorphous film that fully covers and protects the surface. Electron transfer reactions could not proceed through the engineered film as seen with other polycarboxylic species. CHO-1 with Al was also able to passivate a low carbon heat transfer tube and then quickly switch over to cycled cooling water without having the film break. Additionally, CHO-1 with Al was used under low hardness conditions and elevated temperature and low flow, 2 ft/sec, and still was able to engineer a strong electronically insulating passivating film that did not result in any forms of corrosion, Figure 9.

Surface analysis of coupons generated during the passivation process revealed insights into why the CHO-1 with Al system provide the best performance. XPS results suggested the surface is covered by a Ca-Si-O-organic matrix, Table 4. However, XPS only measures the top 10 nm of the surface film and does not elucidate anything regarding the chemistry at the metal oxide interface. As shown with the chromium example, enriching the metal oxide interface initially is the most critical aspect of passivating a metal surface to ensure longevity. Cross sectional analysis of the coupon performed via a focused ion beam, FIB, lift off technique and SEM with EDS mapping, Figure 10. The results were surprising. Given the soluble Al species is fed continuously it was expected that the Al would be present in all areas of the film. Rather, it was revealed that the Al targeted the metal oxide interface versus the capping layer. Like chromium inhibitor example, Al enriched the metal oxide providing the necessary protection and then catalyzed the capping matrix that is formed from the water chemistry and the CHO-1 inhibitor. Without the presence of soluble aluminum species during the passivation step it is more difficult for the CHO-1 inhibitor alone to enrich the metal oxide interface leading to avenues within the surface film for electron transfer to occur resulting in corrosion.

The use of soluble Al species is very effective in forming passivation films. Surface science has revealed how long-term corrosion protection can be achieved; the question remain weather one could do this as effective without the presence of a metal species. Presented here are two examples of how surface films can be engineered with minimal laboratory iterations when equipped with the necessary connection between the role of inhibitor, water chemistry, and metal surface. EXP1 inhibitor, which also falls under the CHO class of inhibitors, was able to passivate the metal surface in the absence of soluble Al species, transition over to cycled water conditions, and provide acceptable protection of admiralty brass coupons while protecting low carbon steel from galvanic corrosion, Figure 11. EXP2 inhibitor represents a non-toxic, biodegradable, and environmentally friendly solution that could passivate several metal surface types under non-phosphorus conditions. Under low hardness passivation conditions, it was able to passivate a low carbon heat transfer tube comparable to CHO-1 plus soluble Al species, Figure 12. The film was robust enough to tolerate a rapid switch to cycled cooling water, heat load, and residual chlorine. Unlike the CHO-1:Al system the EXP2 inhibitor does not need to be fed after passivating the surface. Surface analysis of these species are ongoing and not fully completed for this publication. Nonetheless, it represents exciting developments for future industrial corrosion control program design.

Conclusions

The initial passivation of the base metal oxide layer is a necessary requirement to ensure extended use lifetimes of heat exchanger tube and metal pipping. Examining an ADM heat exchange tube with 42 years of service revealed the initial passivation with chromium aided in protecting the pipe from a wide range of harsh conditions experienced at a refinery. Engineering film technology can mimic the admiralty heat exchange tube characteristics versus traditional industrial water cooling polycarboxylic acid derivatives in the absence of adding phosphorus species to the chemical treatment package. The use of a CHO inhibitor enriches the metal interface with either a soluble aluminum complex or ionic salts present in the water. Selecting the CHO inhibitor is critical to performance and CHO-1 inhibitor with the soluble aluminum complex outperforms PAA, PMA, and a polyhydroxy starch. Surface analysis reveals the CHO-1 inhibitor with soluble aluminum complex forms an analogous passivation film as seen in the 42-year service admiralty heat exchanger tube. Using the acquired knowledge form surface analysis of metal surfaces two new chemistries were explored that can passivate the metal surface without the use a cationic metal species and be robust enough to handle synthetic cycled cooling water. These new chemistries are currently being explored to understand their passivation mechanism and chemistry.

References

B. Boffardi "Corrosion Control of Industrial Cooling Water Systems," NACE, Houston, TX; 1993

3. C. C. Pierce, P. R. Frail, G. Zorn, R. Sharghi-Moshtahin "Surface Characterization of Interfacial Layers to Study the Performance and Evolution of Phosphate Based Programs in Cooling Water Applications," IWC-16-71 2017
4. J. F. Harrison, N. S. Sherwood, "Optimization of Corrosion Control in Alkaline Cooling Water Systems Through the Use of Organic Inhibitors", Corrosion/86, Paper 18, 1986
5. W. J. Beer, J. F. Ertel, "Experience with High-Phosphate Cooling Water Treatment Programs," Corrosion/85, Paper No. 125, 1985
6. R. C. May, G. E. Geiger, D. A. Bauer, "A New Non-Chromate Cooling Water Treatment Utilizes High Orthophosphate Levels without Calcium Phosphate Fouling," Corrosion/80, Paper No. 196, 1980
7. G. E. Geiger, J. F. Ertel, "Advances in Alkaline Cooling Water Treatment Technology," Corrosion/84, Paper No. 320, 1984
8. USEPA "Overview of Impaired Waters and Total Maximum Daily Loads Program" https://www.epa.gov/tmdl
9. USEPA "State Development of Numeric Criteria for Nitrogen and Phosphorous Pollution" https://www.epa.gov/nutrient-policy-data/state-development-numeric-criteria-nitrogen-and-phosphorous-pollution

TPI Tower Performance, Inc.

Exclusive Bayonet Nozzle Adapter
(Convert from Twist-Lock to Threaded Adapter)

If you have one of these

And this happens to you

dek-Spray® Nozzle

Poor Water Distribution

You need one of these

To adapt with one of the state-of-the-art low clogging nozzles—S.P. or L.P.

S.P. Nozzle

L.P. Nozzle

Contact:
Jalene Fritz
800-314-1695
jfritz@towerperformance.com

10. Quality Criteria for Water 1986, EPA 440/5-86-001, Office of Water Regulations and Standards, Washington, D.C.: p. 240
11. Illinois Water Pollution Control Rule, Part 304 Effluent Standards, Section 304.123 Phosphorous, August 30, 1991.
12. C. C. Pierce, C. Sui, G. E. Geiger, "Cooling Treatment Performance Optimization under Alkaline Stressed Conditions" Corrosion/2010, Paper No. 10046, 2010.
13. A. Roman, P. Labine, "Reviews on Corrosion Inhibitor Science and Technology," 1989, National Association of Corrosion Engineers
14. Amjad, Z. "The Science and Technology of Industrial Water Treatment," 2010, CRC Press
15. C. C. Pierce, P. D. Deck, R. Crovetto, B. George, R. P. Kalakodimi, G. Sundararajan, D. W. Whisenhunt Jr. US8021607B2
16. G. Zorn, M. Karadge, C. C. Pierce, J. I. Melzer, M. M. Morra "Advanced Analytical Characterization of Multilayered Thin Films for Corrosion Inhibition" Amer. Vac. Soc. Contributed poster TF-ThP5, Tampa, FL 59th International Symposium and Exhibition, October 29 – November 2, 2011
17. P. R. Frail, G. Zorn, S. -M. Reza, M. M. Morra "Performance Analysis of Commercial Azoles for Yellow Metal Corrosion Control Utilizing Surface Analysis and Electrochemistry" Corrosion/2014, paper no 4246. San Antonio, TX: NACE, 2014.
18. P. R. Frail, G. Zorn, S. – M. Reza, M. M. Morra "Elucidating the Differences Between Weight Loss and Instantaneous Corrosion Rates on Azole Film on Copper Metallurgies" Corrosion/2015, paper no 5924. Dallas, TX: NACE, 2015
19. P. R. Frail, G. Zorn, E. J. Urankar, M. M. Morra "New Yellow Metal Corrosion Inhibitors Targeting Surface Chemistry of Industrial Systems" Corrosion/2017. New Orleans, LA: NACE 2017
20. J. M. Brown, W. S. Carey, J. F. McDowell "Development of an Environmentally Acceptable Cooling Water Treatment Program: Non-Phosphorus Scale Inhibitor" Corrosion/93, paper no 463. Houston, TX: NACE 1993
21. R. M. Post, R. H. Tribble, J. R. Richardson "Development of Next Generation Phosphorus-Free Cooling Water Treatment Technology" 2010 IWC
22. R. M. Post, P. Kalakodimi, R. Tribble "Development and Application of Phosphorus Free Cooling Water Technology" Cooling Technology Institute, Paper no. TP14-14, Houston, TX: CTI 2014
23. M. Felipe, D. Fulmer, C. Sandu, B. Guo, K. Nguyen "Novel and Efficient Non-Phosphorous Cooling Water Corrosion Inhibitor" Cooling Technology Institute, Paper no. TP16-06, Houston, TX: CTI2016
24. B. Chen, Y. Tong, S. Banerjee, J. Zhang, Y. Xie, X. Want, A. Mantis "A Robust Non-Phosphorous Corrosion and Scale Control Program for Cooling Systems" IWC 2017
25. M. LaBrosse, D. Erickson "The Pursuit of a Green Carbon Steel Corrosion Inhibitor" Parts 1 -4, Water & Wastewater, January – April 2015
26. J. Matheis, A. Stratmann, W. Hater, F. Wolf, R. Lunkenheimer, C. Foret "Investigations about a New Heavy Metal Free, Low P-content Corrosion Inhibitor for Evaporative Cooling Systems based on Phosphorous Modified Organic Acid" Corrosion/2016, Paper no 7018, Vancouver, CA: NACE 2016
27. E. C. Ward, E. M. Crane, G. J. Koniges "New Phosphorous-Free Corrosion Inhibitor Technology" AWT 2016

Tables and Figures

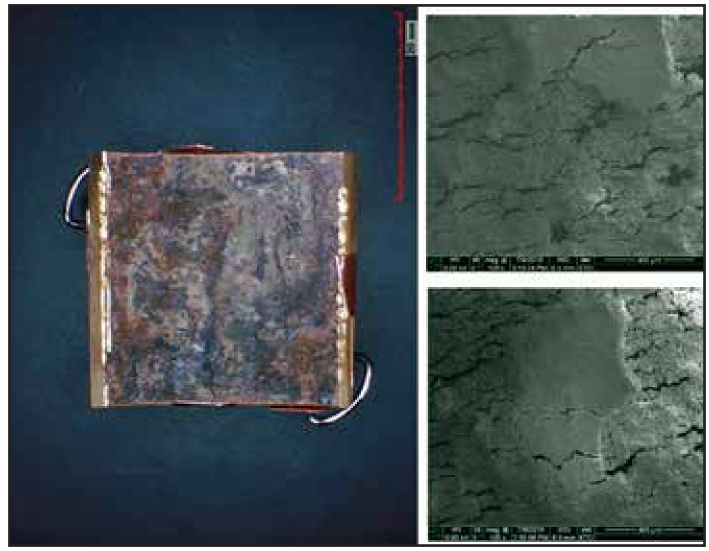

Figure 1 – Photo (left) of inner admiralty heat exchanger tube with 42 years of service at a US West Coast refinery. SEM images (right) of the inner tube exposing the surface film and numerous crevices in the deposited layer, SEM images are focused on the top layer of the exposed inner admiralty heat exchanger tube.

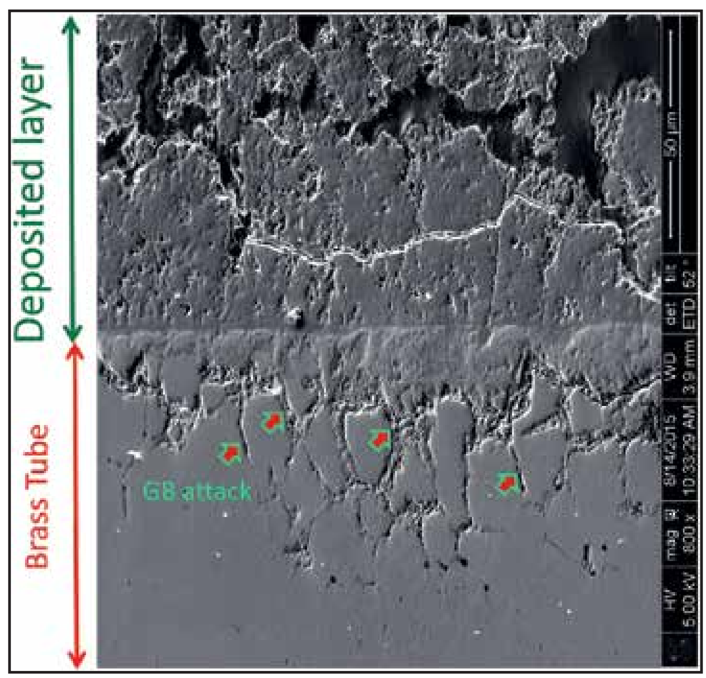

Figure 2 – Cross sectional SEM image of the admiralty heat exchanger tube exposes the extensive grain boundaries because of extensive lifetime.

	ave	stdev
C	37.0	1.7
N	0.7	0.1
O	42.4	0.1
Cu	5.1	0.3
Zn	3.6	1.2
Si	4.6	3.4
Ca	2.1	1.7
P	4.5	2.0

Table 1 – XPS results of the top layer of the admiralty heat exchanger tube

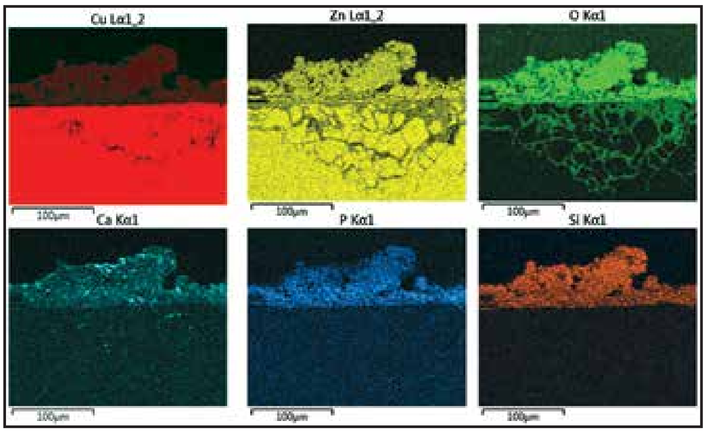

Figure 3 – Cross sectional SEM image with elemental EDS mapping of the admiralty heat exchanger tube. The oxygen and zinc images reveal the extensive grain boundaries that appear to be caused by dezincification and internal oxidation.

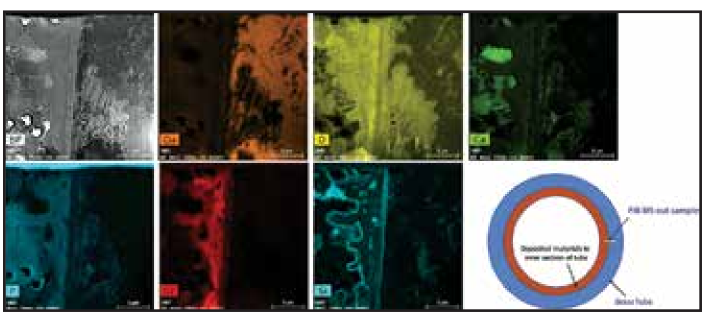

Figure 4 – Focused Ion Beam lift out technique was used to produce a cross sectional sample for TEM imaging with EDS mapping of an admiralty heat exchanger tube with Cr overlay. The chromium film enriches the base metal oxide layer providing the necessary protection for extensive use lifetime. A capping layer builds on top of the initial chromium layer providing additional detection.

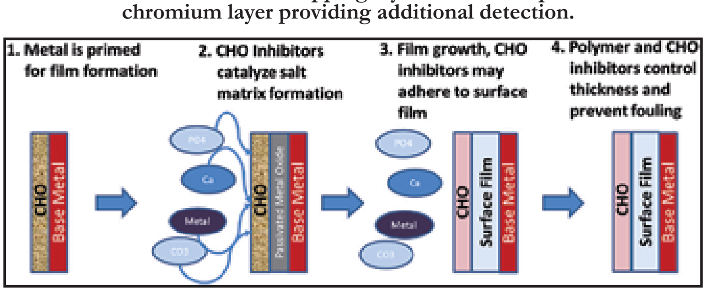

Figure 5 – Engineered passivation technology will build a surface film at the metal oxide interface utilizing Carbon-Hydrogen-Oxygen inhibitor. The role of the CHO inhibitor is to act as a surface buffering agent while facilitating the construction of the passivation film with the ions in the aqueous electrolytic medium. Selection of CHO inhibitor is critical to forming robust passivation films under non-phosphorus conditions and chemical treatments.

Treatment	Dose (ppm active)	Characteristics	Low Hardness passivation (no heat)	low hardness passivation (with heat load)
Polyacrylic acid, PAA	25	MW = 2 - 5K	Failed, high pit density	test stopped
Polymaleic acid, PMA	25	MW = 300 - 1000	Failed, high pit density	test stopped
Polymaleic acid, PMA	50	MW = 300 - 1000	Failed, high pit density	test stopped
Polyhydroxy Starch	25	MW = 300 - 1000	borderline, localized corrosion cells	Failed, high pit density with tubercles
CHO-1	25	proprietary	Pass	Borderline, localize corrosion cells
CHO-1 with Al	25 and 0.25 Al	proprietary	Pass	Pass
EXP1 - no metals	25	proprietary	Pass	Pass
EXP2 - no metals	25	proprietary	Pass	Pass

Table 2 – Common polycarboxylic acid industrial cooling treatments versus CHO-1 inhibitor and their ability to effectively passivate a low carbon steel heat exchange tube under low hardness conditions.

Water Chemistry	Passivation	Transition Water	Passivation (high heat)
Ca as CaCO3	56	600	120
Mg as CaCO3	48	300	55
M-alk as CaCO3	100	200	142
o-PO4	0.3	1	0
SiO2	30	50	65
Cl	62	424	
SO4	52	240	
Dispersant	6	8	

Table 3 – Low hardness water testing conditions

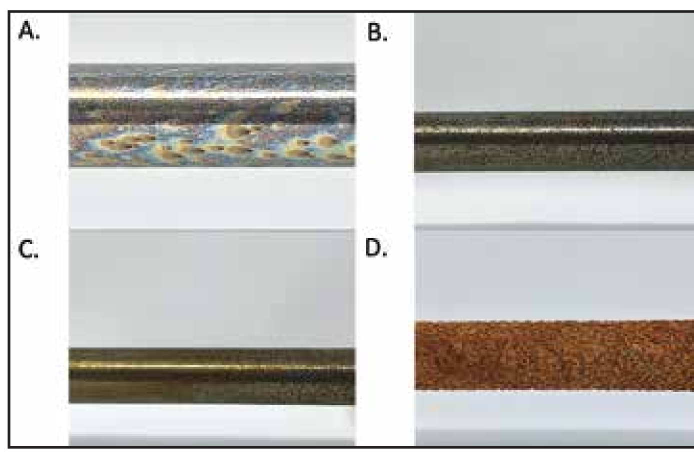

Figure 6 – Comparison of low hardness passivation with common polycarboxylic acid industrial cool chemistries: A. 25 ppm PAA; B. 25 ppm PMA; C. 50 ppm PMA; D. 25 ppm Polyhydroxy Starch, failed after turning on a heat load of 135 °F skin temperature.

Figure 7. CHO-1 passivation under low hardness conditions of a heat exchanger tube with a heat load.

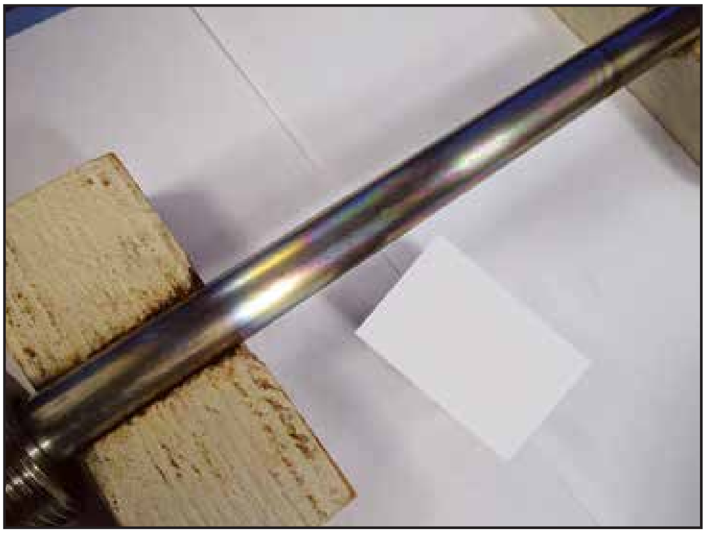

Figure 8 – Low Hardness passivation with CHO-1 and Al soluble complex. The initial step without and with heat load were successful and the experiment was continued with the low hardness water with the addition of free residual chloride of 0.3 ppm for seven days.

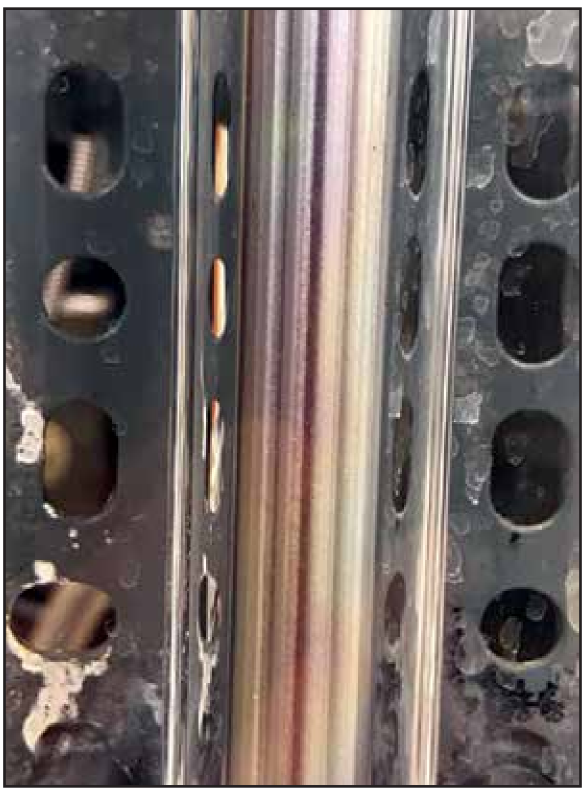

Figure 9 – Low hardness passivation with CHO-1 with soluble Al complex and transition to higher temperature, 160 °F skin.

	Average	stdev
C	42.8	1.1
O	37.5	1.0
Fe	0.4	0.03
N	1.7	0.3
Ca	9.8	0.2
P	5.1	0.7
Si	2.7	0.4

Table 4. XPS atom percentages of the top 10 nm of the passivation film from treating low carbon steel with CHO-1 and a soluble Al complex.

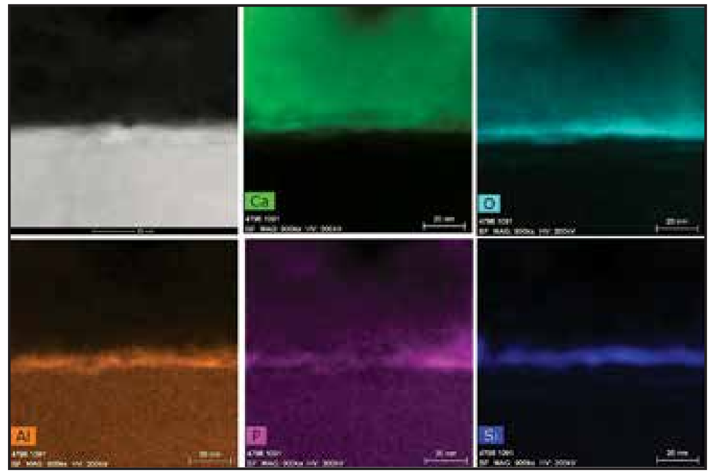

Figure 10 – SEM cross sectional imaging with EDS mapping for CHO-1 with soluble Al complex. The metal oxide interface is enriched with Al and then capped with Si-Ca-O-P layer.

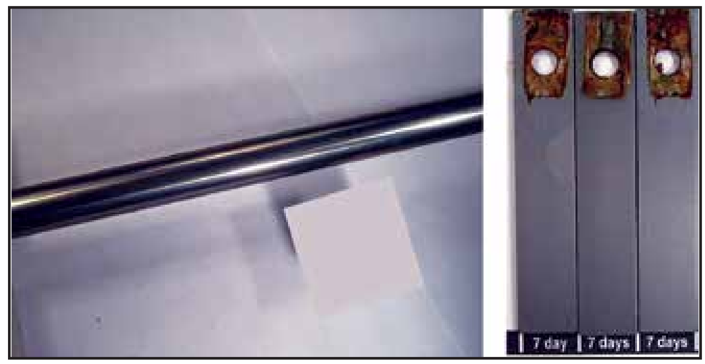

Figure 11 – Engineering Film Technology focused on chemistries that can enrich the metal oxide interface and build the capping layer without the use of metals under low hardness conditions. EXP1 was successful at passivating under low hardness conditions and was transferred over to synthetic cycled cooling water. Below are photos of the low carbon steel heat transfer tube and coupons after seven days with residual chlorine levels of 0.3 ppm.

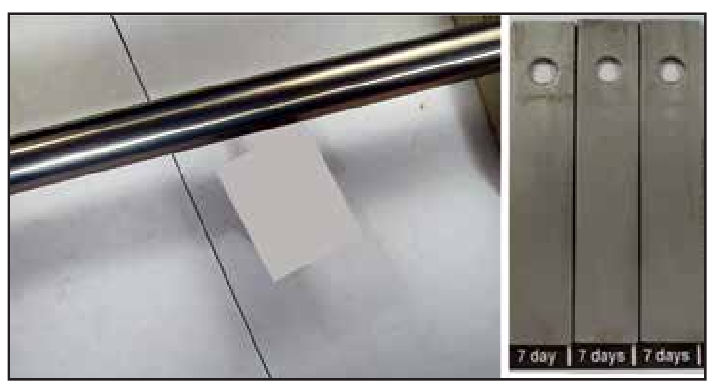

Figure 12 - Engineering Film Technology focused on chemistries that can enrich the metal oxide interface and build the capping layer without the use of metals under low hardness conditions. EXP2 was successful at passivating under low hardness conditions and was transferred over to synthetic cycled cooling water. Below are photos of the low carbon steel heat transfer tube and coupons after seven days with residual chlorine levels of 0.3 ppm.

Moore Sets The Standard In Axial Flow Fans.

Class 10000 Defines Efficiency.

Since 1940, Moore Fans has provided customers with high-efficiency, high-quality Axial Flow Fans for industrial applications worldwide. Operating in air-cooled heat exchangers and cooling towers, Moore fans keep liquids cool in refineries, power plants, process plants, gas compressors and limitless other industrial settings.

Latest Resilient Mount design developed through 50 years of operating experience.

Special Design Features Of The Class 10000 Fan

- Resilient Blade Mounting – For more than half a century, all Moore fan blades have been designed with a resilient blade mount, virtually eliminating all moment forces on the hub and shaft; improves durability; ideal under extreme operating conditions.
- Chord Width – Improve performance with fewer number blades for the same performance requirements, resulting in a lower overall cost.
- Blade Angle Adjustment – Blades are factory preset for specified performance conditions eliminating the need to set during field installation.
- Ring Depth – Designed to operate in a reduced fan ring depth.
- Adjustable Diameter – Designed to permit fan diameter adjustment by as much as +/-1.5 inches (3.81cm), greatly easing installation.
- Ideal For Variable Speed – With Moore's resilient mount system, there are virtually no critical speeds to be avoided.
- Available Blades – Available in both odd and even number of blades, up to 16.
- Low Noise – Where noise levels are critical, combine Vortex tips, wider chord width and increased number of blades for maximum noise reduction.
- Strengthened Design – For engine drive and larger fan diameter applications from four to 28 feet.

Today, Moore Fans has some 150,000 fans in operation around the world. And with sales offices in North America and in Europe, Moore factory engineers and customer service representatives stand ready to help you analyze your air moving requirements, choose the right product, and provide reliable service and support, before and after the sale.

For more information on the Class 10000 Fans or any of the family of quality products from Moore Fans call **660-376-3575** or visit us online at **moorefans.com.**

Moore® FANS

MOORE FANS LLC, MAIN SALES OFFICE & FACTORY
800 South Missouri Avenue, Marceline, MO 64658 USA
Phone: 660-376-3575 • Fax: 660-376-2909
www.moorefans.com

MOORE FANS LTD, EUROPEAN SALES OFFICE
2-3 Claremont • Hastings • East Sussex • TN341HA • UK
Tel: +44 1424 436815 • Fax: +44 1424 422789
E-mail: mail@moorefans.eu.com

INDUSTRIAL AIR MOVING EQUIPMENT

Using An Ultrasound Measurement Technology To Monitor Real-Time Biofilm Activity Cooling Systems

Shihhsiang Sean Chien, Michael Bluemle

Solenis Llc

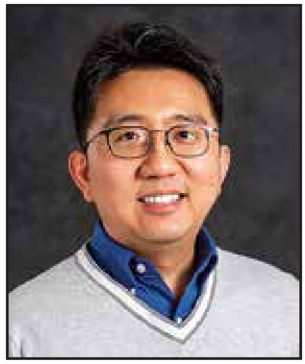

Shihhsiang Sean Chien

Abstract

Microbial (MB) growth management in cooling systems requires an integrated approach to control both suspended (planktonic) and sessile bacteria (biofilm) through proper chemical treatment and monitoring. Technologies are now moving toward in-situ monitoring of microbial growth in the cooling system. This paper reviews an advanced technology to monitor and, ultimately, to optimize the chemical usage for MB control. The core of the integrated MB control solution is based on a real-time monitoring device that employs both an ultrasonic thickness sensor and a thermal resistance sensor to detect biofilm growth. Evaluation was conducted under both laboratory and field conditions. Results indicate that not only the biofilm can be detected in the early stage, but also the instantaneous biofilm thickness measurement was responsive to different MB treatment programs. Case studies demonstrating successful MB growth management with the application of the technology in power, refinery, and chemical production industries will be discussed.

Introduction

Microbiological (MB) growth management in recirculating cooling systems requires an integrated approach to control both heterotrophic and sessile bacteria through proper chemical treatment and monitoring. The suspended (planktonic) bacteria enter the system from various makeup water sources. Once attached to the surface, heterotrophic bacteria produce extracellular polymeric substances (a.k.a. slime) and form a biofilm to protect the bacterial colonies from environmental and mechanical stresses. Biofilm is a loose matrix of different kinds of microorganisms that is held together with a slimy substance called extracellular polysaccharide (EPS). A large portion of a biofilm is simply water (Zhang et al., 1998), but the exact composition and structure is determined by the available nutrients and surrounding environment (Stoodley et al., 1998). Biofilm formation poses a significant problem to cooling water systems as a major source of process yield reduction due to low heat transfer efficiency and frequent corrosion issues. The formation of biofilm can be affected by surface temperature and water composition. Higher surface temperatures not only drive faster microbial growth cycles (Herald and Zottola, 1988), but also enhance colonization with higher bio-volumes, higher percent moisture and higher ratios of anaerobic to aerobic bacteria (Beardwood & Therrien, 1999). Most microorganisms can form biofilm and are able to accumulate on heat exchanger surfaces within 4 to 8 hours (Rossmoore, 1996). A combination of mineral fouling and biofilm not only significantly decreases heat transfer and pumping efficiency, but also promoting the oxidation of metals. Recirculating cooling systems are also a major pathogenic source of Legionella disease with inappropriate treatment programs. Therefore, monitoring biofilm formation in the early stages is critical to suppress the bioactivity in the cooling system.

Advances in monitoring technology, especially since the late 1990s, have yielded various types of online and real-time biofouling monitors. Electrochemical-based technologies use electrical resistance techniques to quantify the existence of living biofilm (Liu, 2012). Thermal transmittance-based technologies use heat transfer resistance to recognize the formation of scale or biofilm (Wan and Xiao, 2011). A recent study introduces a device, the piezo crystal balance, which precisely measures the increase in weight caused by deposition/biofouling (Fu et al., 2017). These technologies provide measurements of biofilm growth based on indirect parameters and rely on multiple measurements to calculate specific coefficients, such as heat transfer coefficient (U). Unless the testing conditions are normalized, a slight change in process water flow, bulk water temperature or heat exchanger surface temperature can affect the accuracy of the measurements. Beardwood (2011) demonstrated that a significant increase in foulant coverage in a steam surface condenser was required to yield similar fouling readings measured by a side-stream testing section. Under such conditions, detection of biofouling would not be expected until a mature and uniform biofilm had developed.

Technologies are now moving toward in-situ monitoring of microbial growth in the cooling system. This paper reviews an advanced technology to monitor and, ultimately, to optimize the chemical usage for MB control. Mauricio et al. (2013) showed the usefulness of non-invasive ultrasound to determine biofilm thickness inside potable water supply pipes. This method allows direct measurement of existing biofilm in the liquid phase based on the analysis of ultrasound pulse-echo behavior. However, whether this technology has the ability to detect biofilm at early stages or is applicable in highly stressed industrial systems is unknown. The core of the integrated MB control solution is based on a real-time monitoring device that employs both an ultrasonic thickness measurement and a thermal resistance sensor to indicate biofilm growth. The device is designed to simulate process conditions that are conducive to MB activity, which can provide an early warning of biofilm growth. With the ability to track biofilm thickness in real-time, the device can initiate and optimize chemical treatment programs through built-in algorithms.

Evaluation of the technology was first conducted on a pilot cooling system using synthetic cooling water with cultured heterotrophic bacteria. Results show that the device was able to detect the establishment of sessile bacteria in real-time during the bacterial growth phase under laboratory conditions. The second part of the lab validation focused on optimizing MB treatment process using the technology. When the biofilm growth reached either a heat transfer reduction or biofilm thickness threshold, the system was automatically treated with organic dispersant and oxidizing biocide in a pre-defined sequence. Various organic dispersants and biocides were also evaluated for optimal biofilm removal efficacy. Lastly, field trials were conducted to verify the applicability of the technology under real world condition. Results of field trials demonstrated that the instantaneous biofilm thickness measurement was responsive to different MB treatment programs. Case studies of successful MB growth management when applying the technology in power, refinery, and chemical production industries will also be discussed in the paper.

Instrument Development

The heat transfer sensor and ultrasound thickness measurement sensor designs were adapted from previous work (Bierganns et al., 2016; Chien et al., 2018), which successfully monitored inorganic scale growth in multiple industrial applications. A heated stainless steel surface target, which is suitable for biofilm growth, is used in the device. The built-in variable heating element provides consistent heat output to maintain the desired surface temperature while built-in thermocouples measure temperature differences in real time. With the assistance of a pre-programmed algorithm, the heat transfer reduction sensor also reports the development of biofilm as a fouling factor and a heat transfer reduction index. The heat transfer reduction index is defined as the difference between the surface and the bulk water temperature at time zero (equilibrium) and at time X.

$$\textbf{Heat transfer reduction index} = \Delta T_X - \Delta T_0 \quad \textbf{(Eq.1)}$$

where $\Delta T_X = T_{surface} - T_{water}$ at time X; $\Delta T_0 = T_{surface} - T_{water}$ at time zero (equilibrium)

The ultrasound thickness-measuring device was invented to measure mineral deposition with a minimal thickness of 0.001 mm (Seida et al., 2009). An ultrasound transducer capable of sending and receiving low-frequency signals (5–15 MHz) at a speed of 1480 m/s (4856 ft/s) was employed to determine the time difference (a.k.a. run time or lag time) between each transmission and reflection. The time difference measured after time zero can then be converted to distance change between the transducer and the target surface. The change is due to the accumulation of a foulant. The transducer has a resolution of 120 picoseconds, which could be converted into a theoretical thickness of 0.2 μm.

Additionally, the ultrasound sensor can distinguish biofilm from different types of foulants by amplifying signals at specific gain setting. The resistance of propagating sound, acoustical impedance, is the commonly used physical property for ultrasound technology because it varies based on material density and complexity. It is a combined impact of speed of sound in different medium and reflection probability of deposit surface. The corresponding reflective sound signals could be used not only for measuring, but also for differentiating the type of deposit. For example, mineral scales typically have high densities, while biofilm may contain up to 90% water and non-homogenous organic content.

The acoustic impedance, percentage of deposit content and associated deposit characteristics for different materials are summarized in Table 1. The observed percentage of deposit helps to determine whether to amplify or to reject the weak reflecting echoes (signals) for better resolution. For example, the received signals for biofilm accumulated on the stainless steel surface consisted of 0.4% of the weak reflection from actual biofilm, and 86% of the strong signals from the SS surface. Therefore, the process could be modified to determine all three forms of deposits (Seida et al., 2013; 2015). On-board algorithms also were developed to correct and compensate for changes in bulk water temperature, pressure and ionic strength, which affect the speed of sound in water. The final design of the integrated heat transfer reduction sensor and the ultrasound thickness sensor is illustrated in Figure 1 (Seida, et al., 2013).

Material	Acoustical Impedance, 10^6 kg/m²sec	Detected material based on received ultrasound signals			
		Deposit, %	Characteristics	Non-deposit, %	Characteristics
Water	1.5	-	N/A	~ 100	N/A
Biofilm	1.7	0.4	Soft surface, weak signal	86.0	Hard surface, strong signal
Scale	20	74.0	Hard surface, strong signal	0.5	Hard surface, weak signal
Steel	45	~ 100	Hard surface, strong signal	-	N/A

Table 1. Percentage Distribution of Ultrasound Reflection

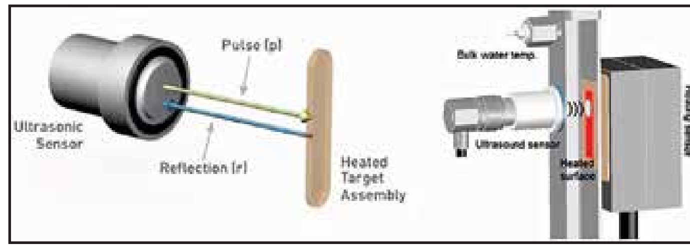

Figure 1. Side stream integrated heat transfer reduction sensor and ultrasound sensor.

Parameters, such as temperature, pressure, and ionic strength, can affect the speed of sound in water or any type of media (Medwin, 1975). For example, the difference of thickness calculation between 1 and 50 mS/cm water sample is about 3 μm with a 10 nanosecond time difference between pulse and reflection signals at a bulk water temperature of 86 °F (30 °C). An average compensation of 7 μm per 1 mS of conductivity increase at 10 mS conductivity water is needed for an accurate measurement. Temperature swings exert an even larger discrepancy, where a 30 μm thickness increase is observed per 0.56 °F (1 °C) increase in water temperature. Therefore, measurement corrections are needed and algorithms were developed to compensate for changes in bulk water temperature, pressure inside the flow channel, and conductivity. Additional details regarding the design and specifications of the ultrasound sensor can also be found elsewhere (Chien et al., 2017; Bierganns et al., 2016, 2017).

Before initiating pilot studies, , the new technology described in this paper was validated through third party using actual biofilm growth under static and dynamic laboratory conditions (not discussed in this paper). The accuracy of the ultrasound thickness measurement sensor was verified by using optical biofilm thickness measurements at outside testing facilities. The non-destructive, in situ technique, Optical Coherence Tomography (OTC), was used and provided comparable biofilm thickness measurements. The results demonstrated great correlation of ultrasound and OCT-based thickness measurements in the range of 25 to 100 μm (R2 = 0.9094). Details of the work can be found elsewhere (Wagner, 2016, 2017; Bierganns et al., 2017).

Materials And Methods

The objective of this paper is to investigate the applicability of the new technology for biofilm measurement and corresponding biofilm growth control under different industrial applications. Standard methods used to determine microbiological growth and experimental setup are described below.

Enumeration Of Biofilm

Laboratory-cultured bacteria was used in all benchtop and pilot studies. The planktonic bacteria culture was obtained from a full-scale, operational cooling tower and was fed with a nutrient-rich medium (containing 50 ppm glucose, 44 ppm NO3 and 12.5 ppm PO4). Microorganisms in this growth medium could reach a stationary growth phase within 72 hours under neutral pH and ambient temperature. The prepared culture then was used to inoculate the target testing system with a microbial population between 104 and 106 CFU/mL.

Planktonic bacteria were enumerated directly using the plate count method following the serial dilution technique. Biofilm, measured as sessile bacteria, was first scraped off of the attached surface using sterilized cotton swabs. Sessile bacteria were then dislodged from the biofilm matrix by sonicating a cotton swab (with the biofilm sample) fully immersed in phosphate-buffered water. The number of viable sessile bacteria were calculated by dividing the total cells in the buffered water with the total surface area of the sample collected. Planktonic and sessile bacteria are reported in colony forming units (CFU) per milliliter and CFU per square centimeter, respectively.

In addition to the traditional viable count method, biofilm coverage also was determined using a direct microscopic method. The biofilm images were recorded using a live/dead stain indicator and a fluorescence microscope with a magnification power of 50X. Microbial cells treated with live/dead stain appear green if they have intact membranes and are healthy. They appear red after the membranes are compromised, indicating the cells are either dying or dead. Yellow cells are believed to represent an intermediate state of damage. Black areas on the sampling specimen are film-free sections. The percent of coverage of the red and green areas on the images are determined using computerized image analysis software containing a built-in algorithm. Three fields of each coupon are imaged, quantified and averaged to obtain the average percent coverage.

Pilot Testing System

The pilot cooling tower (PCT) is designed to evaluate the efficacy of cooling water treatment programs for scale, corrosion and microbiological control with actual or synthetic makeup water under a wide range of operating conditions. The PCT consists of a central human machine interface (HMI) controller, a primary logic controller (PLC) with a touch screen panel, and analyzers (pH, oxidation-reduction potential (ORP) and conductivity). The central HMI controller and PLC have two-way communication for online performance control and data transfer to cloud-based data management. Chemical feed pumps are interfaced to the controller, which can be used to maintain pH, biocide residual and chemical doses at desired set points. The central HMI controller also maintains the cycles of concentration by monitoring either the conductivity or the fluorescent-based tracking chemical.

Figure 2. Overview of pilot scale testing apparatus. Biofilm monitoring and control device (indicated by arrow) is located on the center-right and biofilm sampling rack is on the left side of the image.

Results And Discussion

The following studies aimed at verifying the reliability of the integrated ultrasound sensor under realistic conditions using the PCT. Results of two pilot studies and two field trials are representative of several different types of industry configurations. The water compositions for each trial are summarized in Table 2. In addition to mineral salts used to make the ions, organic and suspended solids also were added to simulate actual organic loading. For the PCT studies, the cooling system was gradually cycled up to the desired cycles of concentration (CoCs) and then inoculated with a prepared inoculum (104 –106 CFU/mL of heterotrophic planktonic bacteria) to accelerate biofilm formation. Nutrient-rich medium was continuously added to the system to maintain healthy microbial activities.

PCT study #1 simulates a cooling system in a chemical processing plant using influent with high silica content. Besides having a premier cooling water treatment program with continuous bleach feed, the cooling system also was treated with additional bromide activated chloramine (BAC) to further improve corrosion inhibition and microbiological control (Beber, 2016). The makeup tank was agitated with a sump pump to keep the contents homogenized.

PCT study #2 simulates a cooling system with a bulk water temperature of 29 ºC (85 ºF) and a linear flow velocity greater than 1 m/s (3.5 ft/s). To induce microbial growth, glucose was added continuously to the cooling tower sump using a peristaltic pump.

Parameters	PCT* #1	PCT #2	CPI**	BIO-R***
pH	7.92 ± 0.03	7.88 ± 0.10	7.4-7.7	8.2-8.3
Conductivity, mS/cm	1345 ± 27	2326 ± 43	1803	2252
PALK, ppm $CaCO_3$	< 0.1	< 0.1	< 0.1	43.7
MALK, ppm $CaCO_3$	59.7 ± 4.0	66.8 ± 14.0	99.4	396.9
CaH, ppm as $CaCO_3$	174.5 ± 8.0	287.1 ± 14.5	290	845
MgH, ppm $CaCO_3$	83.3 ± 4.6	182.8 ± 9.6	124	435
Cl, ppm	143.3 ± 7.3	288.4 ± 26.3	457	43.3
SO_4, ppm	328.8 ± 9.6	712 ± 50.7	142	996
Al, ppm	1.12 ± 0.09	0.1 ± 0	1.5	0.1
$OrthoPO_4$, ppm	3.64 ± 0.27	5.42 ± 0.50	7.3	0.5
Polyphosphate, ppm	1.73 ± 0.42	1.42 ± 0.24	11.6	1.2
Soluble silica, ppm	115.2 ± 9.5	2.8 ± 0.3	55.9	131
Bacteria, CFU/mL (Max)	1.0E+04	2.7E+06	N/A	N/A

* PCT: Pilot cooling tower; ** CPI: Chemical processing industry; *** BIO-R: Biorefining industry.

Table 2. Water Compositions of Pilot Studies and Field Trials

The chemical processing industry (CPI) and the biorefining industry (BIO-R) trials used process waters supplied from side streams at customer sites to demonstrate the performance of the biofilm monitor. Data were collected through an online data management system and water analyses were reported by a certified laboratory.

Pilot Study #1

The first validation approach aimed at verifying the growth of biofilm in the test apparatus and the correlation between heat transfer reduction and biofilm thickness. The experiment started on August 10th, 2016 and the PCT system was maintained at the desired CoCs. The system was treated with a continuous sodium hypochlorite feed and a periodic BAC feed to remove any existing biofilm formation. On August 23rd, two weeks into equilibrium, we suspended the biocide treatment and seeded the cooling water reservoir with clarifier sludge collected from a local wastewater treatment facility to encourage bacterial growth. Within 72 hours of adding the clarifier sludge, biofilm accumulation was observed.

Both ultrasound thickness measurement and heat transfer reduction sensors detected the biofilm formation within reasonable timeframe (Figure 3). Results show that the heat transfer reduction index responded to microbial activity slightly faster than the biofilm thickness measurement. However, this is not surprising because the scattered polysaccharide layer (Island Growth) may have affected heat transfer before a biofilm colony formed. At the end of the test period, the biofilm thickness reached 40 µm with an associated heat transfer reduction index between 0.4 and 0.5 °C (7.2 – 9.0 °F). Visual observation of the heating block confirmed the biofilm growth and is displayed in Figure 4. The planktonic bacterial counts in the recirculating water were 104 CFU/mL, and the sessile bacterial counts collected from the heated target were 2.6x104 CFU/cm2.

With the capability to detect biofilm formation in early stage, the next step is to determine if the analyzer could response to treatment program. Monitoring the performance of the MB treatment program is critical because undertreatment would lead to exaggerated biofouling problem (Lechevallier, 1988). After biofilm attached to the surface, we used stainless steel coupons and the direct microscopic method to evaluate the impact of adding biopenetrant and biocide. The image analysis of biofilm was not aimed at providing direct counts of bacteria; the commonly used viable count is readily available. In addition, viable cells inside bacteria were not uniformly distributed. Although the area to be digitized was selected at random, aggregates of organic deposition can still bias the final counting of the bacterial population. However, when we compared the bacterial numbers obtained by manual counts and through image analysis, we found reasonable agreement (Figure 5).

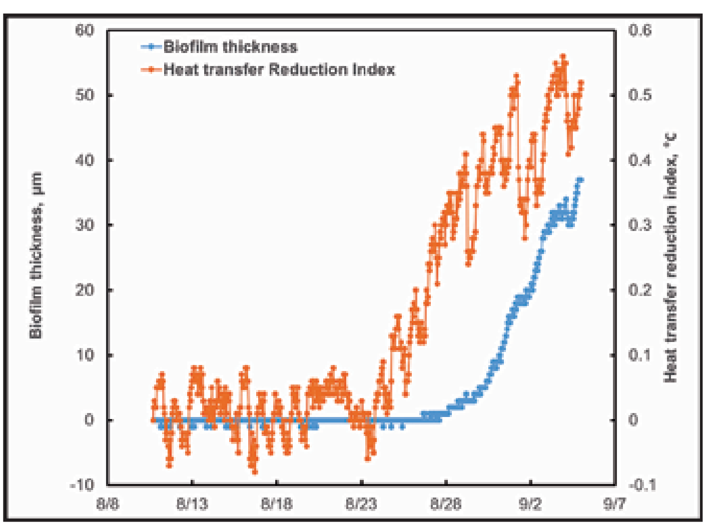

Figure 3. The orange and blue lines show the heat transfer reduction indices and the biofilm thickness measurements, respectively, caused by biofilm growth on the heated target.

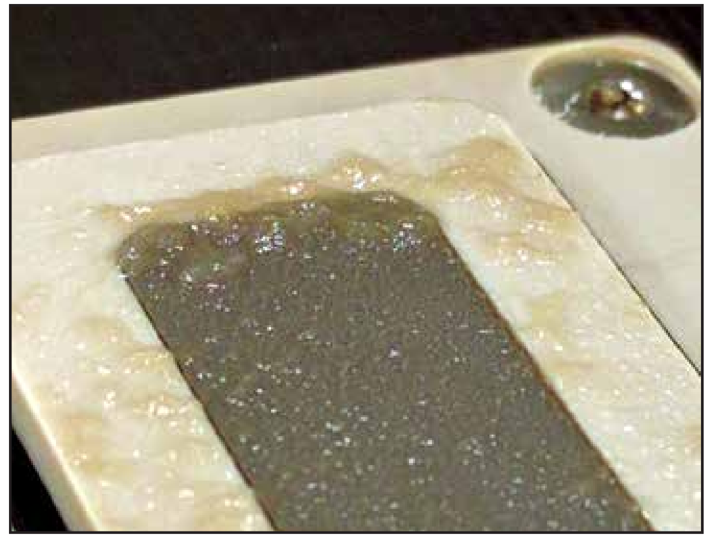

Figure 4. Visual representation of microbial growth on the heated target.

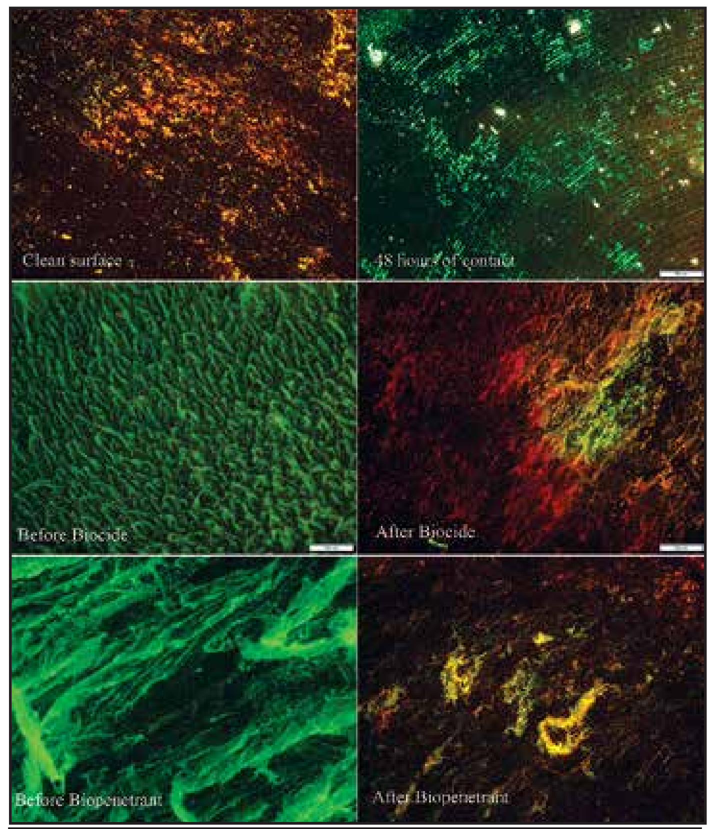

Scenario	% Coverage		Planktonic, CFU/mL		Sessile, CFU/cm^2	
	Before	After	Before	After	Before	After
48 hours contact time	13.3	-	3.2E+03	-	3.2E+04	-
Biocide – 100 ppm	52.6	17.6	4.5E+06	1.2E+05	2.7E+05	5.7E+03
Biopenetrant – 25 ppm	56.3	20.2	4.5E+06	2.2E+06	3.1E+04	1.8E+05

Figure 5. Biofilm coverage on stainless steel specimens under different scenarios. Pilot Study #2

After confirming that growing biofilm inside the PCT was feasible, the focus of the validation work shifted to testing an automatic, performance-driven treatment. The concept was to have an algorithm initiate chemical dosing, at the early stages of biofilm growth, based on the values of the key performance indicators reported by the integrated biofilm sensor, including either the heat transfer reduction index or the biofilm thickness. The proposed treatment program, including the proper interval between chemical doses for thorough mixing and better synergy, emphasizes the combination of biopenetrant and biocide. The use of biopenetrant changed the attached biofilm structure, which eventually led to easier biofilm removal (Seo and Bishop, 2007). The work by Simões et al. also demonstrated that biofilm removal efficacy was improved using a combination of biopenetrant and biocide (2005).

The PCT cooling system was inoculated with 106 CFU/mL planktonic bacteria immediately after reaching the desired CoCs. A 50 ppm dose of glucose was maintained by peristaltic pump to stimulate microbial activity. When the biofilm growth reached the heat transfer reduction threshold of 0.2 °C (0.36 °F), the system automatically dosed 10 ppm of biopenetrant and 100 ppm active hypochlorite, in sequence, at a pre-defined, 30-minute interval. The heat transfer reduction indices, chemical feed indications and ORP readings throughout the study are shown in Figure 6. Note that 30 minutes after dosing, the free and total chlorine residuals were measured at 1 and 4 ppm, respectively. Such a high biocide demand was expected because of the amount of glucose in the cooling system. The integrated sensor was able to initiate three treatment events after self-diagnosis and thereby remove biofilm before a loss in water flow disrupted the testing. After the study, an additional algorithm was implemented to prevent false treatment due to abnormal readings (compare e.g., after 118 hours in Figure 6.) within short periods and unexpected loss of water supply.

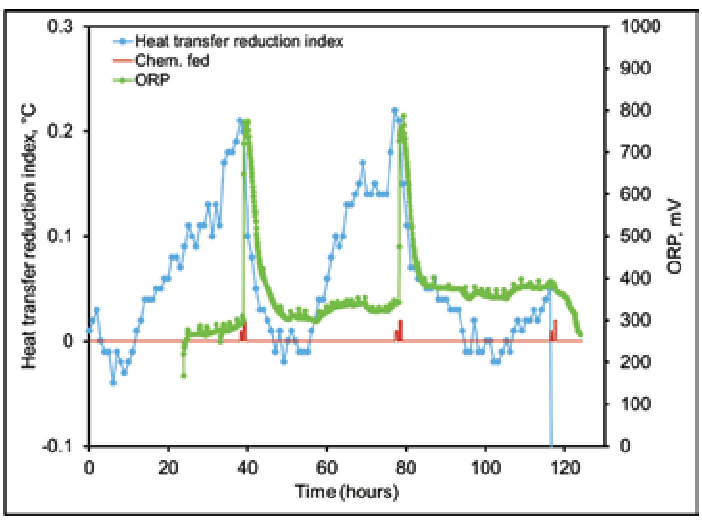

Figure 6. Automatic biopenetrant and biocide treatment in response to biofilm growth.

Case Study: Chemical Processing Industry

The real-time biofilm monitor was implemented in a large chemical production facility in the southern United States. The plant has two cooling towers that cool and recirculate process water streams containing small amounts of ethylene glycol. The cooling system previously experienced intermittent shutdowns due to organic/biofilm accumulation on the high efficiency fill film, which inevitably led to a tower collapse.

The biofilm monitoring system was installed on a side stream and operated with a flowrate of 15 LPM (3.96 GPM). With the change of season, the bulk water temperature varied between 18 and 32 °C

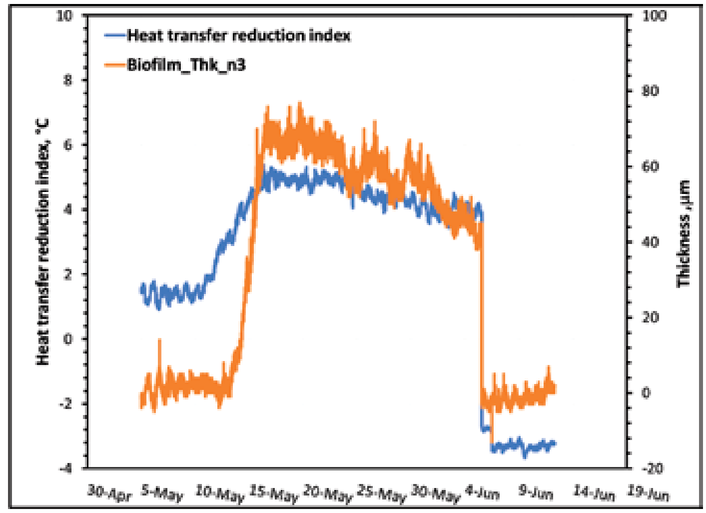

Figure 7. Heat transfer reduction index and thickness measurements at the CPI site.

(64 and 90 °F). The installed biofilm monitor was able to detect microbial activity in response to the increased temperature and the process leaks that occurred between May 10th, 2017 and May 15th, 2017. Heat transfer reduction and biofilm thickness measurements are shown in Figure 7. The biofilm thickness reached 80 µm on May 15. Since then, bromide activated chloramine treatments were introduced periodically to inactivate the viable biofilm. The treatment was effective and reduced the entire biofilm thickness to 40 µm. Mechanical cleaning with increased flowrate at 30 LPM (7.93 GPM) was employed on June 4. Results indicate that most of the deposition has since been removed and the readings have returned to baseline. The transition from continuous feed of oxidizing chemical to performance-based BAC feed not only reduced the overall chemical expense, but also significantly reduced the corrosion potential.

Case Study: Biorefining Industry

An ethanol production plant that has been operating since the 1990s has experienced excessive fouling on cooling tower fill, which impeded evaporation and reduced cooling capacity of individual heat exchangers, condensers, and centrifugal chillers. The current oxidizing biocide treatment was known to be aggressive and inevitably contributed to unacceptable corrosion rates.

Performance improvements were desired; therefore, a new microbiological control program was implemented together with the installation of the real-time biofilm sensor. To model the critical heat exchanger at fermentation cooler, we utilize the combination of hardware (sensors, flow regulators, heating elements) and customized algorithms in OnGuard 3B to replicate its operating conditions. The flow regulation and heating element help to simulate the flow condition (Reynold's number) and heating stress (BTU output). A side-stream of actual cooling water runs through the unit under the same operating characteristics (shown in Figure 8).

The graphical results, shown in Figure 9, reveal the biofilm growth was limited to less than 10 µm after switching from the previous biocide program to a bromide activated chloramine program. The biofilm sensor ensured that BAC was fully controlling biofilm growth in real time and allowed scale and corro-

sion inhibitor feeds to be optimized and met desired key performance indicators.

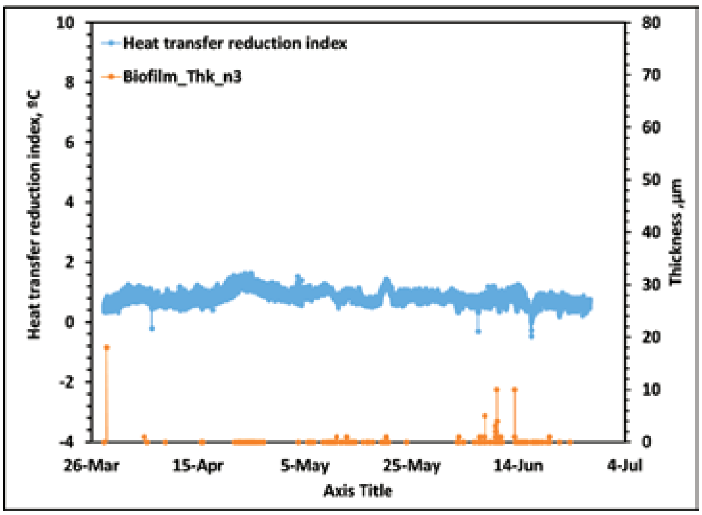

Figure 8. The biofilm monitoring device was installed together with other online analyzers at a side stream near the cooling system.

Figure 9. Heat transfer reduction index and thickness measurements at biorefining site.

Visual observation of traditional corrosion coupons collected before and after switching the biocide program show great improvement (Figure 10). Both the microbiologically induced corrosion and pitting were limited, and the carbon steel corrosion rates decreased from 5.6 MPY (91-day sample) to 0.2 MPY (102-day sample).

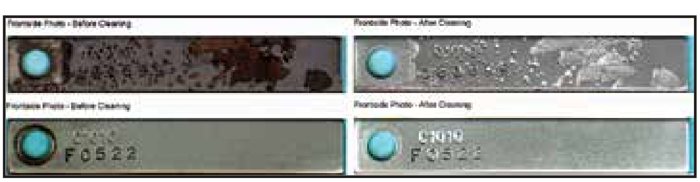

Figure 10. Carbon steel coupons collected before (top) and after switching biocide program (bottom) at biorefining site.

Conclusions

A real-time biofilm sensor that complements microbiological control programs has been developed for industrial water applications. With the combination of heat transfer reduction and biofilm thickness measurements, the analyzer is capable of identifying biofilm growth in its earliest stages. The pulse-echo ultrasound method provides a unique approach to directly measure scale, organic deposition, and biofilm thicknesses with a resolution down to the micrometer scale while the heat transfer reduction sensor clearly indicates the occurrence of fouling. Pilot tests confirmed the integrated sensor is capable of monitoring and treating biofilm growth using self-diagnosis function. The use of microscopic image analysis verified the biofilm coverage and the associated biofilm disruption after treatments. Finally, field trials demonstrated that the integrated sensor is reliable for biofilm monitoring and is responsive to microbial treatments under various industrial configurations. Additionally, the application of intermittent bromide activated chloramine was very effective against biofilm growth. In summary, the integrated biofilm sensor was proven to promptly identify and to mitigate biofilm problems.

Acknowledgements

The authors would like to thank the following people for their contribution to this paper; Terry Bliss, Timothy Patterson, Tracy Cordell, Markus Broecher, Christian Flocken, Donald Holt, Christina Moering, Edward Beardwood, Frank Seida, Michael Schultz, Nathan Schuster, Thomas Clay, Andrew Ledlie, Timothy Duncan, Robert Ferguson, Corinne Consalo and John Chapman.

Reference

1. Beardwood, E.S. and Therrien, J.K. (1999). Implications of Various Dispersants on Biofilm Clean-Up Processes, NACE International, Corrosion/99 Symposia, Paper 301
2. Beardwood, E.S. (2011). Treatment and Management for cooling Waters, NACE International, Houston, Texas, Corrosion 2011 Conference & Expo, Paper No. 11388.
3. Beber, A. (2016) Reduction on Water Consumption on a Cooling Tower with the Application of a Novel Biocide, IWC, 16-23
4. Bierganns, P. (2016). OnGuard 3PB Biofilm Monitor-IWT1216, Solenis Internal Research and Development Report
5. Bierganns, P. and Beardwood, E.S. (2017). A new and novel abiotic-biotic fouling sensor for aqueous systems, Heat Exchanger Fouling and Cleaning
6. Chien, S-H., Bluemle, M., Holt, D., and Young, J. (2018) Monitoring and Prevention of Mineral Scale Formation in Open Cooling Systems with an Inline Fouling Monitor, International Water Conference proceeding, IWC18-61

7. Fu, Y.Q.; Luo, J.K.; Nguyen, N.T.; Walton, A.J.; Flewitt, A.J.; Zu, X.T; Li, Y.; McHale, G.; Matthews, A.; Iborra, E.; Du, H. and Milne, W.I. (2017) Advances in piezoelectric thin films for acoustic biosensors acoustofluidics and lab-on-chip applications, Progress in Materials Science, pp. , 2017, ISSN 00796425.
8. Herald, P.J. and Zottola, E.A. (1988). Attachment of Listeria monocytogenes to stainless steel surfaces at various temperatures and pH values, Journal of Food Science, Vol. 53, Issue 5, page: 1549-1562; DOI: 10.1111/j.1365-2621.1988.tb09321.x
9. Lechevallier, M.W., Cawthon, C.D. and Lee, R.G. (1988) Factors promoting survival of bacteria in chlorinated water supplies. Appl. Environ. Microbiol., 54(3), pp.649-654.
10. Liu, C.C. (2012) Electrochemical Based Biosensors, Biosensors, 2(3), 269-272; DOI:10.3390/bios2030269
11. Maurício, R.; Dias, C.J.; Jubilado, N. and Santana, F. (2013). Biofilm thickness measurement using an ultrasound method in a liquid phase, Environ Monit Assess, 185(10):8125-33. doi: 10.1007/s10661-013-3160-0
12. Rossmoore. H.W. (1996). Handbook of biocide and preservative use, Blackie Academic and Professional, Glasgow, xiv., ISBN 0 7514 0212 5. J. Chem. Technol. Biotechnol., 66: 213. doi:10.1002/(SICI)1097-4660(199606)66:2<213::AID-JCTB2498>3.0.CO;2-W
13. Seida, F.; Flocken, C.; Poschmann, R.; Schultz, M.; Klaua, R. and Dietrich, G. (2009). Method and Device for High Precision Measurement of a Characteristic of a Fouling and / or Scaling Deposit Inside a Fluid Vessel or a Characteristic of a Portion of the Wall Inside a Fluid Vessel by Using Ultrasound, International Patent Publication, Number WO 2009/141135 A1
14. Seida, F.; Flocken, C.; Bierganns, P.; and Schultz, M. (2013). Method and Device for Detecting and Analyzing Deposits, International Patent Publication, Number WO 2013/092819 A3
15. Seida, F.; Flocken, C.; Bierganns, P.; and Schultz, M. (2015). Method and Device for Detecting and Analyzing Deposits, US Patent #2015/0000406 A1
16. Seo, Y. and Bishop, P.L. (2007). Influence of Nonionic Surfactant on Attached Biofilm Formation and Phenanthrene Bioavailability during Simulated Surfactant Enhanced Bioremediation, Environ. Sci. Technol., 41 (20), pp 7107–7113
17. Simões, M.; Pereira, M.O. and Vieira, M.J. (2005). Action of a cationic surfactant on the activity and removal of bacterial biofilms formed under different flow regimes, Water Research, Volume 39, Issue 2, Pages 478-486
18. Stoodley, P.; Dodds, I.; Boyle, J. D. and Lappin-Scott, H. M. (1998). Influence of hydrodynamics and nutrients on biofilm structure, Journal of applied microbiology, 85(S1).
19. Wagner M. (2016). Research Reports for Solenis, 08.08.2016 and 09.11.2016., Karlsruhe Institute of Technology (Engler-Bunte-Institut), Water Chemistry and Water Technology, Engler-Bunte-Ring 1-7, 76131 Karlsuhe, Germany
20. Wagner M. (2017). Research Reports for Solenis, 24.01.2017., Karlsruhe Institute of Technology (Engler-Bunte-Institut), Water Chemistry and Water Technology, Engler-Bunte-Ring 1-7, 76131 Karlsuhe, Germany
21. Wan, Z. and Xiao, C. (2011). Deposition sensor based on differential heat transfer resistance, US Patent# US2011/0096807 A1.
22. Zhang, X.; Bishop, P.L.; Kupferle, M.J. (1998). Measurement of polysaccharides and proteins in biofilm extracellular polymers, Water Science and Technology, Volume 37, Issues 4–5, 1998, Pages 345-348, DOI: 10.1016/S0273-1223(98)00127-9

Cooling Technology Institute Licensed Testing Agencies

For nearly thirty years, the Cooling Technology Institute has provided a truly independent, third party, thermal performance testing service to the cooling tower industry. In 1995, the CTI also began providing an independent, third party, drift performance testing service as well. Both these services are administered through the CTI Multi-Agency Tower Performance Test Program and provide comparisons of the actual operating performance of a specific tower installation to the design performance. By providing such information on a specific tower installation, the CTI Multi-Agency Testing Program stands in contrast to the CTI Cooling Tower Certification Program which certifies all models of a specific manufacturer's line of cooling towers perform in accordance with their published thermal ratings.

To be licensed as a CTI Cooling Tower Performance Test Agency, the agency must pass a rigorous screening process and demonstrate a high level of technical expertise. Additionally, it must have a sufficient number of test instruments, all meeting rigid requirements for accuracy and calibration.

Once licensed, the Test Agencies for both thermal and drift testing must operate in full compliance with the provisions of the CTI License Agreements and Testing Manuals which were developed by a panel of testing experts specifically for this program. Included in these requirements are strict guidelines regarding conflict of interest to insure CTI Tests are conducted in a fair, unbiased manner.

Cooling tower owners and manufacturers are strongly encouraged to utilize the services of the licensed CTI Cooling Tower Performance Test Agencies. The currently licensed agencies are listed below.

Licensed CTI Thermal Testing Agencies

Clean Air Engineering
7936 Conner Rd, Powell, TN 37849
865.938.7555
Fax 865.938.7569
www.cleanair.com / khennon@cleanair.com
Contact: Kenneth (Ken) Hennon

Cooling Tower Technologies Pte Ltd
17 Mandai Estate #06-02, Hwa Yew Industrial Building
SINGAPORE S729934
+65.98251247
johnny@coolingtwrtech.com
Contact: Johnny Ong

Cooling Tower Test Associates, Inc.
15325 Melrose Dr., Stanley, KS 66221
913.681.0027 / (F) 913.681.0039
www.cttai.com / cttakc@aol.com
Contact: Kullin Elliot

DMT GmbH & Co. KG
Am Technologiepark 1, 45307 Essen, Germany
+49.201.172.1164
www.dmt-group.de / meinolf.gringel@dmt-group.com
Dr. -Ing. Meinolf Gringel

McHale Performance
4700 Coster Rd, Knoxville, TN 37912
865.588.2654 / (F) 865.934.4779
www.mchaleperformance.com
ctitesting@mchaleperformnce.com
Contact: Gabriel Ramos

Licensed CTI Drift Testing Agencies

Clean Air Engineering
7936 Conner Rd, Powell, TN 37849
865.938.7555
Fax 865.938.7569
www.cleanair.com / khennon@cleanair.com
Contact: Kenneth (Ken) Hennon

McHale Performance.
4700 Coster Rd, Knoxville, TN 37912
865.588.2654 / (F) 865.934.4779
www.mchaleperformance.com
ctitesting@mchaleperformance.com
Contact: Gabriel Ramos

Cooling Technology Institute Sound Testing

Cooling towers are used extensively wherever water is used as a cooling medium or process fluid, ranging from HVAC to a natural draft cooling tower on a power plant. Sound emanating from a coooling tower is a factor in the surrounding environment and limits on those sound levels, and quality, are frequently specified and dictated in project specefications. The project specifications are expected to conform to local building codes or safety standards. Consequently, it may be in the best interest of the cooling tower purchaser to contract for field sound testing per CTI ATC-128 in order to insure compliance with specification requirements associated with cooling tower sound.

Licensed CTI SoundTesting Agencies

Clean Air Engineering
7936 Conner Rd
Powell, TN 37849
800.208.6162 or 865.938.7555
Fax 865.938.7569
www.cleanair.com
khennon@cleanair.com
Contact: Kenneth (Ken) Hennon

Cooling Tower Test Associates, Inc.
15325 Melrose Dr, Stanley, KS 66221
913.681.0027 / (F) 913.681.0039
www.cttai.com / cttakc@aol.com
Contact: Kullin Elliot

McHale Performance
4700 Coster Rd
Knoxville, TN 37912
865.588.2654
Fax 865.934.4779
www.mchaleperformance.com
ctitesting@mchaleperformance.com
Contact: Gabriel Ramos

Cooling Technology Institute Certification Program STD-201 for Thermal Performance

As stated in its opening paragraph, CTI Standard 201... " sets forth a program whereby the Cooling Technology Institute will certify that all models of a line of water cooling towers offered for sale by a specific Manufacturer will perform thermally in accordance with the Manufacturer's published ratings..." By the purchase of a "certified" model, the User has assurance that the tower will perform as specified, provided that its circulating water is no more than acceptably contaminated-and that its air supply is ample and unobstructed. Either that model, or one of its close design family members, will have been thoroughly tested by the single CTI-licensed testing agency for Certification and found to perform as claimed by the Manufacturer.

CTI Certification under STD-201 is limited to thermal operating conditions with entering wet bulb temperatures between 12.8°C and 32.2°C (55°F to 90°F), a maximum process fluid temperature of 51.7°C (125°F), a cooling range of 2.2°C (4°F) or greater, and a cooling approach of 2.8°C (5°F) or greater. The manufacturer may set more restrictive limits if desired or publish less restrictive limits if the CTI limits are clearly defined and noted in the publication.

Those Manufacturers who have not yet chosen to certify their product lines are invited to do so at the earliest opportunity. You can contact Virginia A. Manser, Cooling Technology Institute at 281.583.4087, or vmanser.cti.org or PO Box 681807, Houston, TX 77268 for further information

Licensed CTI Thermal Certification Agencies

Agency Name / Address	Contact Person / Website / Email	Telephone / Fax
Clean Air Engineering 7936 Conner Rd Powell, TN 37849	Kenneth (Ken) Hennon www.cleanair.com khennon@cleanair.com	865.938.7555 (F) 865.938.7569
Cooling Tower Test Associates, Inc. 15325 Melrose Dr. Stanley, KS 66221	Kullin Elliot www.cttai.com cttakc@aol.com	913.681.0027 (F) 913.681.0039
Cooling Tower Technologies Pte Ltd 17 Mandai Estate #06-02B, Hwa Yew Industrial Building S729934 Singapore	Johnny Ong coolingtwrtech@bigpond.com johnny@coolingtwrtech.com	+65.98251247
DMT GmbH & Co. KG Am Technologiepark 1 45307 Essen, Germany	Dr. Ing. Meinolf Gringel meinolf.gringel@dmt-group.com	+49.201.172.1164
McHale Performance 4700 Coster Rd Knoxville, TN 37912	Gabriel Ramos www.mchaleperformance.com ctitesting@mchaleperformance.com	865.588.2654 (F) 865.934.4779

Order Today
Call 281-583-4087

> *"The Performance Curve method is widely recognized as a more accurate method of determining tower capability from measured test data. The new CTI ToolKit Tab Application provides a quick and easy method for anyone to evaluate a performance test using the procedures prescribed in the ATC-105 code."*
> - Larry Burdick, ATC-105 Task Group

Bill to: ____

____

____

____

Phone: ____________________ **Fax:** ____________________

Email Address: ____________________

Ship to: ____

____

____

____

Phone: ____________________ **Fax:** ____________________

Email Address: ____________________

Charges can be made to Visa, MasterCard or American Express

Card No.: ______________________________ Expiration Date: ____________________

Signature: ______________________________ CVV; CVC; CID Code:____________________

Product		Unit Price	Quantity	Total
CTI ToolKit Version 3.2 (single user license)				
	CTI Member	$395		
	Non-member	$450		
CTI ToolKit Version 3.2 (Upgrade from V1.0 and V2.0)				
	CTI Member	$ 95		
	Non-member	$120		
CTI ToolKit Version 3.2 (Upgrade from V3.0)				
	CTI Member	$ 25		
	Non-member	$ 40		
Shipping for Flash Drive (from Texas): *Priority mail $6; 2nd Day Air $18; Overnight Domestic $28; / International (DHL) TBA*				
Multi-user site licenses and educational institution pricing available on request				

System Requirements:
Microsoft Windows®
95/98, 2000, XP, and
Windows 10

©

Phone: **281.583.4087**
Fax: **281.537.1721**
Web: **http://www.cti.org**

Cooling Towers Certified by CTI

As stated in its opening paragraph, CTI Standard STD-201 "...sets forth a program whereby the Cooling Technology Institute will certify that all models of a line of evaporative heat rejection equipment offered for sale by a specific Manufacturer will perform thermally in accordance with the Manufacturer's published ratings..."

By the purchase of a ***CTI Certified*** model, the Owner/Operator has assurance that the tower will perform as specified*.

**Performance as specified when the circulating water temperature is within acceptable limits and the air supply is ample and unobstructed. CTI Certification under STD-201 is limited to thermal operating conditions with entering wet bulb temperatures between 10°C and 32.2°C (50°F to 90°F), a maximum process fluid temperature of 51.7°C (125°F), a cooling range of 2.2°C (4°F) or greater, and a cooling approach of 2.8°C (5°F) or greater. The manufacturer may set more restrictive limits if desired or publish less restrictive limits if the CTI limits are clearly defined and noted in the publication.*

For each certified line, all models have undergone a technical review for design consistency and rated performance. One or more representative models of each certified line have been thoroughly tested by a CTI Licensed testing agency for certification and found to perform as claimed by the Manufacturer.

The CTI STD-201 Thermal Performance Certification Program has grown rapidly since its' inception in 1983 (see graphs that follow). A total of 79 cooling tower manufacturers are currently active in the program. In addition, 17 of the manufacturers also market products as private brands through other companies.

While in competition with each other, these manufacturers benefit from knowing that they each achieve their published performance capability and distinguish themselves by providing the Owner/Operator's required thermal performance. The participating manufacturers currently have 176 certified product lines plus 26 product lines marketed as private brands which result in approximately 50,000 CTI Certified cooling tower models to select from.

For a complete listing of certified product lines, and listings of all CTI Certified models, please see:

https://www.coolingtechnology.org/certified-towers

Those Manufacturers who have not yet chosen to certify their product lines are invited to do so at the earliest opportunity. Contact the CTI Administrator at vmanser@cti.org for more details.

Thermal Certification Program Participation

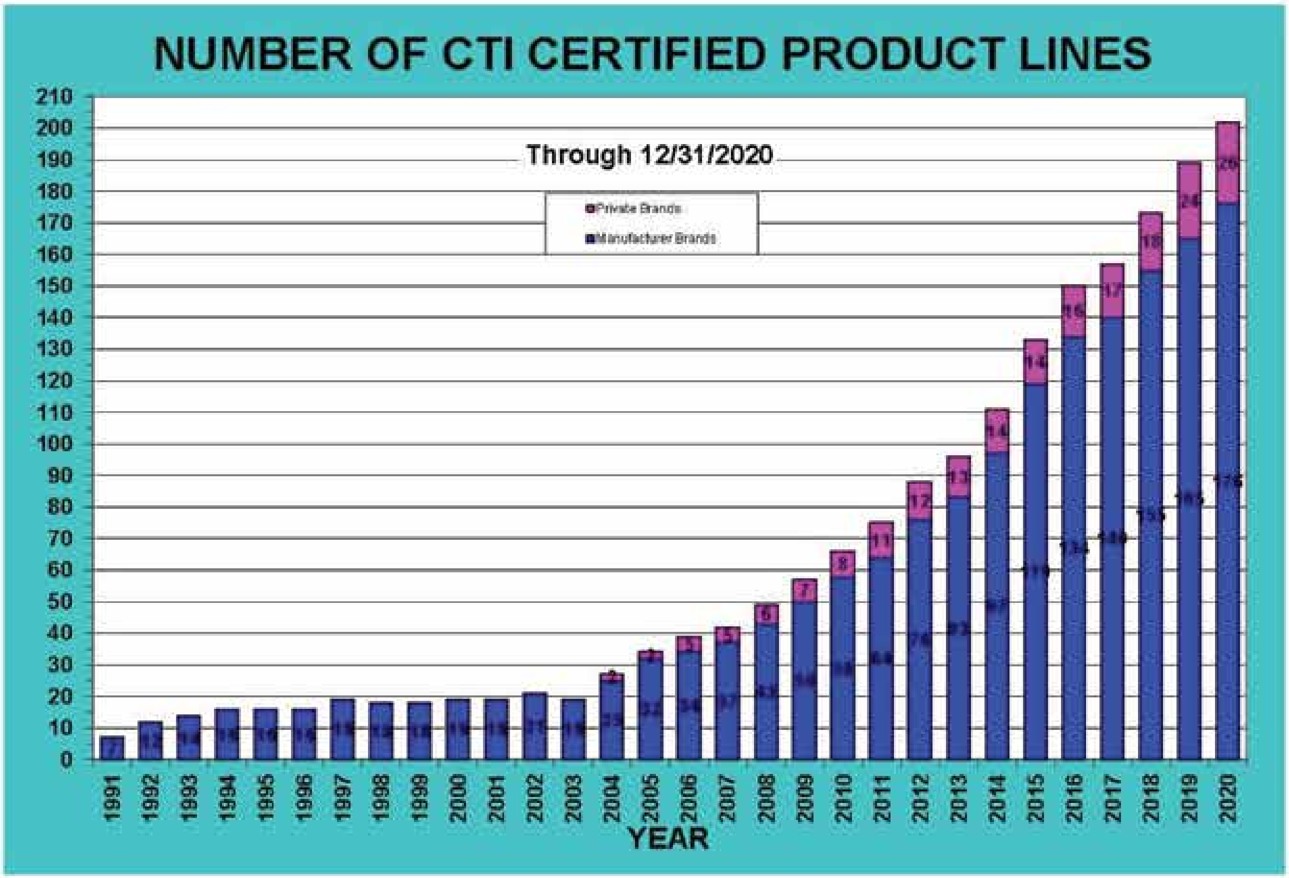

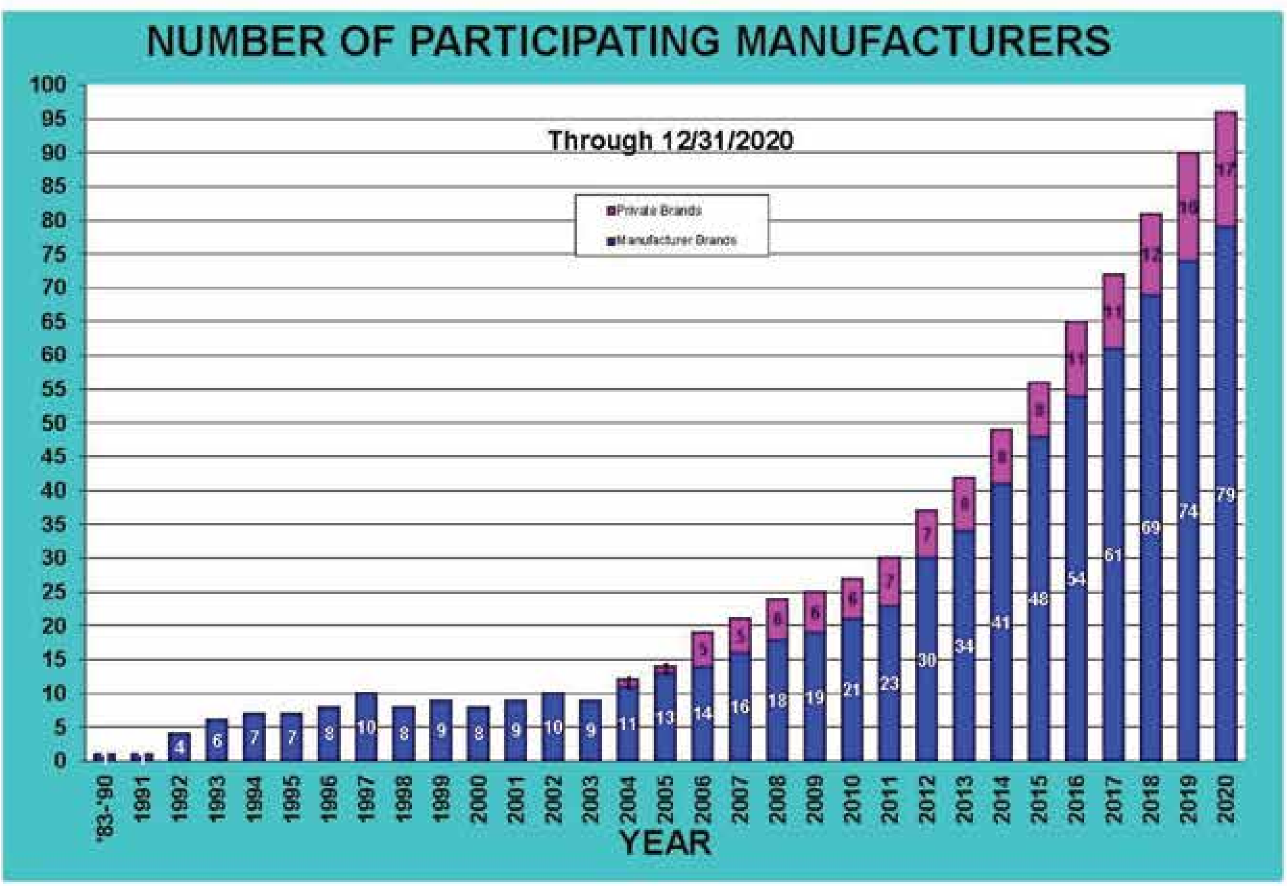

Current Program Participants

(as of December 31, 2020)

Program Participants and their certified product lines are listed below. Only the product lines listed here have achieved CTI STD-201 certification. For the most up-to-date information and a complete listing of all CTI Certified models please visit:

https://www.coolingtechnology.org/certified-towers

Current Certified Model Lists are available by clicking on the individual line names beneath the Participating Manufacturer name.

Catalog information and product selection data are also available by clicking on the links beneath each listed line.

A

Advance GRP Cooling Towers, Pvt.,Ltd.
Advance 2020 Series A *Validation No. C31A-07R03*
NTM Line *Validation No. C31B-19R00*

Aggreko Cooling Tower Services
AG Line *Validation No. C34A-08R02*

Amcot Cooling Tower Corp.
AST *Validation No. C106A-19R00*
Series R-LC *Validation No. C11E-11R03*

American Cooling Tower, Inc.
ACF Series *Validation No. C38D-18R00*
ACX Series *Validation No. C38C-18R00*

AONE E&C Corporation, Ltd.
ACT-C Line *Validation No. C28B-09R01*
ACT-R/ACT-RU Line *Validation No. C28A-05R05*

Approach Engineering Co., Ltd
NSA Line *Validation No. C76B-20R00*

Axima (China) Energy Technology Co., Ltd.
EWX Line *Validation No. C72A-15R03*

B

Baltimore Aircoil Company, Inc.
FXT Line *Validation No. C11A-92R02*
FXV Line *Validation No. C11J-98R10*
NXF Line *Validation No. C11Q-18R01*
PF Series *Validation No. C11P-12R02*
PT2, PTE & PCT Series *Validation No. C11L-07R05*
Series V Closed *Validation No. C11K-00R02*
Series V Open *Validation No. C11B-92R06*
Series S1500 *Validation No. C11H-94R09*
Series 3000A,C,D,E, Compass & Smart *Validation No. C11F-92R19*

Bell Cooling Tower Pvt, Ltd
BCTI Line *Validation No. C43A-12R02*

Brapu (China) Cooling Equipment Co., Ltd
BPC-DE/CH Series *Validation No. C110A-20R00*
BPO-DE/CH Series *Validation No. C110B-20R00*

C

Cenk Endüstri Tesisleri Imalat Ve Taahüt A.Ş.
LEON Line *Validation No. C89A-17R02*
LISA Line *Validation No. C89B-17R01*
ISTANBUL Line *Validation No. C89C-19R00*
ODIN Line *Validation No. C89D-20R01*

Chengdu Xingli Refrigeration Equipment Co., Ltd
HBL-HS Series *Validation No. C115A-19R00*

Chongqing Yinengfu Technology Co., Ltd
YNF Series *Validation No. C103A-18R00*

Composite Cooling Solutions Inc.
PhoenixPL *Validation No. C79B-20R00*

Cool Water Technologies
RTAi Line *Validation No. C52A-13R03*
RTi Line *Validation No. C52A-13R02*

D

Dalian Spindle Environmental Facilities Co., Ltd
DC Series *Validation No. C112A-19R00*
DF Series *Validation No. C112B-19R01*
DX Series *Validation No. C112C-19R01*

Decsa
TMA-EU Series *Validation No. C42C-17R00*

Delta Cooling Tower, Inc.
TM Series *Validation No. 02-24-01*

Delta (India) Cooling Tower Pvt, Ltd
DFC-60UX Line *Validation No. C85A-18R00*

Dezhou Beitai Refrigeration Equipment Co. Ltd.
$DBHZ_2$ *Validation No. C104A-19R00*

Dongguan Kuken Cooling Tower Co.,Ltd.
GXC Series *Validation No. C81B-16R01*
GXE Series *Validation No. C81A-16R0*

Dongguan Ryoden Cooling Equipment Co., Ltd
RT-L&U Series *Validation No. C71A-15R03*
RTM-L Series *Validation No. C71B-15R00*

Dunham-Bush (China) Co., Ltd
BHC Series *Validation No. C107A-19R00*

E

Elendoo Technology (Beijing) Co., Ltd.
EL Line *Validation No. C50C-15R04*
ELOP Line *Validation No. C50B-14R04*

Ebara Refrigeration Equipment & Systems Co.
CDW Line *Validation No. C53A-13R04*
CNW Line *Validation No. C53C-18R00*
CXW Line *Validation No. C53B-14R02*

Evapco, Inc.
AT Series *Validation No. C13A-99R22*
ATWB Series *Validation No. C13F-09R10*
AXS Line *Validation No. C13K-15R03*
ESWA, ESWB, & ESW4 Series *Validation No. C13E-06R12*
L Series Closed *Validation No. C13G-09R04*
L Series Open *Validation No. C13C-05R03*

F

Flow Tech Air Pvt Ltd
FTA Series *Validation No. C69A-16R02*

G

Genius Cooling Tower Sdn Bhd
MK Series *Validation No. C67C-18R01*
MT Series *Validation No. C67A-16R01*
MX Series *Validation No. C67B-16R00*

Guangdong EnZen Energy Saving Technology Co., Ltd
YZC Series *Validation No.C109A-19R00*

Guangdong Feiyang Industry Co., Ltd
RT-L&U Series *Validation No.C71A-15R03*

Guangdong Green Cooling Equipment Co., Ltd
GLR-E Series *Validation No.C97B-18R01*

Guangdong Zhaorin Industrial Co., Ltd
SRN Series *Validation No.C95A-17R01*

Guangdong Liangken Cooling and Heating Equipment Technology Co., Ltd
LRT Series *Validation No.C66A-15R02*
LYH Series *Validation No.C66B-20R00*

Guangzhou Goaland Energy Conservation Tech Co., Ltd.
GLH Series *Validation No. C96A-17R01*

Guangzhou Laxun Technology Exploit Co., Ltd.
LC Line *Validation No. C45F-16R01*
LMB Line *Validation No. 12-45-02*
PG Line *Validation No. C45G-17R00*
PL Line *Validation No. C45E-16R03*

Guangzhou Single Beam All Steel Cooling Tower Equipment Co., Ltd.
SLH Line *Validation No.C91E-16R02*

H

Hanf Cooling Equipment Co., Ltd
GTC Series *Validation No. C101B-19R01*
GTN Series *Validation No. C101A-18R01*
GTS Series *Validation No. C101C-20R00*

Hon Ming (Guang Dong) Air Conditioning Equipment Company, Ltd.
HM Series *Validation No. C66B-20R00*
MK Series *Validation No. C66A-15R02*

Hunan Yuanheng Technology Company, Ltd.
YCH-F Line *Validation No. C40C-16R02*
YCN-F Line *Validation No. C40D-18R00*
YHD Line *Validation No. C40B-15R00*
YHW Line *Validation No. C40E-18R00*

HVAC/R International, Inc.
Therflow Series TFC *Validation No. C28B-09R01*
Therflow Series TFW *Validation No. C28A-05R05*

I

İMAS KLİMA SOĞUTMA MAKİNA SANAYİ TİCARET ve MÜMESSİLLİK A.Ş.
TA Line *Validation No. C114B-20R00*
TAK Line *Validation No. C114A-20R00*

J

Jacir
DTC *Validation No. C46E-18R01*
VAP Line *Validation No. C46C-16R02*

Jiangsu Greenland Heat Transfer Technology Co.
GBH-TS Line *Validation No. C87A-18R01*

Jiangsu i-Tower Cooling Technology Co., Ltd.
REH Series *Validation No. C75B-16R01*
TMH Series *Validation No. C75A-16R02*

Jiangsu Ocean Cooling Equipment Co., Ltd.
TKS Series *Validation No. C41D-18R00*

Jiangxi Ark Fluid Science Technology Co., Ltd.
FBFJ Line *Validation No. C83B-18R00*
FBNJ Line *Validation No. C78B-20R00*
FKH Line *Validation No. C83A-17R01*

Ji'Nan Chin-Tech Thermal Technology Co., Ltd.
CCOX Line *Validation No. C91F-20R00*
CTHX Line *Validation No. C91E-16R02*

K

Kelvion B.V.
Polacel CF Series *Validation No. C25A-04R02*

KIMCO (Kyung In Machinery Company, Ltd.)
CKL Line *Validation No. C18B-05R04*

KIMCO (Kyung In Machinery Company, Ltd.)
Endura Cool Line *Validation No. C18A-93R09*
GX Line *Validation No. C18D-18R01*

King Sun Industry Company, Ltd.
HKD Line *Validation No. C35B-09R06*
KC Line *Validation No. C35C-11R02*
KFT Line *Validation No. C35D-16R01*

Korytko Systems, Ltd.
KDI Line *Validation No. C70A-16R02*

KSN Co., Ltd
KSNC Series *Validation No. C44A-12R03*
KSNX Series *Validation No. C44B-12R01*
KSNC-C Series *Validation No. C44C-14R01*
KSNX-C Series *Validation No. C44D-14R01*

L

Liang Chi Industry Company, Ltd.
LCTD Line *Validation No. C20J-18R00*
LCTR Line *Validation No. C20H-17R00*
Series C-LC *Validation No. C20B-09R02*
Series D-LC *Validation No. C20F-14R02*
Series R-LC *Validation No. C20E-11R03*
Series U-LC *Validation No. C20D-10R04*
Series V-LC *Validation No. C20C-10R01*
TLC Line *Validation No. C20G-16R00*
V-LN Line *Validation No. C20K-20R00*

M

Marley (SPX Cooling Technologies)
Aquatower Series *Validation No. 01-14-05*
AV Series *Validation No. C14D-98R03*
DTW Series *Validation No. C14N-16R02*
LW Series *Validation No. C14P-16R01*
MCW Series *Validation No. 06-14-08*
MD and CP Series *Validation No. C14L-08R10*
MH Series *Validation No. C14G-04R11*
NC Series *Validation No. C14A-92R21*
NX Series *Validation No. C14M-15R01*
Quadraflow Line *Validation No. 92-14-02*

Mesan Cooling Tower, Ltd.
MCC Series *Validation No. C26G-12R03*
MFD Series *Validation No. C26J-16R01*
MHD Series *Validation No. C26K-20R00*
MXC Series *Validation No. C26H-12R01*
MXR-KM, MXL, MXH Series *Validation No.C26C-08R09*

MITA S.r.l.
PM Series *Validation No. C56B-16R02*

N

NIBA Su Sogutma Kulerleri San, ve Tic, A.S.
HMP-NB Line *Validation No. C55A-14R02*

Nihon Spindle Manufacturing Company, Ltd.
KG Line *Validation No. C33B-12R05*

O

Ocean Cooling Tower Sdn Bhd
OCBSD *Validation No. C86B-19R00*
YC Series *Validation No. C86A-17R00*

OTT Company, Ltd.
OTTC Series *Validation No. C44A-12R03*
OTTX Series *Validation No. C44B-12R01*
OTTC-C Series *Validation No. C44C-14R01*
OTTX-C Series *Validation No. C44D-14R01*

P

Paharpur Cooling Tower, Ltd.
CF3 Series *Validation No. C51A-13R03*
OXF-30K Series *Validation No. C51B-14R00*
Series RXF *Validation No. C51C-19R00*

Protec Cooling Towers, Inc.
FRS Series *Validation No. 05-27-03*
FWS Series *Validation No. C27A-04R06*

Q

Qinyang Zhonghe Zhi Da Technology Co., Ltd.
HLO Series *Validation No. C99B-20R00*
HL-SC Series *Validation No. C99A-18R00*

R

Reymsa Cooling Towers, Inc. (Fabrica Mexicana de Torres, SA de CV)
HFC Line *Validation No. C22F-10R06*
RT & RTM Series *Validation No. C22G-13R08*

Rosemex, Inc.
RC (RCS/D) Series *Validation No. C54A-13R04*
RO (ROS/D) Series *Validation No. C94A-14R03*

RSD Cooling Towers
RSS Series *Validation No. C32A-08R01*

Ryowo (Holding) Company, Ltd.
FDC Series *Validation No. C27E-11R00*
FRS Series *Validation No. 05-27-03*
FVS Series *Validation No. 12-27-06*
FWS and FCS Series *Validation No. C27A-04R06*
FXS Series *Validation No. C27B-20R00*

S

Shangdong Grad Group Co., Ltd.
GAT Series *Validation No. C88A-17R00*

Shanghai ACE Cooling Refrigeration Technology Col, Ltd.
AC Line *Validation No. C80A-17R01*

Shanghai Baofeng Machinery Manufacturing Co., Ltd.
BTC Line *Validation No. C49A-12R01*

Shanghai Liang Chi Cooling Equipment Co., Ltd.
LCP Line *Validation No. C62D-18R00*
LNCM Line *Validation No. C62B-16R00*
LRS Line *Validation No. C62C-16R00*
LRCM-DD Line *Validation No. C62E-19R00*

Shanghai Tyacht Cooling System Co.,Ltd.
TMC Line *Validation No. C93C-18R00*

Shanghai Wanxiang Cooling Equipment Co., Ltd.
FBH/HL Line *Validation No. C54A-13R04*
FKH/FKHL Series *Validation No. C94A-14R03*

Shanghai Zendia Cooling Equipment Co., Ltd.
ZHF-7000 Series *Validation No. C111A-19R00*

Sinro Air-Conditioning (Fogang) Company, Ltd.
CEF Line *Validation No. C37D-20R00*
CEF-A Line *Validation No. C37B-11R03*
SC-B Series *Validation No. C37C-11R02*
SC-H Series *Validation No. C37A-10R03*

Sung Ji Air-Conditioning Technology Co., Ltd.
SJCO Series *Validation No. C74B-16R01*
SJMO Series *Validation No. C74A-16R00*

T

Ta Shin F.R.P. Company, Ltd.
TSS Series *Validation No. C32A-08R01*

The Cooling Tower Company, L.C
TCIA Series *Validation No. C29C-19R01*

Thermal-Cell sdn bhd
THW Line *Validation No. C40E-18R00*

Thermax Cooling Solutions Limited
Enerflow (CM) Line *Validation No. C117A-20R00*

Tower Tech, a div. of CPK Manufacturing, LLC
TTXL Line *Validation No. C17F-08R05*
TTXR Line *Validation No. C17F-15R00*

Truwater Cooling Towers Sdn Bhd
EC-S Series *Validation No. C41A-12R04*
EX-S and VX-S Series *Validation No.C41B-12R07*
TKS Series *Validation No.C41D-18R00*

W

Wuxi Ark Fluid Science Technology Co., Ltd.
FBF Series *Validation C83B-18R00*
FBN Series *Validation C78B-20R00*

Wuxi Fangzhou Water Cooling Equipment Co., Ltd.
FFB Line *Validation C64D-20R00*

Wuxi Zhishui Environmental Co., Ltd.
ZSBN Series *Validation C113A-20R00*

Y

YM Tech Co., Ltd.
Csta Line *Validation No. C108D-20R00*
Xsta Line *Validation No. C108B-19R01*
YFO Line *Validation No. C108A-19R00*
YFOL Line *Validation No. C108C-20R00*

York (By Johnson Controls)
AT Series *Validation No. C13A-99R22*
LSTE Line *Validation No. C13G-09R03*

Z

Zhejiang Dongjie Cooling Tower Co., Ltd.
DHC Line *Validation No. C63B-15R00*

Zhejiang Haicold Cooling Technology Co., Ltd
SFN Line *Validation No. C76B-20R00*

Zhejiang Jinling Refrigeration Engineering Co.,Ltd.
JFT Series *Validation No. C28C-16R02*
JNC Series *Validation No. C28B-09R01*
JNT Series *Validation No. C28A-05R05*

Zhejiang Ryoden Cooling Equipment Co., Ltd.
RT/SB Series *Validation No. C102A-18R00*

Zhejiang Shangfeng Cooling Tower Co., Ltd.
SFB Line *Validation No. C73A-15R01*
SFCFG Line *Validation No. C73B-20R00*

Zhejiang Wanxiang Science and Technology Company, Ltd.
WBH Line *Validation No. C96A-17R01*

Always Look For the CTI Certified Label with Validation Number on Your Equipment

Index to Advertisers

Aggreko Cooling Tower Services .. 36-37

Amarillo Gear Company .... IBC

Amarillo Gear Service 3

Arvind 7

Bailsco Blades & Castings, Inc 2

Brentwood Industries.......................... 41

ChemTreat, Inc..................................... 35

Composite Cooling Solutions ....IFC

Cooling Tower Resources 4

CTI License Testing Agencies............. 62

CTI Sound Testing/Thermal Performance.... 63

CTI ToolKit..................................... 64-65

CTI Certified Towers........................ 66-71

Denso.. 47

Experience - Power 31

FanTR 11

Fuel Ethanol Workshop 21

Harmony Integrated............................. 6

Kipcon 5

Moore Fans 53

Precision Cooling Towers.................... 43

Rexnord Industries.............................. 27

Seagull Cooling Towers 17

C.E. Shepherd Company, LP 23

SPX Cooling Technologies .... OBC

Tower Performance, Inc. 49, 72

Turbo Machinery.................................. 61

MARLEY®

Use Our Tools to Extend Your Cooling Tower's Life

Tower Inspections with Report:

Using our proprietary MarleyInspections™ app, our inspector carefully documents tower conditions and generates a comprehensive written report in 24 hours.

Components Inventory:

Our extensive Parts and Service facilities have the essential cooling tower components you need. Gearbox repairs? We've got you covered!

Rapid Recon Resources:

Our experienced crews have exemplary safety records and can quickly mobilize to support your emergent needs and ongoing projects.

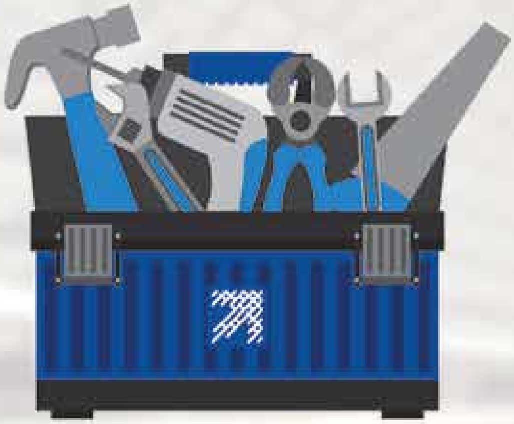

Modular Tower Build Solutions:

We have the engineering know-how and construction muscle to speed design and accelerate erection to meet your outage schedule.

For the Long Haul:

Count on our extensive Engineering, Manufacturing and Construction resources to assess, protect and extend the operational condition of your cooling tower.

In ordinary or extraordinary times, you can count on #SPXMarley.

24/7 Response: 800-4Marley; after hours emergency: 913-707-4631
www.spxcooling.com/process-cooling

Follow us on social media: **spxcooling.com/connect**

800.4.Marley | spxcooling.com

SPX®